Pro- and antiapoptotic events in Herpes simplex virus type 1 (HSV-1) infection of immature dendritic cells

D I S S E R T A T I O N

zur Erlangung des akademischen Grades

doctor rerum naturalium
(Dr. rer. nat.)
im Fach Biologie

eingereicht an der
Mathematisch-Naturwissenschaftlichen Fakultät I
Humboldt-Universität zu Berlin

von
Diplombiologin Angela Kather

Präsident der Humboldt-Universität zu Berlin:
Prof. Dr. Jan-Hendrik Olbertz

Dekan der Mathematisch-Naturwissenschaftlichen Fakultät I:
Prof. Dr. Andreas Herrmann

Gutachter:
1. Prof. Dr. Detlev H. Krüger
2. Prof. Dr. Birgit Sawitzki
3. PD Dr. Sebastian Voigt

eingereicht am: 01.04.2011
Tag der mündlichen Prüfung: 19.10.2011

Abstract

Herpes simplex virus type 1 (HSV-1) is a human pathogen which belongs to the family *Herpesviridae*. This virus family is characterized by a large genome encoding many genes, which shape the virus-host interaction. Furthermore, herpesviruses are able to remain lifelong in the host in a latent state from which they can reactivate in order to replicate again. Reactivation of HSV-1 can cause recurrent disease, Herpes labialis, characterized by vesicle formation in the skin of the lips. Sporadically, HSV-1 infection can cause other clinical manifestations, such as encephalitis with poor prognosis.

Virus infection is controlled at the cellular level as well as by the immune system. Cells can respond to virus infection by induction of apoptosis, a strictly regulated form of physiological cell death. This can efficiently limit replication of the virus and spread of the virus to surrounding cells. However, to resolve peripheral lesions and prevent disease in the central nervous system, a specific cytotoxic T cell immune response to HSV-1 is crucial. The most potent activators of T cells are dendritic cells (DCs). Immature dendritic cells (iDCs) patrol in peripheral tissues and take up antigens. Upon encounter with specific structures of pathogens or inflammatory signals, DCs mature, migrate to the draining lymph nodes and are able to present antigens to T cells and activate them. HSV-1 can infect local iDCs and severely impair their phenotype, function and viability. However, uninfected bystander iDCs take up antigen from HSV-1 infected cells and mount a protective immune response.

HSV-1 encodes several genes, which serve to efficiently prevent apoptosis in most infected cell types, thereby ensuring successful virus replication. In contrast, HSV-1 infected iDCs undergo apoptosis and virus replication in this cell type is low. So far, the mechanisms underlying apoptosis of HSV-1 infected iDCs are poorly defined. However, it has been shown that the antiapoptotic cellular protein c-FLIP is reduced in HSV-1 infected iDCs. The mechanism and impact of HSV-1 induced c-FLIP reduction was not investigated up to now. Furthermore, it is not known why antiapoptotic HSV-1 genes are not functional in iDCs.

In this work, the amount of c-FLIP was for the first time successfully reduced in iDCs by RNA interference. This confirmed the importance of c-FLIP for viability of iDCs. Therefore, it is likely that the reduction of the amount of c-FLIP after HSV-1 infection could also sensitize iDCs to apoptosis.

The mechanism of HSV-1 induced c-FLIP reduction was resolved to a large extent. It could be demonstrated that a viral or induced cellular protease directly degrades c-FLIP, while the amount of cytoplasmic c-FLIP mRNA was not reduced. HSV-1 induced c-FLIP degradation occurred at late stages of infection and was dependent on proper expression of early and leaky late virus genes. Degradation of c-FLIP after HSV-1 infection was independent from the proteasome and binding to the death inducing signaling complex. Co-transfection studies indicated that viral protein kinase U_S3 and c-FLIP co-localize. This could be an indication that U_S3 is involved in HSV-1 induced degradation of c-FLIP.

Surprisingly, c-FLIP reduction after HSV-1 infection was not only observed in iDCs, but also in human umbilical vein endothelial cells (HUVECs), primary epithelial cells (keratinocytes), primary connective tissue cells (fibroblasts) and cells of hematopoietic origin (Hodgkin/Reed-Sternberg cells). However, in these cell

types no apoptosis was observed after HSV-1 infection. It was hypothesized that effective antiapoptotic viral factors compensate the HSV-1 induced loss of c-FLIP in most cell types, but not in iDCs. In order to investigate whether antiapoptotic HSV-1 genes possibly are insufficiently expressed in iDCs, a microarray analysis of HSV-1 gene expression in apoptotic iDCs compared to nonapoptotic epithelial cells was conducted. Intriguingly, the abundance of transcripts of most antiapoptotic HSV-1 genes was not different in iDCs compared to epithelial cells. However, latency-associated transcripts (LATs) were significantly lower expressed in iDCs. It is known that in neurons and epithelial cells, LATs possess a potent antiapoptotic activity. This could compensate the lack of c-FLIP. Consistent with this hypothesis, a LAT deletion mutant of HSV-1 induced more apoptosis in iDCs compared to the respective wild type virus.

In this work it is shown for the first time that in addition to changes in the cellular apoptosis signaling network, the lack of one antiapoptotic viral factor contributes to apoptosis of HSV-1 infected iDCs. The expression of HSV-1 antiapoptotic factors appears to be cell type dependent, as shown here for LATs. The cell type specific induction or prevention of apoptosis might be one tool of HSV-1, which might contribute to maximize its spread, replication and establishment of latency without excessive damage to the host.

Zusammenfassung

Herpes simplex Virus Typ 1 (HSV-1) ist ein humanpathogenes Virus und gehört zur Familie *Herpesviridae*. Diese Virusfamilie ist durch ein sehr großes Genom gekennzeichnet, das viele an der Virus-Wirt Interaktion beteiligte Gene enthält. Herpesviren sind in der Lage lebenslang im Wirt zu überdauern, in einer latenten Form aus der sie reaktivieren und erneut replizieren können. Die Reaktivierung von HSV-1 kann mit wiederkehrenden Krankheitserscheinungen einhergehen, vor allem den charakteristischen Lippenbläschen (Herpes labialis). Vereinzelt kann eine HSV-1 Infektion auch andere klinische Manifestationen zeigen, zum Beispiel Enzephalitis mit schlechter Prognose.

Virusinfektionen werden sowohl auf Zellebene als auch durch das Immunsystem eingedämmt. Zellen können auf eine Virusinfektion durch Induktion von Apoptose reagieren, einer genau regulierten, physiologischen Form des Zelltods. Dadurch kann die Virusreplikation und die Virusausbreitung auf benachbarte Zellen stark verringert werden. Für die Heilung peripherer Läsionen und für den Schutz des Zentralnervensystems vor Schäden ist jedoch eine spezifische zytotoxische T-Zell Immunantwort gegen HSV-1 entscheidend. Die potentesten Aktivatoren von T-Zellen sind dendritische Zellen (DCs). Unreife dendritische Zellen (iDCs) patrouillieren in peripheren Geweben und nehmen Antigene auf. Wenn sie auf spezifische Strukturen von Pathogenen oder auf Entzündungssignale treffen, reifen die DCs, wandern zu den abführenden Lymphknoten und sind in der Lage, T-Zellen Antigene zu präsentieren und sie zu aktivieren. HSV-1 kann die lokalen iDCs infizieren und ihren Phänotyp, ihre Funktion und ihre Lebensfähigkeit stark beeinträchtigen. Nicht infizierte „bystander" iDCs nehmen jedoch Antigene von HSV-1 infizierten Zellen auf und induzieren eine schützende Immunantwort.

HSV-1 besitzt mehrere Gene, die dazu dienen, in den meisten infizierten Zelltypen Apoptose effektiv zu verhindern, um eine erfolgreiche Virusreplikation sicherzustellen. Im Gegensatz dazu gehen HSV-1 infizierte iDCs in Apoptose und die Virusreplikation ist in diesem Zelltyp gering. Bis jetzt sind die Mechanismen, die der Apoptose in HSV-1 infizierten iDCs zu Grunde liegen, nur unzureichend aufgeklärt. Es wurde jedoch gezeigt, dass das antiapoptotische zelluläre Protein c-FLIP in HSV-1 infizierten iDCs reduziert ist. Der Mechanismus und die Auswirkungen der HSV-1 induzierten c-FLIP Reduktion wurden bisher nicht untersucht. Weiterhin ist nichts darüber bekannt, warum die antiapoptotischen HSV-1 Gene in iDCs nicht funktionieren.

In dieser Arbeit wurde die c-FLIP Menge in iDCs erstmalig mit Hilfe von RNA Interferenz erfolgreich reduziert. Dies bestätigte die Bedeutung von c-FLIP für die Lebensfähigkeit von iDCs. Folglich ist es wahrscheinlich, dass auch die Reduktion der c-FLIP Menge nach HSV-1 Infektion iDCs für Apoptose empfindlich machen könnte.

Der Mechanismus der HSV-1 induzierten c-FLIP Reduktion wurde weitgehend aufgeklärt. Es konnte gezeigt werden, dass eine virale oder induzierte zelluläre Protease c-FLIP direkt abbaut, während die Menge zytoplasmatischer c-FLIP mRNA nicht reduziert war. Der HSV-1 induzierte c-FLIP Abbau fand in späten Stadien der Infektion statt und war abhängig von der ordnungsgemäßen Expression viraler „early" und „leaky late" Gene. Der Abbau von c-FLIP nach HSV-1 Infektion war unabhängig vom Proteasom und der Bindung an den „death inducing signa-

ling complex“. Kotransfektionsuntersuchungen deuteten darauf hin, dass die virale Proteinkinase U_S3 und c-FLIP kolokalisieren. Dies könnte ein Hinweis darauf sein, dass U_S3 am HSV-1 induzierten Abbau von c-FLIP beteiligt ist.

Überraschenderweise war eine c-FLIP Reduktion nach HSV-1 Infektion nicht nur in iDCs zu beobachten, sondern auch in Endothelzellen aus Nabelschnurvenen (HUVECs), primären epithelialen Zellen (Keratinozyten), primären Bindegewebszellen (Fibroblasten) und Zellen hämatopoetischen Ursprungs (Hodgkin/-Reed-Sternberg Zellen). Jedoch war in diesen Zelltypen keine Apoptose nach HSV-1 Infektion zu beobachten. Es könnte vermutet werden, dass effektive antiapoptotische virale Faktoren den HSV-1 induzierten Verlust von c-FLIP in den meisten Zelltypen kompensieren, jedoch nicht in iDCs. Um zu untersuchen, ob antiapoptotische HSV-1 Gene möglicherweise unzureichend exprimiert sind, wurde eine Microarray-Analyse der HSV-1 Genexpression in apoptotischen iDCs im Vergleich zu nicht apoptotischen epithelialen Zellen durchgeführt. Interessanterweise war die Menge der Transkripte der meisten antiapoptotischen HSV-1 Gene nicht unterschiedlich in iDCs im Vergleich zu epithelialen Zellen. Jedoch waren in iDCs „latency-associated transcripts“(LATs) signifikant geringer exprimiert. Es ist bekannt, dass LATs in Neuronen und epithelialen Zellen eine antiapoptotische Aktivität besitzen. Diese könnte den Mangel an c-FLIP kompensieren. Übereinstimmend mit dieser Hypothese induzierte eine HSV-1 LAT-Deletionsmutante mehr Apoptose in iDCs im Vergleich zum entsprechenden Wildtyp -Virus.

In dieser Arbeit wurde erstmals gezeigt, dass zusätzlich zu Veränderungen im zellulären Apoptosesignalnetzwerk der Mangel an einem antiapoptotischen viralen Faktor zur Apoptose von HSV-1 infizierten iDCs beiträgt. Die Expression antiapoptotischer Faktoren von HSV-1 scheint vom Zelltyp abhängig zu sein, wie hier für LATs gezeigt. Die zelltypspezifische Induktion oder Verhinderung von Apoptose könnte ein Werkzeug von HSV-1 sein, das dazu beiträgt, seine Verbreitung, seine Replikation und die Etablierung von Latenz zu maximieren, ohne übermäßigen Schaden für den Wirt.

Inhaltsverzeichnis

Abbreviations

aa	Amino acids
ACV	Aciclovir
ADP	Adenosine diphosphate
APS	Ammonium persulfate
ATP	Adenosine triphosphate
bp	Base pairs
BSA	Bovine serum albumin
CD	Cluster of differentiation
c-FLIP	Cellular FLICE inhibitory protein
c-FLIP$_L$	Long isoform of c-FLIP
c-FLIP$_S$	Short isoform of c-FLIP
co	Control
C-terminus	Carboxyl-terminus of a protein
DAPI	4′,6-Diamidino-2-phenylindole
DC	Dendritic cell
DD	Death domain
DED	Death effector domain
DISC	Death inducing signaling complex
DKFZ	German cancer research center
DMEM	Dulbecco's modified Eagle's medium
DNA	Desoxyribonucleic acid
E	Early
EDTA	Ethylenediaminetetraacetic acid
EGFP	Enhanced green fluorescent protein
FACS	Fluorescence-activated cell sorter
FADD	Fas-associated death domain
FCS	Fetal calf serum
FITC	Fluorescein isothiocyanate
FLICE	Fas-associated death domain-like interleukin-1-β-converting enzyme
FLIP	FLICE inhibitory protein

gD	Glycoprotein D of HSV-1
gJ	Glycoprotein J of HSV-1
GM-CSF	Granulocyte-macrophage colony-stimulating factor
h	Hour or hours
HaCaT	Human keratinocyte cell line
HeLa	Human cervix carcinoma cell line
HEp-2	HeLa subpopulation cell line
hi-HSV-1	Heat inactivated HSV-1
HRS	Hodgkin/Reed-Sternberg cells
h p. i.	Hours post infection
HSV-1	Herpes simplex virus type 1
HUVEC	Human umbilical vein endothelial cells
Hve	Herpes virus entry mediator
IAP	Inhibitor of apoptosis protein
ICP	Infected cell protein
iDCs	Immature dendritic cells
IB	Immunoblot
IE	Immediate early
IF	Immunofluorescence
IL	Interleukin
IR_L	Internal repeat long of HSV-1 genome
IR_S	Internal repeat short of HSV-1 genome
kbp	Kilo-base pairs
L	Late
LAT	Latency-associated transcript
LATs	Latency-associated transcripts
LPS	Lipopolysaccharide
MACS	Magnetic-activated cell sorting
MG132	Proteasome inhibitor
MHC	Major histocompatibility complex
min	Minutes
MOI	Multiplicity of infection
mRNA	Messenger RNA
NFκB	Nuclear factor kappa-light-chain-enhancer of activated B cells
N-terminus	Amino-terminus of a protein
ORF	Open reading frame
PAMPs	Pathogen-associated molecular patterns
PBMC	Peripheral blood mononuclear cells
PBS	Phosphate buffered saline
PCR	Polymerase chain reaction
PFA	Paraformaldehyde
PI	Propidium iodide
PKR	Protein kinase R
PRRs	Pattern recognition receptors

PVDF	Polyvenylidene difluoride
RNA	Ribonucleic acid
ROS	Reactive oxygen species
RPMI	Roswell Park Memorial Institute medium
RT-PCR	Reverse transcriptase-PCR
s	Seconds
SD	Standard deviation
SDS-PAGE	Sodium dodecyl sulfate polyacrylamide gel electrophoresis
siRNA	Small interfering RNA
TNF	Tumor necrosis factor
TR_L	Terminal repeat long of HSV-1 genome
TR_S	Terminal repeat short of HSV-1 genome
TRAIL	TNF-related apoptosis-inducing ligand
TxR	Texas Red
U_L	Unique long region of HSV-1 genome
U_S	Unique short region of HSV-1 genome
uv-HSV-1	Ultraviolet light inactivated HSV-1
v-FLIP	Viral FLICE inhibitory protein
VP	Virion polypeptide
wt	Wild type

1 Introduction

Virus infections are controlled by powerful and precisely adjusted defense mechanisms of the host. In multicellular organisms, each cell possesses strategies to avert the danger of takeover by a virus. In addition a complex network of specialized cells, the immune system, has evolved to defend the host organism against damage or death due to excessive virus replication. Viruses in turn have acquired means to evade the defense mechanisms of the host in order to maximize their replication and spread within the organism and between individuals.

Herpes simplex virus type 1 (HSV-1) can infect and impair dendritic cells, which play a pivotal role in orchestrating the immune system [23, 97, 114, 115, 133, 143]. This is one of the several immune evasion strategies of HSV-1. In this thesis, crucial mechanisms of the impairment of dendritic cells by HSV-1 are studied.

1.1 Herpes simplex virus type 1 (HSV-1)

HSV-1 is a human herpesvirus. There exists a second serotype, Herpes simplex virus type 2 (HSV-2) [150]. HSV-2 differs from HSV-1 in some aspects, for example the preferred site of infection [120] and sensitivity to antiviral drugs [3, 49]. The experiments presented in this thesis were exclusively conducted with HSV-1.

HSV-1 is distributed worldwide and the human being is the only host. The frequency of seropositive individuals is high, ranging in young adults from 50 % in developed countries to over 80 % in less industrialized countries [142].

1.1.1 HSV-1 infection and disease

HSV-1 infection can occur at different sites of the body. HSV-1 infects skin and mucosa of lips and mouth and less often genital, perigenital, and anal skin. The virus replicates in epithelial cells, resulting in cell lysis and release of mature virus progeny. This can cause primary disease. The released virions can infect sensory nerve endings, which innervate the infected area of the skin. By retrograde transport virions or deenveloped virus particles reach the neuron cell bodies located in the trigeminal ganglia or dorsal root ganglia. There, HSV-1 replicates without destroying the cell and finally establishes a latent state. During latency, the virus does not replicate and no viral proteins are synthesized. HSV-1 can exist latently in neurons for years. Triggers, which are not fully understood, periodically cause the virus to replicate again. Progeny viruses are transported down the axon (anterograde transport) to the epithelial tissues where primary infection took place. Then, HSV-1 infects epithelial cells again and replicates efficiently,

which can result in recurrent disease. Recurrent replication increases the probability of spread of HSV-1 to a new individual [142].

Primary infection and also recurrent replication of HSV-1 often occur without significant symptoms. Symptomatic primary disease (oropharyngeal Herpes) is characterized by sore throat, ulcerative and vesicular lesions, gingivostomatitis and localized lymphadenopathy with fever and malaise. Symptomatic recurrent disease (Herpes labialis) is characterized by a prodrome of pain and itching, which is followed by vesicle formation in the skin of the lips and around the mouth. The vesicles progress to the pustular, ulcerative and crusting stage and finally heal, which is associated with pain. Rare, but severe complications of HSV-1 infection are keratoconjunctivitis, encephalitis, and disseminated infections [142].

Pathology due to replication of HSV-1 is similar for both primary and recurrent infection. The pathologic changes represent a combination of virally mediated cell death and inflammatory immune response. Infected epithelial cells enlarge and loose intact plasma membranes, finally forming multinucleated giant cells. When the cells lyse, clear fluid appears between the epidermis and dermal layer. This vesicular fluid contains large amounts of virus, cell debris, and inflammatory immune cells. In dermal substructures an intense inflammatory immune response is evident. There are also vascular changes in the area of infection, such as perivascular cuffing and some hemorrhagic necrosis. During healing of the vesicle, more inflammatory immune cells are recruited and the vesicular fluid becomes pustular. Finally the vesicle scabs and does usually not leave a scar [142].

Although life-threatening complications of HSV-1 induced disease are rather rare, many people experience frequent recurrent disease, which is painful and incriminating [142]. HSV-1 caused disease is therefore a relevant socio-economic factor.

1.1.2 HSV-1 structure and morphology

HSV-1 is a member of the family *Herpesviridae*, which is defined by certain properties of the virion. The virion of a herpesvirus has a core, which contains the linear double-stranded DNA representing the genome of the virus. The core is surrounded with an icosadeltahedral capsid composed of 162 capsomeres which have a hole running down the long axis. The capsid is approximately 100 to 110 nm in diameter and is surrounded with asymmetric material called tegument. The outer lining of the virus particle is a trilaminar lipid layer, designated envelope, containing viral glycoprotein spikes. The typical appearance of a herpesvirion in electron microscopy is shown in figure 1.1A, while in figure 1.1B the components are schematically depicted. All herpesviruses are characterized by four significant biologic properties: 1) They encode a large array of enzymes involved in DNA synthesis, nucleic acid metabolism and processing of proteins. 2) Viral DNA replication and assembly of the capsid take place in the nucleus. 3) Successful replication of the virus results in destruction of the cell. 4) They are able to remain in their natural hosts in a latent state [142].

The genome of HSV-1 is a linear double-stranded DNA molecule with a length of approximately 150 kbp [16, 33]. It encodes more than 80 open reading frames (ORFs).

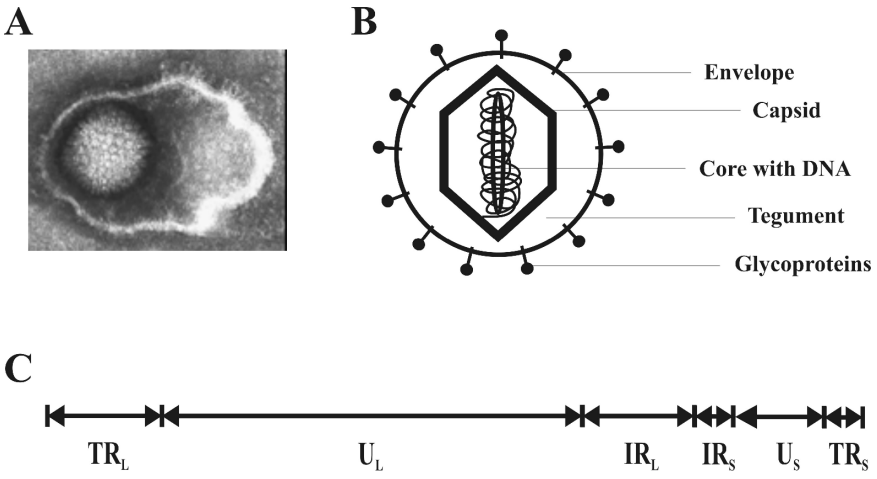

Figure 1.1: **Characteristics of HSV-1. A)** Electron microscopy of a herpesvirion. **B)** Schematic depiction of herpesvirion components. **C)** Schematic depiction of HSV-1 DNA sequence arrangement. The HSV-1 DNA molecule consists of two components, the long (L) region and the short (S) region. Each component consists of a unique sequence (U_L, unique long; U_S, unique short) flanked by inverted repeats (TR_L, terminal repeat long; IR_L, internal repeat long; TRS, terminal repeat short; IRS, internal repeat short). According to references [139, 142].

Therefore, HSV-1 is a rather huge virus, bringing many of the enzymes needed for replication with it. Furthermore it contains numerous genes which play a role in the complex interaction with the host [142].

The genome consists of two components, the long (L) region and the short (S) region. Each component consists of a unique sequence flanked by inverted repeats, as shown in figure 1.1C. Genes located in the unique long region are designated U_L followed by a number indicating the position in the order of genes on that segment, for example U_L54 (infected cell protein (ICP)27 or α27, a regulatory protein). Genes in the unique short region are designated U_S plus number, for example U_S6 (gD, glycoprotein D). Genes located in the inverted repeats of the long region are γ34.5 (ICP34.5, counteracts activation of protein kinase R), α0 (ICP0, a regulatory protein), and the latency-associated transcript (LAT). Only one gene is located in the inverted repeats of the short region, that is α4 (ICP4, a regulatory protein) [139].

1.1.3 Replication of HSV-1

Entry and release of viral DNA

The entry of HSV-1 into a cell occurs in three stages. First, the virion attaches to the surface of the cell by interaction of the viral envelope protein gC with heparan sulfate on the cell. Second, HSV-1 glycoprotein gD in the envelope of the virion binds to one of

several coreceptors on the cell surface. There exist three different types of coreceptors: members of the tumor necrosis factor (TNF) receptor family (*herpes virus entry mediator* A, HveA), coreceptors of the immunoglobulin superfamily (HveB and HveC), and 3-*O*-sulfated heparan sulfate [44]. In addition, HSV-1 envelope glycoprotein gB binds to non-muscle myosin heavy chain IIA (NMHC-IIA), which is expressed in many human cell types [5]. In the third stage, the HSV-1 envelope fuses with the plasma membrane of the host cell and the tegument-coated capsid is released into the cytoplasm [44].

The capsid with associated tegument structures is then transported to the cell nucleus with the help of the microtubular network and dynein. The capsids associate with the nuclear pore complexes and the viral DNA is released into the nucleus, where it rapidly circularizes. Some tegument proteins, for example the virion host shutoff (*vhs*) protein (UL41), are released into the cytoplasm. Other tegument components stay associated with the capsid and some are transported into the nucleus, such as the transcription stimulator VP16/αTIF (U_L48) [142].

Transcription of HSV-1 genes

The transcription of viral genes takes place in the nucleus, mediated by host RNA polymerase II. Several viral gene products may be involved, which modify the activity and structure of RNA polymerase II. Expression of viral genes occurs sequentially in a tightly regulated cascade. Very soon after infection (2-4 h post infection with MOI 10 - 20), VP16/αTIF (U_L48) stimulates the expression of the first virus genes, the immediate early (IE) or α genes. These include α4 (ICP4), α0 (ICP0), U_L54 (ICP27), U_S1 (ICP22), U_S12 (ICP47), and $U_S1.5$. All IE proteins, except ICP47, are regulatory proteins important for proper expression of the following temporal classes of HSV-1 genes [142]. ICP47 is involved in immune evasion of HSV-1 by blocking antigen presentation to T cells [185].

The next (4-8 h post infection) viral genes expressed are the early (E) or β genes. They require at least the transactivating function of the immediate early protein ICP4 but not the onset of viral DNA synthesis. Almost all early genes encode proteins which are involved in nucleotide metabolism and DNA replication. Prominent examples are U_L23 (thymidine kinase), U_L39 (ICP6, large subunit of ribonucleotide reductase), U_L50 (dUTPase), and U_L30 (DNA polymerase) [142].

As soon as the early genes are expressed, viral DNA replication takes place. The expression of the third temporal class of HSV-1 genes, the leaky late or γ_1 genes, starts at low levels before viral DNA replication begins, but is strongly enhanced thereafter. In contrast, expression of the last set of HSV-1 genes, the true late or γ_2 genes, is strictly dependent on viral DNA replication [142]. γ_2 genes are not expressed in the presence of inhibitors of viral DNA synthesis, for example aciclovir (ACV) [36]. Many late (L) HSV-1 genes represent virion components, for example U_S2 (tegument protein [142]) or mediate interaction with the host, like $\gamma_1$34.5 (ICP34.5, precludes shutoff of protein synthesis by activated PKR [60]), and U_S3 (protein kinase [39], blocks apoptosis [103]).

Expression of some early and most late HSV-1 genes is dependent on the immediate early protein ICP27 [146]. Therefore, it represents one of the two essential IE pro-

teins, besides ICP4. While ICP4 exerts its effect directly at the transcriptional level [47], ICP27 can act at both the transcriptional and posttranscriptional level. ICP27 appears to modulate virtually every aspect of mRNA metabolism, including primary transcription, polyadenylation, nuclear export of intronless mRNA, splicing, and mRNA stability and translation. At early times post infection, ICP27 is predominantly found in the nucleus. However, after 4 h post infection, ICP27 starts to shuttle between the nucleus and the cytoplasm. This is essential for nuclear export and translation of most late HSV-1 transcripts [146].

DNA replication, virion assembly, and egress

Replication of HSV-1 DNA takes place in the nucleus of the host cell. The new DNA is synthesized by a rolling-circle mechanism. The resulting concatemers are cleaved into monomers during assembly of nucleocapsids. The mature, DNA containing capsids bud through the inner lamella of the nuclear membrane. During this process, the tegument and a first version of the envelope are acquired. The virion is then transported through the trans-Golgi network, where the envelope obtains its final composition and posttranslational modifications of the glycoproteins occur. Viral glycoproteins, for example gD, do not only accumulate in intracellular membranes, but also in the plasma membrane of the cell. This can be used to detect infected cells by staining with gD-specific antibodies. HSV-1 virions are finally released from the cell through secretory vesicles [142].

HSV-1 microarray

Wagner and his co-workers have developed a HSV-1 microarray which allows a global monitoring of HSV-1 gene expression [158, 177]. This technique makes it possible to analyze the complex HSV-1 transcription program under various conditions of infection and in different cell types. Differences in the expression of viral genes observed with the microarray yield new indications about the function and importance of the respective HSV-1 genes in the biological processes examined. This is of high value, as the function of several HSV-1 genes is still not known or only poorly defined.

The procedure of HSV-1 microarray analysis is similar to the technique of microarray analyzes already established and widely used for human or microbe gene expression. For the HSV-1 microarray analysis, 52 oligonucleotide probes which are complementary to specific HSV-1 sequences are spotted on glass slides. Total RNA is isolated from infected cells or tissues and oligo-dT-primed cDNA is synthesized, which is tagged with a fluorescent dye. The cDNA is hybridized with the probes on the glass slide and after washing away unbound cDNA, the fluorescence signal is detected with a laser-based imaging device. The presence of a signal indicates that the respective HSV-1 gene is expressed at the selected time point post infection and under the conditions of the conducted experiment. The intensity of the fluorescence signal correlates with the amount of transcripts present in the cell [158, 177].

Because the isolation of mRNA and the generation of cDNA is achieved using the poly(A) tail, the selection of sequences for the oligonucleotide probes is restricted to the 52 polyadenylation sites known within the genome of HSV-1. Oligonucleotide probe sequences are located immediately adjacent to the polyadenylation sites because incorporation of the fluorescence tags into cDNA is not highly efficient, resulting in cDNA lengths of only 3-400 nucleotides. Only a bit more than one half of the total viral transcripts are terminated with a unique polyadenylation site and can therefore be uniquely specified. The remaining HSV-1 genes belong to coterminal transcript families and the signal obtained with the microarray can not distinguish between the different transcripts. This weakens the utility of the HSV-1 microarray [158, 177].

The HSV-1 microarray was successfully used in different experimental settings and revealed interesting new aspects of HSV-1 biology. For example it could be shown that the efficient export of the majority of viral transcripts does require the RNA and TAP/NXF1 binding activity of ICP27 [79] and that the viral transcriptional program is not disturbed after inhibition of stress-activated kinase p38 [83].

1.1.4 HSV-1 latency

The host-virus interaction of HSV-1 is predominated by establishment and maintenance of latency rather than occurrence of disease [142]. The virus invades the host in order to stay and replicate from time to time without causing severe damage. Thereby, the virus ensures efficient spread among individuals.

HSV-1 establishes latency in the nucleus of the sensory nerves innervating the skin area of primary infection. The HSV-1 genome in latently infected neurons displays the characteristics of endless or circular DNA. However, virus replication is not detected. No viral function is absolutely required for the establishment of latency. The current hypothesis assumes that latency is automatically established if the initial, sustained expression of α genes is missing. Expression of α genes is lacking in neuronal cells because of several reasons, including absence of trans-activating host factors in the nucleus and hormonally regulated repression of viral gene expression [142].

During maintenance of latency almost no viral gene expression is detectable. The only transcripts which are abundantly expressed in latently infected neurons are the latency-associated transcripts (LATs) [139, 176]. LATs presumably promote latent infection by repression of lytic gene expression and protection of the latently infected neurons from apoptosis [129, 152].

Reactivation of latent HSV-1 occurs after local or systemic stimuli. Injury or stimulation of cells in the tissue innervated by the latently infected dorsal root neuron can trigger reactivation. Systemic triggers are physical or emotional stress, hyperthermia, exposure to UV light, and hormonal imbalance. No single viral gene is responsible for HSV-1 reactivation. Rather, a joint action of several HSV-1 genes is necessary. After injury of neurons, the cellular transcription factors *oct-1*, c-*jun*, and c-*fos-1* rapidly increase. They might play a role in triggering of reactivation, because the promoters of the viral transactivator ICP0 and the viral repressor LAT contain binding sites for these

factors. Presumably, the balance between ICP0 and LAT expression regulates reactivation [142].

Latency-associated transcripts

LATs are the only HSV-1 transcripts abundantly expressed during latency. The coding region for LATs is located in the inverted repeats of the long region of the HSV-1 genome. The primary transcript is 8.5 kb in length and polyadenylated. It is hardly detectable in latently infected neurons. Splicing of the primary transcript yields a circularized 2 kb stable intron, which is not capped or polyadenylated and represents the major LAT transcript during latency. The remaining 6.5 kb LAT molecule is unstable and usually not detectable. The 2 kb stable LAT can be spliced further to yield a 1.5 kb intron [139, 176].

LATs are also expressed during lytic infection. Transcripts of 1.6, 2, and 8.5 kb length can be detected in lytically infected cells. In contrast to latently infected cells, all LATs found in lytically infected cells are polyadenylated. The expression of lytic LATs might be regulated by a different promoter and occurs late during HSV-1 infection [28, 32].

Although open reading frames have been identified within the LAT sequence, no corresponding protein has been found up to now. It must be assumed that the functions of LATs are executed by the RNA itself. Recent studies have identified small RNAs [152] and microRNAs [170] in the LAT region, which influence viral gene expression and apoptosis.

The expression of LATs significantly enhances the latency-reactivation cycle in small animal models. Spontaneous reactivation in rabbits and induced reactivation in mice is severely impaired, though not completely abrogated, after infection with LAT deletion mutants of HSV-1 [129]. The function important for wild-type reactivation of HSV-1 is located within the first 1.5 kb of the LAT coding sequence. This part of the sequence includes the first 837 nucleotides of the stable intron detected in latently infected neurons [130]. The most important function of LATs during the latency-reactivation cycle appears to be inhibition of apoptosis. The antiapoptotic function of LATs is described in detail in section 1.2.5.

1.1.5 Impact of HSV-1 infection on the host cell

The infection of cells with HSV-1 results in fundamental structural and biochemical changes, designated as “cytopathic effect" (CPE), that ultimately lead to cell death. These changes are caused by irreparable injury due to virus replication and by cellular responses to infection [142].

Structural changes observed after HSV-1 infection are detachment and rounding up of the cells, disaggregation of the nucleolus, distortion of the nucleus, formation of intranuclear inclusion bodies, duplication and folding of intracellular membranes as well as fragmentation and dispersal of Golgi stacks [142].

HSV-1 also fundamentally alters the metabolism of the host cell. Cellular processes are shut off or redirected in order to serve the successful replication of the virus. Host

protein synthesis is inhibited in a multiphase process. The first phase of this shutoff is mediated by the HSV-1 virion host shutoff *vhs* protein, encoded by ORF UL41. *vhs* causes disintegration of cellular polyribosomes and degradation of present host mRNA [98, 126]. The second phase of shutoff requires the HSV-1 immediate early protein ICP27 and reduces the remaining amount of host protein synthesis by inhibition of pre-mRNA splicing [56, 57]. In addition to inhibition of protein synthesis, selected cellular proteins are degraded or destabilized and the function of many host proteins is altered in order to perform virus specific tasks [142].

Finally, after virus replication is completed, infected cells die. Death of cells after infection with wild-type HSV-1 is considered to be a form of necrosis [123, 142]. However, if synthesis of viral proteins is blocked after wild-type HSV-1 infection or if cells are infected with a mutant of HSV-1 which is impaired in expression of post-α genes, infected cells undergo apoptosis [7, 8, 92]. From these observations it was concluded that the cell recognizes infection with HSV-1 and induces apoptosis in order to block virus replication. However, viral proteins synthesized during infection with HSV-1 are able to prevent the induced apoptosis from taking place, thereby keeping the cells alive until the virus has completed its replication.

1.2 Apoptosis

In contrast to necrosis, which is a pathological uncontrolled form of cell death, apoptosis represents a tightly controlled physiological process. Necrosis is accompanied by the leakage of cell components out of the cell, which is a strong inflammation inducing signal. In contrast, the remnants of apoptotic cells are taken up by phagocytes without inducing inflammation [100].

Apoptosis is characterized by specific morphological and biochemical changes in the cell. The cells round up, loose cell-cell contacts, and shrink. Because cell junctions are disintegrated, the plasma membrane becomes convoluted and forms the typical apoptotic blebs. Finally the cell breaks up into membrane spheres of various sizes containing packaged cellular contents. These characteristic spheres are called apoptotic bodies. During the process of apoptosis the asymmetry of the plasma membrane breaks down and lipids which are normally only found on the inner side of the membrane are exposed to the outer side. One of these lipids, phosphatidylserine, is recognized by phagocytes which take up the apoptotic bodies. Furthermore, the nucleus is fragmented after chromatin condensation and aggregation. The nuclear fragments are also packed into apoptotic bodies. The DNA is cleaved between nucleosomes by endonucleases leading to DNA fragments, which are multiples of 180 bp in length [100].

Apoptosis is important for the maintenance of multicellular organisms. In order to adjust the number of cells contained in a certain tissue, the surplus of cells must be eliminated [100]. Apoptosis is also used as a defense mechanism. By sacrificing transformed or infected cells the organism as a total is saved from death due to cancer or excessive replication of a pathogen [124].

1.2.1 Pathways of apoptosis induction and regulation

Apoptosis can be induced either via signals originating from outside the cell (extrinsic pathway) or from inside the cell (intrinsic pathway). Basic apoptosis signaling events are depicted in figure 1.2. Extrinsic signals are the so called death ligands, which induce apoptosis by binding to the respective death receptors. Death ligands known up to now are Fas ligand (Fas L or CD95L), tumor necrosis factor α (TNF-α), and TNF-related apoptosis inducing ligand (TRAIL). The intrinsic pathway of induction of apoptosis can be activated by a variety of stress events, for example oxidative stress, treatment with cytotoxic drugs, or virus infection [151].

Regardless of the pathway of induction of apoptosis, the apoptosis inducing signal is transduced within the cell via a cascade of cysteine aspartate proteases, called caspases. The cytoplasmic part of a death receptor, such as Fas (CD95), contains a protein-protein interaction domain called the death domain (DD). Upon activation of Fas the adapter molecule FADD (Fas-associated death domain) is recruited to the death receptor via the DD. The DD of FADD is located at the carboxyl terminus. At the amino terminus, FADD contains a second protein-protein interaction motif, the death-effector domain (DED). Procaspase-8 can bind to the DED of FADD, because it also contains two DED in its amino terminus. The complex of Fas ligand, Fas, FADD, and procaspase-8 is called death inducing signaling complex (DISC). Procaspases possess only limited catalytic activity. However, when two procaspase molecules come into close proximity in the DISC, they cleave each other to form the active homodimer. Activation of the intrinsic pathway results in the release of cytochrome *c* from the mitochondria into the cytosol. Cytochrom *c* triggers forming of the apoptosome, composed of each seven molecules of cytochrome *c*, Apaf-1 (apoptosis protease-activating factor-1), (d)ATP, and procaspase-9. This results in formation of active caspase-9 [151].

The above mentioned caspases 8 and 9 represent initiator caspases. Though activated through different pathways, they all have the same substrate, procaspase-3. Cleavage of procaspase-3 by one of the initiator caspases results in active caspase-3, which is the executioner caspase. Caspase-3 cleaves molecules like ICAD (inhibitor caspase-activated desoxyribonuclease), which leads to activation of CAD (caspase-activated desoxyribonuclease). This mediates the morphological and biochemical changes associated with apoptosis, for example fragmentation of DNA [151].

Induction of apoptosis must be tightly regulated in order to avoid excessive cell death. At several checkpoints in the apoptosis signaling network, antiapoptotic proteins counter-regulate proapoptotic signals. For example, inhibitor of apoptosis proteins (IAPs) can directly bind and inactivate caspases and thereby block apoptosis [20]. Induction of apoptosis via the intrinsic pathway is regulated by the complex interaction of proapoptotic (Bax, Bak, Bad, tBid) and antiapoptotic (Bcl-2, Bcl-xL) members of the B-cell lymphoma-2 (Bcl-2) family of proteins [1]. FLICE (Fas-associated death domain-like interleukin-1-β-converting enzyme) inhibitory protein (FLIP) is a caspase homolog and can therefore bind to the DISC and interfere with binding and activation of initiator caspases. FLIP is therefore able to block the extrinsic pathway of apoptosis induction [66, 96, 148, 169].

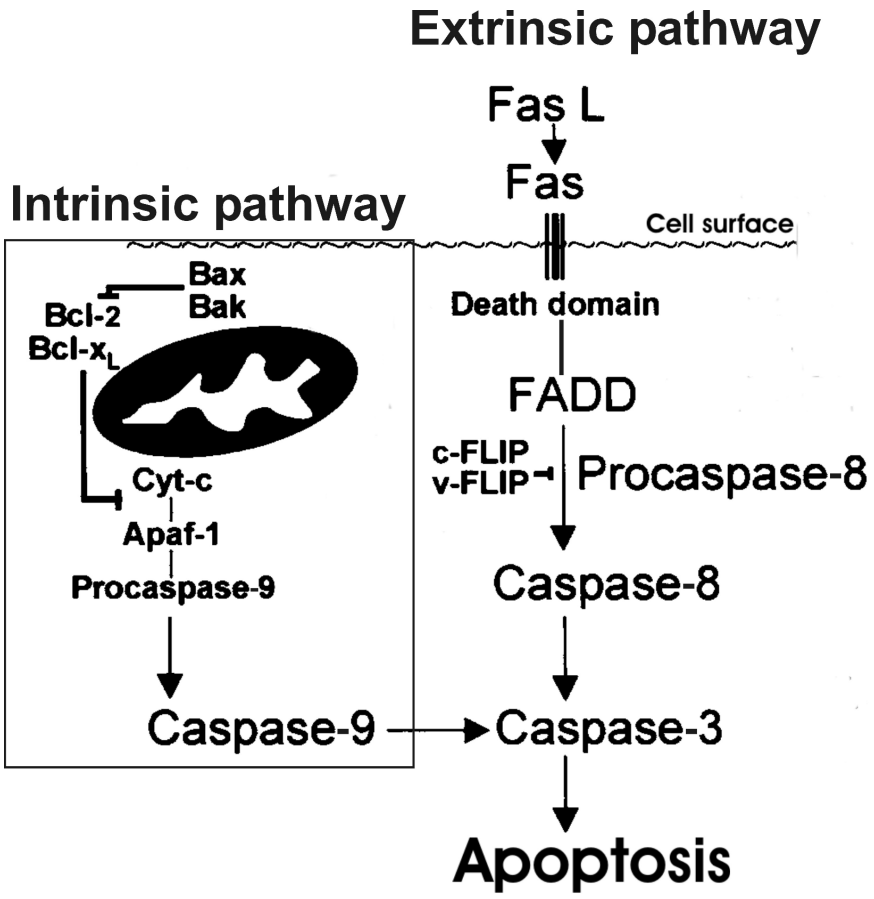

Figure 1.2: **Intrinsic and extrinsic pathways of apoptosis induction.** The extrinsic pathway is induced by binding of death ligands such as Fas ligand (Fas L) to death receptors, for example Fas (CD95). Adapter molecules, in this case FADD (Fas-associated death domain), and procaspase-8 are then recruited via death domains to the cytoplasmic part of the receptor. Aggregated procaspase-8 molecules can cleave each other to form active caspase-8 (FLICE). In the intrinsic pathway of apoptosis induction, cytochrom *c* (Cyt-c) is released from permeabilized mitochondria. Cyt-c, Apaf-1 (apoptosis protease-activating factor-1), (d)ATP, and procaspase-9 form the apoptosome, which enables activation of caspase-9. The initiator caspases 8 and 9 then cleave and activate procaspase-3. Cleavage of caspase-3 substrates ultimately leads to apoptosis. Activation of caspase-8 can be blocked by FLIPs (c-FLIP, cellular FLICE inhibitory protein; v-FLIP, viral FLICE inhibitory protein). Permeabiliziation of mitochondria is regulated by interaction of proapoptotic (Bax, Bak) and antiapoptotic (Bcl-2, Bcl-xL) members of the B-cell lymphoma-2 (Bcl-2) family of proteins. Taken from reference [151], modified.

There are connections between the intrinsic and the extrinsic pathway of apoptosis induction. For example, a signal induced by the extrinsic pathway can be amplified through cleavage of the Bcl-2 family member Bid to proapoptotic tBid by caspase-8, which leads to release of cytochrome *c* from mitochondria [151]. Furthermore, factors released from the mitochondria can modulate the extrinsic pathway, as is the case for Smac/Diablo, which inhibits IAPs and thereby enhances caspase activity.

1.2.2 FLIP

FLIP is a homolog of procaspase-8. The first FLIP molecules found were encoded by viruses and therefore called v-FLIP [165]. In human cells, several splice variants of c-FLIP (cellular FLIP) mRNA have been described, but in most cells only two proteins are expressed: c-FLIP$_L$ and c-FLIP$_S$. The long isoform c-FLIP$_L$ has a domain structure similar to procaspase-8, two DED's in the amino terminus and a caspase like domain in the carboxyl terminus. However, c-FLIP$_L$ is catalytically inactive, because it lacks the conserved cysteine residue of caspases [66]. However, c-FLIP$_L$ can itself be cleaved by caspases at Asp376 to yield c-FLIP(p43) and c-FLIP(p12) [148]. c-FLIP$_S$ consists only of the two death effector domains followed by a short unique carboxyl terminus [66]. c-FLIP$_R$, a third isoform with a structure similar to c-FLIP$_S$, is only found in some cell types of haematopoetic origin [48].

Because of the DEDs, c-FLIP molecules can be incorporated into the DISC (figure 1.3). In the absence of c-FLIP, procaspase-8 aggregates in the DISC and is cleaved and activated. If a sufficient amount of c-FLIP is present in the cell, it can successfully compete with recruitment of procaspase-8 to the DISC. Thereby it can prevent aggregation and activation of procaspase-8 and apoptosis is blocked [66, 96, 148, 169]. Mathematical modeling revealed that the amount of c-FLIP can function as a switch in the decision whether apoptosis takes place or not after stimulation of death receptors [19, 55].

For c-FLIP$_S$ and c-FLIP$_R$ the prevention of activation of procaspase-8 by binding to the DISC is the only mode of action and therefore these two isoforms are exclusively antiapoptotic. c-FLIP$_L$ has more diverse functions. First it has been shown that c-FLIP$_L$ can even promote apoptosis when expressed in low amounts, possibly because the c-FLIP$_L$/caspase-8 heterodimer is also an active protease with comparable activity and specificity as the caspase-8 homodimer. When present in higher amounts, it has been shown that c-FLIP$_L$ can not only efficiently block apoptosis, but its cleavage products can activate the NFκB (Nuclear factor kappa-light-chain-enhancer of activated B cells), ERK (extracellular signal-regulated kinase), and Wnt (wingless type) signaling pathways. Thereby, c-FLIP$_L$ can divert Fas-mediated death signals into signals that lead to proliferation or differentiation of the cell [85].

Transcription of c-FLIP is induced after activation of ERK, PI3K(phosphatidylinositol 3-kinase)-Akt, NFκB [93, 111], NFAT (Nuclear factor of activated T cells), and p53 signaling pathways. In contrast, signaling via c-Myc (myelocytomatosis oncogene cellular homolog) represses c-FLIP mRNA expression. Also signaling through STAT (Signal transducers and activators of transcription) members was shown to regulate c-FLIP expression, either negatively (STAT5) or positively (STAT3) [84].

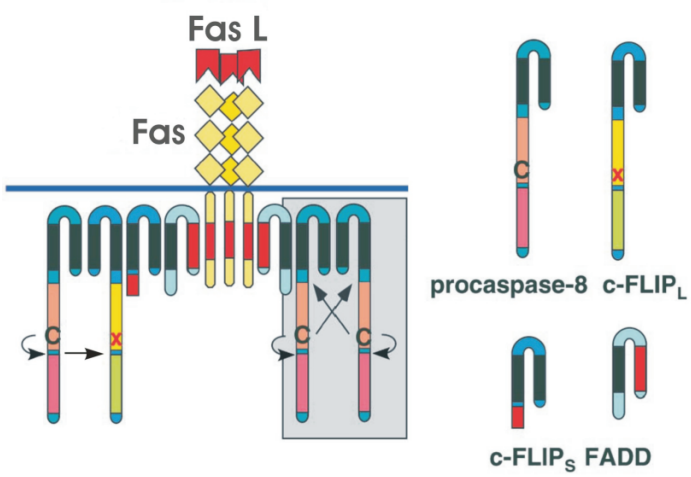

Figure 1.3: **Binding of c-FLIP to the DISC and prevention of procaspase-8 cleavage.** Upon binding of Fas ligand (Fas L) to its receptor (Fas, CD95) several molecules, including FADD (Fas-associated death domain), procaspase-8, c-FLIP$_L$, and c-FLIP$_S$ are recruited to the cytoplasmatic tail of Fas and form the death inducing signaling complex (DISC). If no or little FLIP is present (right part of the figure, on gray background), procaspase-8 can aggregate and cleave itself to form the active caspase-8 homodimer which promotes apoptosis. Presence of high amounts of the catalytically inactive caspase homologs c-FLIP$_S$ or c-FLIP$_L$ (left part of the figure) block procaspase-8 aggregation and cleavage and apoptosis is prevented. However, c-FLIP$_L$ can be cleaved by procaspase-8 to yield c-FLIP(p43) and c-FLIP(p12). These c-FLIP$_L$ cleavage products promote cell survival. The catalytically active site within procaspase-8 is indicated with “C". In c-FLIP$_L$, this site is mutated and catalytically inactive, indicated by “X". Taken from reference [96], modified.

The amount of c-FLIP in the cell is determined not only by the number of mRNAs expressed, but also by posttranslational regulation of protein stability. c-FLIP isoforms are short-lived proteins, which are ubiquitinylated and degraded by the proteasome [41, 89, 128]. The unique carboxyl terminus of c-FLIP$_S$ contains a destabilizing sequence which enhances its ubiquitinylation and proteasomal degradation. Therefore, c-FLIP$_S$ has a shorter half-life compared to c-FLIP$_L$ [135].

Furthermore, c-FLIP can be phosphorylated by different kinases, such as protein kinase C (PKC) [64, 86], p38α [168], and Calcium/Calmodulin-dependent protein kinase II [184]. The phosphorylation status of c-FLIP not only regulates its stability, but also its recruitment to the DISC.

Several soluble factors and small molecules directly or indirectly modulate the c-FLIP amount, for example bacterial lipopolysaccharide (LPS), CD40L, reactive oxygen species (ROS), cycloheximide, and proteasome inhibitors (MG132) [84, 90, 101].

Ishioka *et al.* observed that c-FLIP$_L$ forms aggregates when overexpressed in cells

[67]. These aggregates block the ubiquitine-proteasome system and are therefore resistant to proteasomal turnover. Ishioka *et al.* generated mutants of c-FLIP$_L$ and analyzed their distribution in transfected cells and their ability to block the ubiquitine-proteasome system (figure 1.4).

Wild type c-FLIP$_L$ and the mutant c-FLIP$_L$ D376A form dense aggregates in the perinuclear region and block the ubiquitine-proteasome system. The mutant with a truncated C-terminus (c-FLIP$_L$ 1-438) still blocks the ubiquitine-proteasome system and forms aggregates, however these aggregates are more evenly distributed within the cell. c-FLIP$_L$ 1-202 also aggregates, but in a more filamentous pattern and is not able to block the ubiquitine-proteasome system. Only the two mutants with removed or mutated DEDs (c-FLIP$_L$ 203-480 and c-FLIP$_L$ F23G/F114G) display a homogeneous distribution in the transfected cells and are not able to block the ubiquitine-proteasome system. Taken together, DEDs cause aggregation of overexpressed c-FLIP$_L$. Aggregated c-FLIP$_L$ is resistant to proteasomal turnover. If DEDs are mutated, overexpressed c-FLIP$_L$ does not aggregate and is susceptible to turnover by the proteasome.

1.2.3 Detection of apoptosis

A variety of methods has been established to determine whether cells undergo apoptosis (reviewed in reference [151]). It is possible to detect the activation of the apoptosis signaling pathways as well as the resulting biochemical and morphological changes.

The activation of caspases can be shown using fluorigenic substrates. Cleavage of procaspases and of specific substrates of caspase-3 (for example the DNA repair enzyme poly(ADP-ribose)polymerase, PARP) can be assessed by immunoblot analysis. Permeabilization of the outer mitochondrial membrane is indicated by a shift in the emission spectra of the fluoresce substance JC-1, which accumulates in mitochondria after addition to cells.

The characteristic cleavage of DNA can be visualized after isolation of DNA from cells and subsequent separation in agarose gels, thereby revealing the “laddering" of the DNA in apoptotic cells. Double strand breaks resulting from DNA cleavage can be marked with FITC-conjugated dUTP using terminal desoxynucleotidyl transferase (terminal desoxynucleotidyl transferase nick end-labeling, TUNEL). The condensation of chromatin and the fragmentation of the nucleus in apoptotic cells can be proved by staining with DAPI and subsequent microscopic examination.

Loss of membrane assymetry during apoptosis is accompanied with exposure of phosphatidylserine to the outer side of the cell. FITC labeled AnnexinV binds specifically to phosphatidylserine and thereby apoptotic cells can be detected by flow cytometry. This method allows detection of apoptosis of single cells at early times after induction of apoptosis, because exposure of phosphatidylserine occurs very soon after activation of caspases [155]. But, if the plasma membrane is disintegrated, AnnexinV can reach the inner side of the cell and bind to phosphatidylserine on the inner side of the plasma membrane. Therefore, cells with permeabilized plasma membrane (necrotic cells or cells at the late stage of apoptosis) must be excluded by staining with propidium iodide.

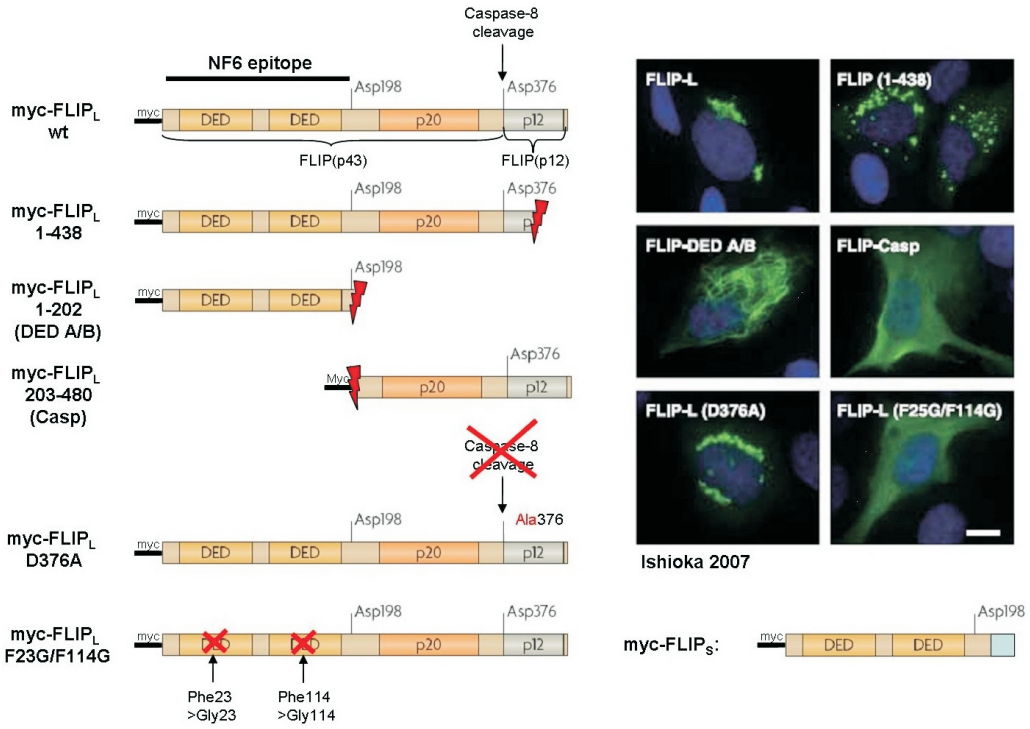

Figure 1.4: **Aggregation of mutated c-FLIP$_L$ overexpressed in cells [67].** On the left side, wild type and mutated forms of c-FLIP$_L$ are schematically depicted. c-FLIP$_L$ consists of two death effector domains (DED) at the N-terminus and a caspase-like domain at the C-terminus, composed of the p20 and p12 subdomains. c-FLIP$_S$ is lacking the caspase-like domain and has a unique C-terminus. c-FLIP$_L$ can be cleaved by caspase-8 at Asp376 into two parts (p43 and p12). c-FLIP$_L$ can homodimerize or heterodimerize with caspase-8. This dimerization is mediated by the DED's. Mutation of Phe23 and Phe114 abrogates the ability of c-FLIP$_L$ to form dimers. On the right side, microscopic examination of transfected HT-1080 cells shows the cellular localization of c-FLIP$_L$ mutants after immunostaining with anti-myc antibody as published by Ishioka *et al.* By accident, c-FLIP$_L$ F23G/F114G was assigned c-FLIP$_L$ F25G/F114G in the publication by Ishioka *et al.* Wild type c-FLIP$_L$ and the mutants c-FLIP$_L$ D376A and c-FLIP$_L$ 1-438 form dense aggregates in the perinuclear region and block the ubiquitine-proteasome system. c-FLIP$_L$ 1-202 aggregates in a more filamentous pattern and is not able to block the ubiquitine-proteasome system. Only the two mutants with removed or mutated DEDs (c-FLIP$_L$ 203-480 and c-FLIP$_L$ F23G/F114G) display a homogeneous distribution in the transfected cells and are not able to block the ubiquitine-proteasome system. The different expression plasmids encoding mutated c-FLIP$_L$ molecules were generated by Ishioka *et al.* The plasmid encoding c-FLIP$_S$ was provided by Krueger *et al.* [96] and is shown in the lower right part of the figure. All c-FLIP molecules are tagged on their N-terminus with the myc-sequence. The epitope of the anti-FLIP antibody (clone NF6) used in immunoblot analysis is indicated.

1.2.4 Modulation of apoptosis by viruses

Apoptosis is an important response of cells to infection by viruses, because sacrifice of some infected cells can save the organism. However, viruses have evolved numerous strategies to counteract apoptosis of the host cell in order to ensure successful replication or maintenance of latency.

The counteracting strategies of viruses target different parts of the apoptosis signaling pathway. The receptors for Fas ligand and TRAIL are cleared from the surface and subsequently degraded by the receptor internalization and degradation complex (RID or E3-10.4/14.5 K) of adenovirus [105]. Downstream signaling of death receptors is blocked by viral homologs of FLIP (v-FLIP) encoded for example by Kaposi's sarcoma-associated herpesvirus (KSHV) and the poxvirus Molluscum contagiosum [165]. Viral Bcl-2 homologs, for example BHRF1 of Epstein-Barr virus (EBV) [63] and E1B 19K of adenovirus [29], block apoptosis signaling via the intrinsic pathway. Murine cytomegalovirus m38.5 protein, which localizes to mitochondria, is another viral inhibitor of intrinsically induced apoptosis [82]. Also caspases can directly or indirectly be inhibited by viral proteins, as it is the case for CrmA of Cowpox virus [190] and IAP of baculovirus [20]. The proapoptotic function of p53 is targeted by many viruses, for example by the E6 protein of Human papillomavirus, the SV40 large T antigen and EBV BZLF1 [124].

However, some viruses also actively induce apoptosis and caspase activation [124]. For example, induction of apoptosis is essential for release of influenza virus progeny [183]. In the case of Aleutian mink disease parvovirus (ADV), cleavage of the essential major nonstructural protein NS1 by effector caspases is essential for its localization to sites of replication. Therefore, blockage of apoptosis or caspase activation results in decreased replication of ADV [20].

1.2.5 Modulation of apoptosis by HSV-1

Apoptosis is induced soon after HSV-1 infection. Expression of mRNA of one immediate early HSV-1 gene, $\alpha 0$, is the crucial proapoptotic event for induction of apoptosis by HSV-1 [25, 145, 147]. This is supported by the fact, that *de novo* protein synthesis is not required for HSV-1 induced apoptosis.

However, wild type HSV-1 infection does not result in apoptosis of epithelial cells, which represent the main host cells for productive replication of HSV-1. This is because during 3 h and 6 h post infection effective antiapoptotic events occur (Figure 1.5A) [123]. This time period is called "apoptosis prevention window" and is characterized by expression of viral proteins, which efficiently block apoptosis [8, 92]. Dependent on the cell type, infection with HSV-1 also confers resistance against apoptosis induced by many agents, including sorbitol, staurosporine, and Fas ligand [8, 43]. Protection of the host cell against apoptosis ensures efficient replication of HSV-1. However, HSV-1 replication finally results in destruction and death of the infected cells. This is considered to be a kind of necrotic cell death due to exhaustion of the cell.

Up to now, several antiapoptotic HSV-1 genes have been identified. Three of them

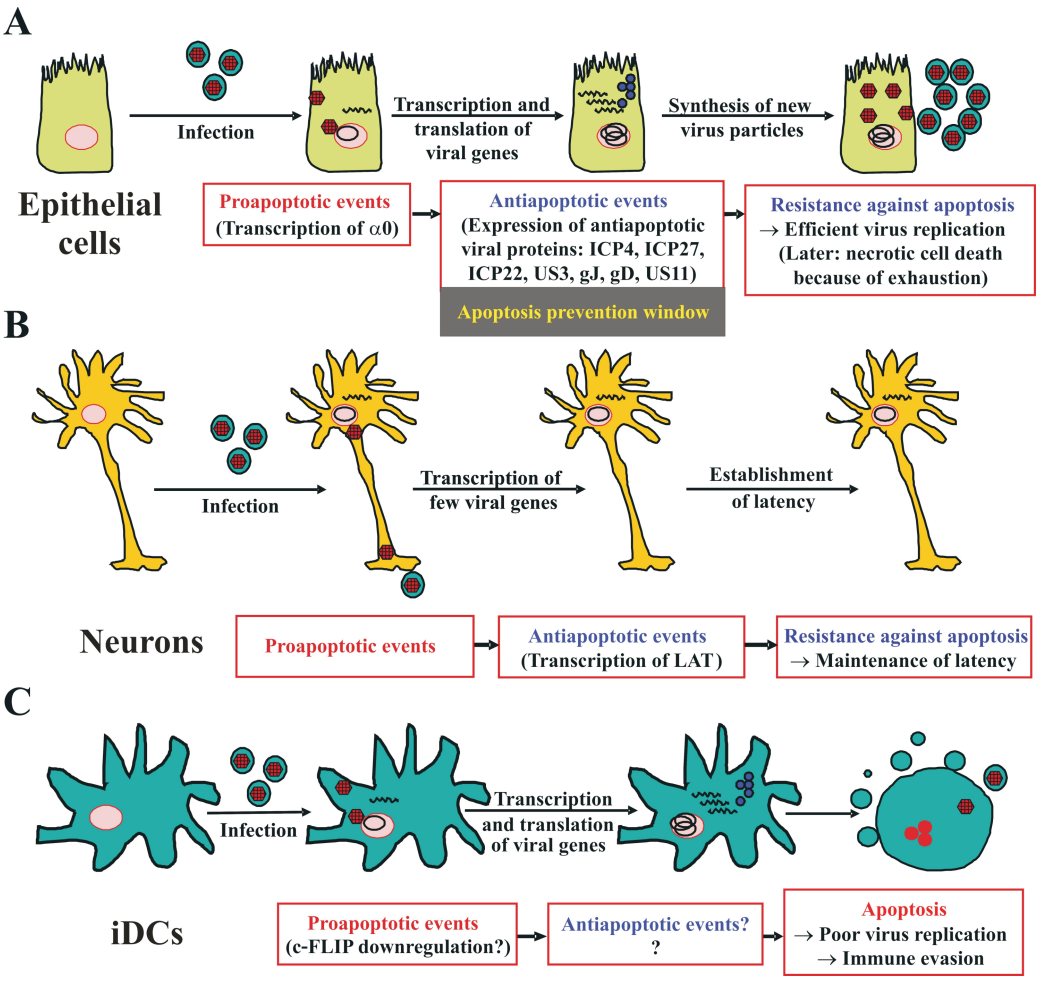

Figure 1.5: **Modulation of apoptosis by HSV-1 in different cell types.** HSV-1 induces apoptosis early after infection. However, in most cell types, like epithelial cells **(A)** and neurons **(B)**, execution of apoptosis is blocked by antiapoptotic viral factors [123]. Consequently, these cells survive and ensure successful virus replication or maintenance of latency. In lytically infected epithelial cells, antiapoptotic proteins are expressed during an apoptosis prevention window between 3 and 6 h after infection. In contrast, HSV-1 infected immature dendritic cells (iDCs) undergo apoptosis and virus replication is low **(C)** [23, 115, 133]. Although downregulation of the cellular antiapoptotic molecule c-FLIP was observed in HSV-1 infected iDCs, it is not known, whether this contributes to apoptosis. The question arises, why the strong antiapoptotic factors of HSV-1 fail to block apoptosis in iDCs.

encode immediate early proteins: ICP4, ICP22, and ICP27. Increased apoptosis is observed in cells infected with HSV-1 mutants lacking one of these proteins [7, 8, 102]. The involvement of ICP4, ICP22, and ICP27 in prevention of apoptosis is likely indirect, because they are essential for proper expression of early and late genes [142], including antiapoptotic genes.

U_S3 codes for a late expressed viral protein kinase with antiapoptotic activity [72, 103]. It has been shown by Benetti and Roizman [17] that U_S3 promotes cell survival by acting like cellular protein kinase A. Furthermore, U_S3 posttranslationally modifies the proapoptotic Bcl-2 protein family member Bad and thereby blocks its activation [26, 119, 118]. Besides that, U_S3 phosphorylates procaspase-3 and prevents its proteolytic cleavage [18].

U_S5 encodes the viral glycoprotein gJ, which is expressed late during infection [142]. Many studies demonstrated its involvement in prevention of HSV-1 induced apoptosis and it was shown that it has a protective effect against apoptosis induced by the effector molecules of cytotoxic T-cells, granzyme B and perforin, when expressed alone [72, 73, 188]. gJ induces formation of reactive oxygen species (ROS) [10], however it is not clear whether this contributes to prevention of apoptosis.

U_S6 encodes the late expressed viral glycoprotein gD. gD possesses antiapoptotic activity, which is separated from its involvement in receptor binding and membrane fusion of the virus particle [188, 187, 189]. The mechanism of apoptosis inhibition by gD remains elusive.

U_S11 encodes a dsRNA binding protein of HSV-1 [6], which is expressed late during infection. Many studies have demonstrated its role in the viral response against host cell defense. Amongst others, U_S11 interferes with the cellular interferon-inducible antiviral response by efficiently inhibiting activation of protein kinase R (PKR) [27, 87]. The diverse effects of PKR activation include activation of the FADD/caspase-8 apoptosis inducing pathway [11]. Furthermore, U_S11 has a direct antiapoptotic function at the level of mitochondrial apoptosis signaling pathways or upstream [70].

LATs also possess antiapoptotic activity [2, 24, 65, 74, 131]. LATs can block apoptosis induced by the extrinsic pathway as well as by the intrinsic pathway [62]. Expression of LATs promotes survival of neurons in infected rabbits and mice [2, 24, 131] and reduces apoptosis during lytic infection of tissue culture cells [2, 75]. Furthermore, LAT alone protects from apoptosis when ectopically overexpressed [2, 65, 74, 131]. Protection of latently infected neurons against apoptosis might be the main function of LATs in the latency-reactivation cycle of HSV-1 (figure Figure 1.5B). This is indicated by the fact that overexpression of other antiapoptotic factors like c-FLIP [77], baculovirus IAP [76] and bovine herpesvirus LAT homolog [117] can rescue the wild-type reactivation phenotype of LAT deletion mutants of HSV-1. Furthermore, both the antiapoptotic function and the reactivation promoting function of LAT reside within the first 1.5 kb of the LAT sequence [2, 24, 65, 74, 130, 131].

In contrast to epithelial cells and neurons, HSV-1 infection results in apoptosis in some cell types of the immune system, such as activated T-cells and immature dendritic cells (Figure 1.5C) [23, 115, 133, 137]. This might be one strategy of immune evasion of HSV-1. Efficiency of HSV-1 replication in these cell types is low. The processes, which

lead to apoptosis instead of protection against apoptosis in these cell types after HSV-1 infection, are not yet unraveled. Infection and impairment of dendritic cells by HSV-1 is discussed in detail in section 1.3.3.

1.3 HSV-1 and the immune system

Skin and mucosal HSV lesions are more severe and more frequent in individuals with impaired immune response [91, 149]. This indicates that the strength of the host immune response largely determines the outcome of HSV-1 infection.

1.3.1 The immune response to HSV-1

Components of the innate immune system represent the first line of defense against pathogens. Natural killer (NK) cells [127], natural killer T (NKT) cells [52], and complement [175] are innate immune factors, which are involved in the control of HSV infections. However, protective immunity against symptomatic HSV infection is dependent on a strong adaptive immune response [91, 113, 171].

The adaptive immune response is based on presentation of processed antigens, such as fragments of viral proteins, on major histocompatibility complex (MHC) molecules on the surface of cells. T cells specifically recognize these antigen-MHC structures and, depending on the type of T cell, either directly kill the antigen presenting cell (cytotoxic T cell) or activate B cells to produce antigen specific antibodies (helper T cell). However, T cells are not able to execute these effector functions until they are activated by dendritic cells (DCs) [69].

1.3.2 Dendritic cells

DCs have received their name based on their tree-like or dendritic shape [157]. Dendritic cells are found at all body surfaces, including the skin, pharynx, and vagina, as well as internal or mucosal surfaces, such as the respiratory tract and the gastrointestinal system. Consequently, DCs are positioned at the sites where the organism gets in contact with invading pathogens for the first time [12, 13].

There exist several different types of DCs. Each type is characterized by a unique set of markers and functions. The majority of tissue resident DCs, like the Langerhans cells of the skin, are of myeloid origin. Type I interferon producing plasmacytoid dendritic cells and some types of DCs in secondary lymphoid organs are of lypmhoid origin [182]. In the laboratory, DCs are differentiated from monocytes of the blood by addition of GM-CSF and IL-4 [144]. In the absence of inflammation, this type of myeloid DC corresponds to mucosal DCs, but not to DCs in lymphoid tissues [173].

DCs differentiate through two major stages. DCs in peripheral tissues represent the immature stage. Immature dendritic cells (iDCs) are characterized by a high phagocytic but low migratory and T cell activating capacity. Consequently, they express the phagocytosis receptor DEC 205 but only little antigen presenting MHC molecules and co-

stimulatory molecules on their surface [35]. Maturation of DCs is induced by pathogen-associated molecular patterns (PAMPs), for example bacterial lipopolysaccharide (LPS), double stranded RNA, and viral envelope proteins or by pro-inflammatory cytokines like IL-1 and TNF-alpha. PAMPs are recognized through pathogen recognition receptors (PRRs), for example Toll-like receptors (TLRs) and retinoic-acid-inducible gene I (RIG-I) [108].

Maturation inducing signals lead to activation of NFκB which induces expression of many genes, resulting in numerous changes in DC phenotype, surface molecule expression, and function [94, 122]. Maturing DCs migrate to the draining lymph nodes. Phagocytic activity is shut down and antigen processing is increased. MHC molecules, co-stimulatory molecules (such as CD80, CD86) and adhesion molecules are upregulated. This phenotype renders mature DCs (mDCs) potent T cell activators, because T cells only become activated if they receive appropriate co-stimulatory signals in addition to the presented antigen [35].

In the absence of infection or inflammation, DCs take up and process tissue antigens or harmless environmental antigens and induce tolerance of the immune system to these antigens [59, 107, 136]. This is important to avoid autoimmune disease and allergy.

Survival and death of DCs must be tightly regulated to ensure an orderly course of the adaptive immune response. Decreased apoptosis of DCs, for example as a result of caspase mutations or chronic stimulation of the antiapoptotic effector molecule CD40, can result in excessive activation of the immune system. This can lead to autoimmunity, chronic inflammation, and lymphoproliferative disease [110, 178]. In contrast, inflammatory diseases can be treated with immunomodulatory drugs, which induce premature death of DCs [180].

Regulation of DC survival is mediated by contact with other cells of the immune system. Activated T cells express ligands (such as CD40L and RANKL) for antiapoptotic receptors on DCs, CD40 and RANK (receptor activator of nuclear factor-κB), and are therefore able to give a survival signal to DCs [81, 181]. However, in some cases activated T cells can also induce death of DCs [40]. DCs express CD95 (Fas), a classical apoptosis inducing receptor. However, engagement of CD95 can trigger activation rather than death in DCs [53, 54, 141]. This is probably enabled by the high amount of c-FLIP expressed in DCs, which blocks the proapoptotic signaling of death receptors in favor of survival pathways [58, 104, 179]. Receptor induced survival of DCs is mainly mediated by activation of transcription factor NF-κB, while death signaling occurs via JNK/AP-1 activation. The balance between NF-κB and JNK/AP-1 activation appears to decide whether DCs live or die, regardless of the receptor, which triggers these pathways [94].

Many viruses infect DCs, including HSV-1, measles virus, vaccinia virus, human immunodeficiency virus [132], and pathogenic hantaviruses [138]. Viruses can interfere with many aspects of DC biology, like migration, antigen processing, maturation, T cell activation, and viability [132]. It can be assumed that viruses thereby shape the immune response to serve their needs.

1.3.3 HSV-1 infection of dendritic cells

HSV-1 can productively infect iDCs but only low titers are achieved [114, 133]. In contrast, infection mDCs is abortive [97]. Infection with HSV-1 induces profound changes in the phenotype of iDCs, as illustrated in figure 1.6. HSV-1 infection results in rounding up of iDCs and in a loss of their ability to form the characteristic dendrites [134, 133]. After HSV-1 infection of iDCs, MHC class II antigen presenting surface molecules as well as the co-stimulatory molecule CD86 are moderately upregulated, which indicates a partial maturation [133, 143]. In contrast, MHC class I molecules are downregulated [143], due to the action of HSV-1 ICP47 protein, which blocks loading of antigens to MHC class I and thereby its transport to the cell surface [185].

Though HSV-1 infection induces a partial maturation of iDCs, maturation in response to LPS is inhibited [133, 143]. The upregulation of co-stimulatory molecules fails, cytokines are not produced, and responsiveness to chemokines is not acquired [143]. As a consequence of the inability of HSV-1 infected iDCs to mature, they also display a strong impairment in the induction of primary and secondary T cell responses [133]. Taken together, HSV-1 is able to efficiently interfere with the function of DCs.

Finally, HSV-1 infected iDCs undergo premature apoptosis and die [23, 115, 133]. HSV-1 induced apoptosis in iDCs involves early and late viral proteins [23] and is associated with activation of caspases, downregulation of the antiapoptotic cellular protein c-FLIP, and upregulation of p53 [23, 115]. Furthermore, expression of TNF-α and TRAIL is enhanced after HSV-1 infection of iDCs [115]. However, inhibition of death ligand binding to their receptors could only partially reduce apoptosis observed in HSV-1 infected iDCs [115]. These studies show that HSV-1 can not only impair the function of DCs, but can also eliminate this cell type, which is critically important for induction of an antiviral immune response.

Though iDCs at the site of infection are damaged, a protective immune response against HSV-1 is mounted and the infection is resolved. This is mediated by uninfected bystander DCs, mainly dermal or submucosal DCs. These uninfected iDCs take up debris of dead infected cells and present the viral antigens to effector cells in the draining lymph nodes, thereby activating HSV-1 specific effector T cells [23]. The impairment of local DCs probably delays the immune response to HSV-1. This delay might enable the virus to gain access to the local sensory nerve endings, infect them and establish latency.

1.4 Objective of this work

HSV-1 caused disease is a relevant socio-economic factor [142]. On the opposite, HSV-1 as been explored as a vehicle for gene therapy which could in the future cure many diseases [88, 99, 172]. Therefore, the detailed investigation of HSV biology is of high relevance. The objective of this thesis is to contribute new insights about the interaction of HSV-1 with the immune system, in particular about the mechanisms of impairment of iDCs by HSV-1.

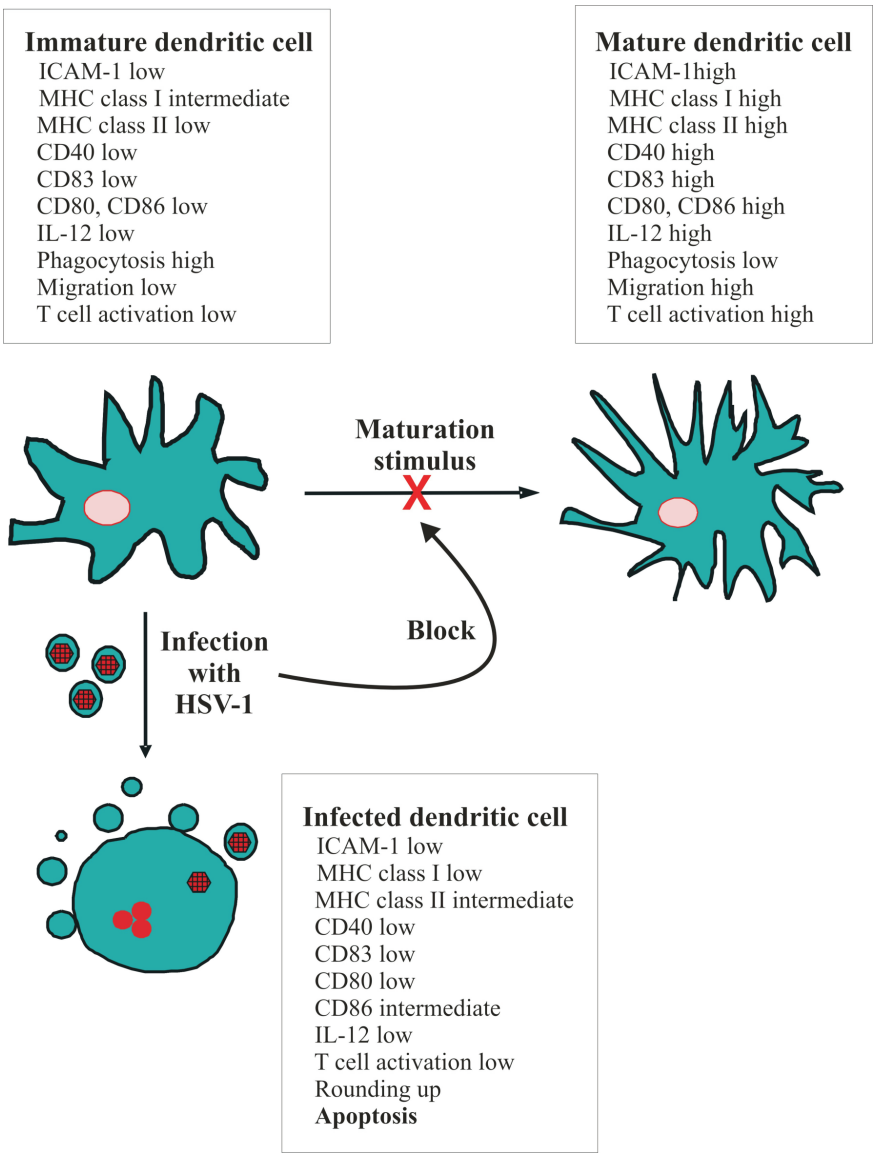

Figure 1.6: **Phenotype of immature and mature DCs and changes induced by HSV-1, according to references [23, 35, 115, 134, 133, 143].**

Several studies have revealed important facts about HSV-1 induced apoptosis of iDCs [23, 115, 133], but the underlying mechanisms are not yet resolved.

Müller *et al.* [115] observed changes in cellular factors, which might be involved in apoptosis induction after HSV-1 infection of iDCs. They showed that HSV-1 infection leads to downregulation of the antiapoptotic cellular protein c-FLIP, but did not dissect the processes, which lead to this downregulation. Therefore, in the first part of this thesis the impact and mechanism of HSV-1 induced c-FLIP downregulation was investigated.

Because HSV-1 possesses several genes, which can efficiently block apoptosis in the host cell [123], it is conceivable that insufficient expression of these genes would contribute to induction of apoptosis after infection of iDCs. Up to now, no studies concerning this hypothesis are published. In the second part of this thesis a microarray analysis was undertaken to find out whether viral antiapoptotic genes are properly expressed in HSV-1 infected iDCs.

The data presented in this thesis indicate that HSV-1 expresses or induces factors, which degrade c-FLIP independent from the proteasome. The importance of c-FLIP for survival of iDCs was demonstrated. Furthermore, it was shown for the first time that poor expression of a viral antiapoptotic gene, LAT, is also involved in apoptosis induction in iDCs after HSV-1 infection.

2 Materials and Methods

2.1 Chemicals

Name	Company
Acetic acid	Roth (Karslruhe, Germany)
APS	Roth (Karslruhe, Germany)
Bromophenolblue	Roth (Karslruhe, Germany)
BSA	Roth (Karslruhe, Germany)
$CaCl_2$	Roth (Karslruhe, Germany)
Chloroform	Roth (Karslruhe, Germany)
Complete Protease Inhibitor Cocktail	Roche (Mannheim, Germany)
Coomassie Brilliant Blue	Serva (Heidelberg, Germany)
DNase	Roche (Mannheim, Germany)
EDTA	AppliChem (Darmstadt, Germany)
Ethanol	Roth (Karslruhe, Germany)
Formaldehyde	Merck (Darmstadt, Germany)
Glycin	Roth (Karslruhe, Germany)
Glycerol	Roth (Karslruhe, Germany)
Goat serum	Dako (Hamburg, Germany)
HEPES	Roth (Karslruhe, Germany)
Isopropanol	Roth (Karslruhe, Germany)
KCl	Roth (Karslruhe, Germany)
KH_2PO_4	Roth (Karslruhe, Germany)
β-mercaptoethanol	Merck (Darmstadt, Germany)
Methanol	Roth (Karslruhe, Germany)
Molecular weight marker	Fermentas (St. Leon-Rot,Germany)
Mounting medium	Dako (Hamburg, Germany)
NaCl	Roth (Karslruhe, Germany)
Na_2HPO_4	Roth (Karslruhe, Germany)
NP 40	Merck (Darmstadt, Germany)
PFA	Roth (Karslruhe, Germany)
Phenol	Roth (Karslruhe, Germany)
Rotiphorese-acrylamid	Roth (Karslruhe, Germany)
SDS	Merck (Darmstadt, Germany)
Sodium azide	Roth (Karslruhe, Germany)
Sucofin skim milk powder	TSI (Zeven, Germany)
TRI REAGENT	Sigma-Aldrich (Deisendorf, Germany)
TEMED	Roth (Karslruhe, Germany)

Name	Company
Tris-aminomethan	Roth (Karslruhe, Germany)
Tris-HCl	Roth (Karslruhe, Germany)
Triton X-100	Merck (Darmstadt, Germany)
Tween-20	Roth (Karslruhe, Germany)

2.2 Buffers and Solutions

Name	Ingredients
AnnexinV-buffer	10 mM HEPES, pH 7.4 0.14 M NaCl 5 mM $CaCl_2$ 5 % FCS 0.02 % sodium azide
Coomassie stain	Destain solution with 2.5 % Coomassie Brilliant Blue
Destain solution	7 % acetic acid 10 % methanol Ad dd H_20
Electrophoresis buffer	0.06 M Tris-aminomethan 0.2 M glycin 0.1 % SDS pH 8.4
FACS-block	PBS with 10 % FCS 0.02 % sodium azide
FACS-wash	PBS with 1 % FCS 0.02 % sodium azide
Fixation solution	PBS with 0.37 % formaldehyde
IB-wash	150 mM NaCl 100 mM Tris-HCl pH 8.0
IF-block	PBS with 3 % goat serum 1 % triton X-100

Name	Ingredients
Loading buffer	0.5 M Tris-HCl 10 % SDS 10 % glycerol 0.05 % bromophenolblue 5 % β-mercaptoethanol
Lysis buffer	50 mM Tris-HCl 10 mM EDTA 80 mM KCl 1 % NP 40 pH 7.5 plus one tablet Complete Protease Inhibitor Cocktail
PBS	150 mM NaCl 6.5 mM Na_2HPO_4 3.5 mM KCl 2 mM KH_2PO_4
Resolving gel buffer	0.9 M Tris-aminomethan 0.4 % SDS pH 8.8
Stacking gel buffer	0.3 M Tris-aminomethan 0.4 % SDS pH 6.8
Transfer buffer	0.8 M Tris-aminomethan 0.4 M glycin 20 % methanol pH 8.0
Triton lysis buffer	50 mM HEPES 5 mM EDTA 150 mM NaCl 1 % triton X-100 pH 7.5

2.3 Cell Culture Equipment

Name	Company
$CaCl_2$	Tebu-bio (Offenbach, Germany)
DMEM	PAA (Marburg, Germany)
DMSO	Roth (Karslruhe, Germany)
ECGF	PAA (Marburg, Germany)
EDGS	Tebu-bio (Offenbach, Germany)
EpiLife	Tebu-bio (Offenbach, Germany)
Fetal calf serum (FCS) HyClone	Perbio (Bonn, Germany)
Heparin	PAA (Marburg, Germany)
HEPES	PAA (Marburg, Germany)
L-glutamine	PAA (Marburg, Germany)
LPS	Sigma-Aldrich (Hamburg, Germany)
MCDB 131	PAA (Marburg, Germany)
MG132	Sigma-Aldrich (Deisendorf, Germany)
Penicillin	PAA (Marburg, Germany)
Recombinant hu GM-CSF	Immunotools (Friesoythe, Germany)
Recombinant hu IL-4	Immunotools (Friesoythe, Germany)
PBS	PAA (Marburg, Germany)
Plastic ware, sterile	TPP (Trasadingen, Switzerland) Nunc (Wiesbaden, Germany) Greiner (Frickenhausen, Germany)
RPMI 1640	PAA (Marburg, Germany)
Streptomycin	PAA (Marburg, Germany)
Trypsin/EDTA	GIBCO® Invitrogen (Karlsruhe, Germany)

2.4 Cell Culture Media

Name	Ingredients
F-medium	DMEM (500 ml) 10 % heat-inactivated FCS 4 mM L-glutamine 100 U/ml penicillin 100 μg/ml streptomycin
PB-medium	RPMI 1640 (500 ml) 10 % heat-inactivated FCS 10 mM HEPES 4 mM L-glutamine 100 U/ml penicillin 100 μg/ml streptomycin

Name	Ingredients
DC-medium	RPMI 1640 (500 ml)
	10 % heat-inactivated FCS
	10 mM HEPES
	4 mM L-glutamine
	100 U/ml penicillin
	100 μg/ml streptomycin
	200 U/ml recombinant hu IL-4
	500 U/ml recombinant hu GM-CSF
HUVEC-medium	MCDB 131 (500 ml)
	10 % heat-inactivated FCS
	10 mM HEPES
	4 mM L-glutamine
	100 U/ml penicillin
	100 μg/ml streptomycin
	50 mg/ml heparin
	10 mg/ml ECGF
Ker-medium	EpiLife (500 ml)
	0.06 mM $CaCl_2$
	100 U/ml penicillin
	100 μg/ml streptomycin
	1 x EDGS

2.5 Kits

Name	Company
BCA Protein Assay Kit	Pierce (Rockford, USA)
CD14 MicroBeads	Miltenyi Biotech (Bergisch-Gladbach, Germany)
Complete Protease Inhibitor Cocktail Tablets	Roche (Mannheim, Germany)
Human Monocyte Nucleofector^{TM} Kit	Amaxa (Cologne, Germany)
MACS columns, Large cell, LD and MS	Miltenyi Biotech (Bergisch-Gladbach, Germany)
Monocyte Isolation Kit II	Miltenyi Biotech (Bergisch-Gladbach, Germany)
MagNA Pure LC mRNA Isolation Kit-I, Lysis Buffer Refill	Roche (Mannheim, Germany)

Name	Company
Plasmid Purification Kit, Midi	Qiagen (Hilden, Germany)
Super Signal West Dura Extended Duration Substrate	Perbio (Bonn, Germany)
Venor GEM-Mycoplasma Detection Kit	Minerva biolabs (Berlin, Germany)

2.6 Antibodies and Fluorescent Dyes

Antibodies and fluorescent dyes were used in the following applications: FACS, Flow cytometry; IB, Immunoblot analysis; IF, Immunofluorescence; S, Stimulation of cells

Primary antibodies

Specificity	Clone	Applic.	Company/Source
Actin (beta)	AC-15 (mouse)	IB	Abcam (Hiddenhausen, Germany)
CD95 (agonistic)	CH-11 (mouse)	S	Beckman Coulter (Roissy, France)
gD (HSV)	DL-6 (mouse)	FACS	Santa Cruz Biotechnology (Heidelberg, Germany)
FLIP (cellular)	NF6 (mouse)	IB, IF	Peter Krammer (DKFZ, Heidelberg, Germany)
Myc-Tag	polyclonal rabbit	IB	Biozol (Eching, Germany)
HSV (McIntyre)	polyclonal rabbit serum	IF	Dako (Hamburg, Germany)

Secondary antibodies

Antibody	Conjugation	Applic.	Company
Goat-anti-mouse F(ab')$_2$	Peroxidase	IB	Dianova (Hamburg, Germany)
Goat-anti-rabbit F(ab')$_2$	Peroxidase	IB	Dianova (Hamburg, Germany)
Goat-anti-mouse F(ab')$_2$	Cy5	FACS	Immunotools (Friesoythe, Germany)
Goat-anti-mouse F(ab')$_2$	FITC	FACS	Immunotools (Friesoythe, Germany)
Goat-anti-mouse F(ab')$_2$	TexasRed	FACS, IF	Immunotools (Friesoythe, Germany)
Goat-anti-rabbit F(ab')$_2$	FITC	IF	Immunotools (Friesoythe, Germany)

Fluorescent dyes

Name	Applic.	Company
AnnexinV-FITC	FACS	Santa Cruz Biotechnology (Heidelberg, Germany)
DAPI	IF	Invitrogen (Karlsruhe, Germany)
Propidium iodide	FACS	Santa Cruz Biotechnology (Heidelberg, Germany)

2.7 Technical Equipment

Name	Company
CCD camera, Kodak Image Station 4000 MM Digital Imaging System	Kodak (Stuttgart, Germany)
Cell counting chamber, Neubauer improved	Roth (Karlsruhe, Germany)
Centrifuge, Megafuge 2.O R	Heraeus (Hanau, Germany)
CO2 Incubator HERACell 150	Heraeus (Hanau, Germany)
Electronic pipetor, Pipetus	Hirschmann Laborgeräte (Eberstadt, Germany)
Electrophoresis System	BIO-RAD Laboratories (München, Germany)
Flow Cytometer, FACSCalibur	BD Biosciences (Heidelberg, Germany)
Fluorescence Microscope, Olympus BX60	Carl Zeiss (Jena, Germany)
Microscope, Axiovert 25	Carl Zeiss (Jena, Germany)
Microscope slides, SuperFrost Ultra Plus	Menzel (Braunschweig, Germany)
NucleofectorTM	Amaxa (Cologne, Germany)
PVDF membranes	Millipore Corporation (Bedford, USA)
Sterile filters 0,2 μm	Schleicher and Schüll (Dassel, Germany)
Sterile Workbench, HERASafe	Heraeus (Berlin, Germany)
Vortex-Genie 2	Scientific Industries (New York, USA)
Waterbath	GFL (Burgwedel, Germany)

2.8 Plasmids

The following mamalian expression plasmids were used in this work:

Plasmid	Parental Vector	Insert	Insertion Site	Source/ Reference
pEGFP-N1	pEGFP-N1	none		Clontech
$FLIP_S$-EGFP	pEGFP-N1	c-$FLIP_S$ lacking last 8 aa	BglII/SacII	[153]
$FLIP_L$-EGFP	pEGFP-N1	c-$FLIP_L$	BglII/SacII	[153]
myc-$FLIP_S$	pcDNA3	myc-c-$FLIP_S$	HindIII/XbaI	[96]
myc-$FLIP_L$	pcDNA3	myc-c-$FLIP_L$	HindIII/XbaI	[121]
myc-$FLIP_L$ 1-438	pcDNA3	myc-c-$FLIP_L$ bases 1-1314	HindIII/XbaI	[67]
myc-$FLIP_L$ 1-202	pcDNA3	myc-c-$FLIP_L$ bases 1-606	HindIII/XbaI	[67]
myc-$FLIP_L$ 203-480	pcDNA3	myc-c-$FLIP_L$ bases 606-1443	HindIII/XbaI	[67]
myc-$FLIP_L$ D376A	pcDNA3	myc-c-$FLIP_L$ with mutated codon 376	HindIII/XbaI	[67]
myc-$FLIP_L$ F23G/F114G	pcDNA3	myc-c-$FLIP_L$ with mutated codons 23 & 114	HindIII/XbaI	[67]
U_S3-EGFP	pEGFP-N1	U_S3 (HSV-1 strain F)	XhoI/BamHI	MJR
gJ-EGFP	pEGFP-N1	gJ (HSV-1 strain F)	XhoI/BamHI	MJR

$FLIP_L$-EGFP and $FLIP_S$-EGFP were kindly provided by Professor Harald Wajant (Department of Molecular Internal Medicine, Medical Polyclinic, University of Würzburg, Würzburg, Germany). myc-$FLIP_S$ was a kind gift of Professor Peter H. Krammer (Division of Immunogenetics, German Cancer Research Center, Heidelberg, Germany). myc-$FLIP_L$, myc-$FLIP_L$ 1-438, myc-$FLIP_L$ 1-202, myc-$FLIP_L$ 203-480, myc-$FLIP_L$ D376A and myc-$FLIP_L$ F23G/F114G were kindly made available by Professor Mikihiko Naito (Institute of Molecular and Cellular Biosciences, University of Tokyo, Tokyo, Japan). The sequences of $FLIP_L$ and $FLIP_S$ are available in the Nucleotide Database under accession numbers U97074 and U97075, respectively. U_S3-EGFP and gJ-EGFP were obtained from Martin J. Raftery (MJR, Institute of Virology, Charité Medical School, Berlin, Germany) with kind permission.

Plasmids were expanded in *Escherichia coli* strain XL-1 blue and purified using Qiagen Midi Plasmid Purification Kit (Qiagen, Hilden, Germany).

2.9 Cells

Cell culture work was carried out following standard sterile working rules in a laminar flow hood using sterile reagents and equipment. Ingredients of the used culture media are listed in section 2.4. FCS was inactivated at 56 °C for 30 min (water bath) before us-

age. For passaging or collection, adherent cells were washed twice with PBS, incubated with trypsin solution (PBS with 0.05 % trypsin and 1 mM EDTA) for 5 min at 37 °C and resuspended in the respective culture medium. Absence of Mycoplasma species from cell lines was regularly tested using Venor GEM-Mycoplasma Detection Kit.

2.9.1 Cell Lines

Name	Origin	Medium
A549	epithelial, human lung carcinoma	F-medium
HeLa	epithelial, human cervix carcinoma	F-medium
HEp-2	epithelial, HeLa subpopulation	F-medium
HaCaT	epithelial, spontaneously immortalized aneuploid human keratinocyte	F-medium
L428	hematopoietic, human, Hodgkin/Reed-Sternberg cells of Hodgkin's lymphoma	PB-medium
L1236	hematopoietic, human, Hodgkin/Reed-Sternberg cells of Hodgkin's lymphoma	PB-medium

HaCaT cells were kindly provided by N. Fusenig (DKFZ, Heidelberg, Germany). L428 and L1236 were obtained from Stefan Mathas (Max Delbrück Center for Molecular Medicine, Berlin, Germany). All other cell lines were obtained from ATCC.

2.9.2 Dendritic Cells

Monocytes were obtained from buffy coats of healthy donors (DRK, Berlin, Germany) by density gradient centrifugation over Ficoll-Paque and subsequent isolation with Monocyte Isolation Kit II. Monocytes were then differentiated into iDCs by culture in DC-medium for 6 days.

2.9.3 Other primary cells

Human umbilical vein endothelial cells (HUVECs) were prepared by the recently modified [166] method of Jaffe *et al.* [68] and maintained in HUVEC-medium on gelatin-coated plates. Primary keratinocytes and fibroblasts (isolated as described in [78]) were obtained from C. Johnen and K. Bräutigam (Department of Surgery, Univer-sitätsmedizin Berlin - Charité, Berlin, Germany). Keratinocytes were maintained in Ker-medium and fibroblasts in F-medium.

2.10 Viruses and Infection

HSV-1 wild type strains KOS, F, and 17 as well as a LAT knockout mutant of HSV-1 (ΔLAT, 17N/H [22]) were propagated on Vero E6 cells. An ICP27 knockout mutant of HSV-1 (ΔICP27, 27-LacZ [154]) was propagated on Vero E6 cells which are stably transfected to complement ICP27 (Vero 2-2). Cell culture supernatant of infected Vero E6 or Vero 2-2 cells was collected and centrifuged at 2,000 g for 10 min. The cleared supernatant was frozen in liquid nitrogen at 0.5 ml aliquots. Titers of virus stocks were determined by measuring TCID50.

For infection experiments, suspension cells were resuspended in and adherent cells were overlayed with a minimal volume of culture medium. Transfected cells were infected 24-35 h post transfection. The appropriate volume of HSV-1 containing supernatant necessary to achieve the desired MOI was added to the cells and mixed. After incubation for 1 h at 37 °C to allow virus adsorption, the virus containing medium was removed and cells were washed two times with medium. A sufficient volume of culture medium was added and cells were maintained under normal culture conditions. As controls, infection was performed with heat-inactivated (56 °C, 30 min) or UV-inactivated (10 min) HSV-1. Efficiency of infection was controlled by staining of cells at 18 h post infection with anti-gD and fluorescence-conjugated secondary antibody, followed by flow cytometry. Background staining was determined by staining of uninfected cells or cells treated with inactivated virus and subtracted.

2.11 Immunoblot analysis

Cells were washed with cold PBS and lysed for 1 h on ice in lysis buffer. After centrifugation at 15,000 g for 30 min, the supernatant containing soluble cytoplasmatic proteins was mixed with loading buffer, incubated at 95 °C for 10 min, and separated by 12-15 % SDS-PAGE. In order to achieve equal loading of lanes, the protein content of lysates was determined using BCA protein assay kit. After transfer to PVDF membranes, the blots were blocked with 5 % BSA or 5 % milk powder in IB-wash and thereafter incubated with primary antibody. After washing 5 times with IB-wash, blots were incubated with peroxidase-conjugated secondary antibody. After washing again 5 times with IB-wash, blots were developed by enhanced chemoluminescence using Super Signal West Dura Extended Duration Substrate. The signal was detected with a charge-coupled device (CCD) camera. After stripping off with 0.4 M glycine/0.2 % SDS (pH 2.2), blots were blocked again and stained against β-actin to check for equal loading. Densitometric analysis of bands on photographs of immunoblots was performed by using ChemiImager 4000 software (Alpha155 Innotech Corporation, San Leandro, CA, USA).

2.12 Flow cytometry and detection of apoptosis

For assessment of infection efficiency, cells were harvested at 18 h post infection with HSV-1 and washed once with FACS-wash. Primary antibody (specific for HSV-1 gly-

coprotein D, gD) was diluted in FACS-block and added to the cells. After 20-30 min, primary antibody was washed from the cells with FACS-wash two times. Thereafter, cells were incubated with secondary antibody in FACS-block for 15-20 min. After a final wash with FACS-wash, cells were resuspended in fixation solution and stored at 4 °C in the dark until analysis. EGFP expressing cells were not fixed after staining, but left in FACS-wash and analyzed immediately. For detection of apoptosis, cells were washed once with AnnexinV-buffer and stained with AnnexinV-FITC for 20 min in the dark. Thereafter, cells were washed two times with AnnexinV-buffer. Propidium iodide was added and cells were directly analyzed. Analysis was done with a FACSCalibur flow cytometer. Data were analyzed with Cellquest Pro software.

2.13 Immunofluorescence

Medium was removed from cells grown on glass plates and washed once with PBS. Fixation of cells was achieved by incubation in PBS/3.7 % PFA for 5 min at room temperature. After washing three times with PBS, cells were permeabilized and blocked with IF-block for 5 min. After washing again three times with PBS, first antibody was added diluted in FACS-block with 5 % goat-serum and left on the cells for 30 min at room temperature. Then, cells were washed 4 times with PBS and incubated for 1.5 h in the dark with secondary antibody diluted in FACS-block with 5 % goat-serum. Finally, cells on glass plates were washed four times with PBS and once with distilled water. Glass plates were then covered with mounting medium and transferred to glass slides for fluorescence microscopy.

2.14 Microarray analysis of HSV-1 gene expression

At different time points post infection, cells were harvested and lysed in TRI REAGENT. Total RNA was extracted with phenol/chlorform and resuspended in sterile water. Total RNA was shipped on dry ice to Rozanne M. Sandri-Goldin and Gayathri Devi-Rao (Department of Microbiology and Molecular Genetics, School of Medicine, University of California Irvine, USA), who carried out the microarray analysis. Fluorescein- or biotin-labeled cDNA was generated from purified poly(A)-containing RNA by random hexamer-primed polymerization using Superscript II reverse transcriptase (Gibco-BRL, Invitrogen, Carlsbad, USA) as described in detail in [161]. Generation of HSV-1 microarrays, as oligonucleotide selection, synthesis and deposition on the chip have been described previously [158, 177]. Position of oligonucleotide probes which are located in the LAT region of the HSV-1 genome is illustrated in figure 2.1. Hybridization of microarrays with labeled cDNA and scanning was carried out as reported recently [161, 160]. Briefly, microarrays were hybridized with cDNA probes for 18 h and rinsed for scanning with a proprietary HiLight dual-color kit (Genicon Sciences, San Diego, USA) at 52 °C in a MAUI hybrid mixer assembly (BioMicro Systems, Salt Lake City, USA). After hybridization, the slides were washed, blocked and bound by the gold

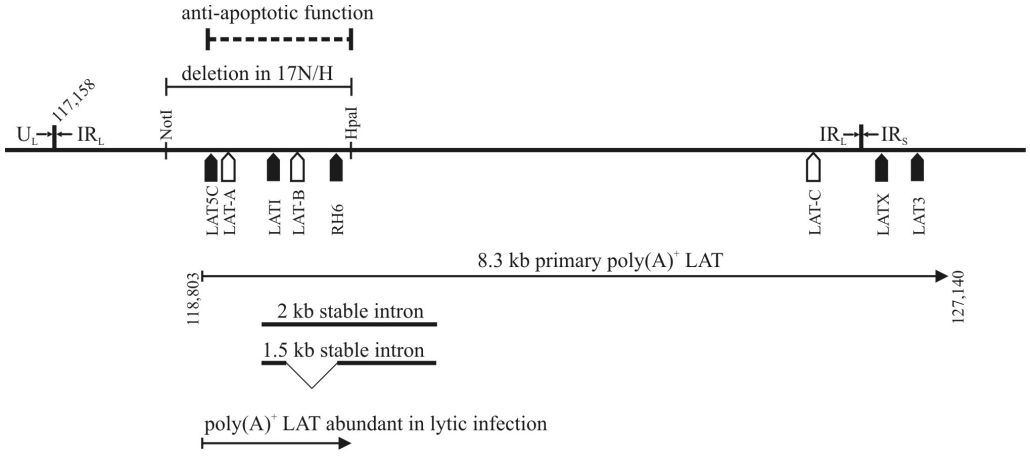

Figure 2.1: **Diagram of the LAT region of the HSV-1 genome showing location of LAT probes used for microarray analysis and quantitative RT-PCR.** Schematic map of the internal repeat and joint region of the HSV-1 genome. Selected restriction sites, the region associated with antiapoptotic function of LAT [24] and the deletion in 17N/H [22] are indicated. Position of probes used in the microarray [177] are marked with filled arrows, position of probes used in quantitative RT-PCR are marked with open arrows. Below the map of the genome important LAT RNA species are depicted based on data published by Devi-Rao *et al.* [32]. For better orientation, base numbers of the total HSV-1 DNA sequence [accession number: X14112] are given for selected positions.

and silver RLS method (two-color nucleic acid microarray resonance light-scattering-based method, Genicon Sciences, San Diego, USA). Microarrays were scanned with a GSD-501 HiLight reader (designed for RLS, Genicon Sciences, San Diego, USA). First, for each gene or coterminal transcript family, a median value was calculated from the net (minus background) hybridization values of the three replicate probe spots on the chip. These median hybridization values were then expressed in percent of the total viral signal of the given hybridization (median hybridization value of probe multiplied with 100, divided by the sum of all hybridization values) to obtain a relative abundance for the respective detected transcript. Microarray analysis of HSV-1 gene expression in each cell type was performed three times with RNA from three independent infection experiments as indicated in table 3.1. Relative abundances of each transcript from the different infections were pooled to calculate final median values displayed in tables 1-4. Relative abundances in iDCs and HaCaT or HeLa cells were compared by Student's two-tailed *t* test, assuming unequal variance and with the null hypothesis being that the true values in the different cell types are identical.

2.15 LightCycler quantitative real-time PCR

Cells were lysed in MagNA Pure lysis buffer and frozen at -80 °C until further processing. mRNA isolation, primer design and LightCycler quantitative real-time PCR was done by Thomas Giese (Institute of Immunology, University of Heidelberg, Heidelberg, Germany). mRNA was isolated with a MagnaPure-LC device using standard protocols. RNA was reverse-transcribed with AMV-RT and oligo(dT) primer (First Strand cDNA synthesis kit, Roche, Mannheim, Germany). For amplification of target sequences, LightCycler Primer Sets (Search-LC, Heidelberg, Germany) were used with LightCycler FastStart DNA Sybr Green I Kit (Roche, Mannheim, Germany). RNA input was normalized by the average expression of the housekeeping genes encoding β-actin and cyclophilin B. By plotting a known input concentration of a plasmid to the PCR cycle number at which the detected fluorescence intensity reached a fixed value, a virtual standard curve was generated. This standard curve was used to calculate transcript copy numbers. The presented relative copy numbers are mean averages of data of two independent analyzes for each sample and parameter. Primers for detection of c-FLIP are located at nucleotides 1163 and 1420 of the c-FLIP$_L$ open reading frame (accession number U97074). Locations on the HSV-1 genome (accession number X14112.1) of probes used to detect different LAT-species (LAT-A: 118987-119182, LAT-B: 119811-119935, LAT-C: 125612-125692) are illustrated in figure 2.1. Locations on the HSV-1 genome (accession number X14112.1) of primers for detection of other HSV-1 genes are listed in the table below.

Gene	5′ primer	3′ primer
UL10	23619-23639	23654-23679
UL54	114982-115002	115160-115184
US1	133304-133325	133541-133565
US3	135451-135476	135539-135562
US5	137806-137821	137890-137910
US6	138750-138773	138983-139001
US11	145087-145110	145008-145031

In one set of experiments, quantitative RT-PCR of c-FLIP was performed separately in nuclei and cytoplasm. Therefore, cells were resuspended in lysis buffer and incubated for 1 h on ice. The lysat was centrifuged and supernatant and pellet separately resuspended in MagNA Pure lysis buffer. The pellet was washed once with lysis buffer before resuspension in MagNA Pure lysis buffer, to remove residual cytoplasm.

2.16 Transfection of cells with mammalian expression plasmids

Transfections were performed with HEp2, A549, or HEK cells and different transfection reagents were used.

For transfection of cells with Lipofectamine^{TM} 2000 Transfection Reagent (Invitro-

gen, Karlsruhe, Germany), adherent cells were trypsinized, washed one time with culture medium and resuspended in 500 µl DMEM/5 % FCS. Separately, 3 µg plasmid was added to 50 µl Optimem and gently mixed. In another tube, 50 µl Optimem was mixed with 5 µl Lipofectamine^{TM} 2000. After 5 min, plasmid solution and Lipofectamine^{TM} 2000 solution were mixed and incubated 30 min at room temperature. Thereafter, the transfection mixture was added to the cells, gently mixed and incubated for 3.5 h in a cell culture incubator (37 °C, 5 % CO_2). Thereafter, cells were washed twice with DMEM/5 % FCS, resuspendended in an appropriate amount of DMEM/5 % FCS and seeded on cell culture dishes.

Transfections with ExGen 500 Universal Transfection Reagent (Fermentas, St. Leon-Rot, Germany) were carried out as follows. Adherent cells were used at 50 % confluency, washed twice with PBS and overlayed with DMEM without additives. 3 µg plasmid were mixed with 200 µl PBS and 9.9 µl ExGen 500 and immediately mixed by vortexing for 10 s. The transfection mixture was then incubated for 10 min at room temperature and thereafter added to the cells, followed by gentle mixing and incubation for 7 h in the cell culture incubator. Then, the transfection medium was exchanged with the regular cell culture medium.

Transfections with FuGENE® 6 Transfection Reagent (Roche, Mannheim, Germany) were performed with adherent cells at 50 % confluency. Before transfection, the culture medium was exchanged with fresh regular cell culture medium. For each plasmid the optimal volume FuGENE® 6 [µl] : mass DNA [µg] ratio was established in preceding optimization experiments. 582 µl DMEM without additives was mixed with 18 µl FuGENE® 6 and incubated for 5 min at room temperature. Then, 6 µg (ratio 3 : 1) or 12 µg (ratio 3 : 2) were added, gently mixed and incubated for another 40 min at room temperature. The transfection mixture was added to the cells in a drop wise manner and distributed by gentle swirling. The transfection medium was left on the cells until they were used for assay of gene expression or virus infection.

For some experiments, TurboFect^{TM} *in vitro* Transfection Reagent (Fermentas, St. Leon-Rot, Germany) was used to transfect cells. Cells were trypsinized, washed once with culture medium and resuspended in 100 µl DMEM without additives. Separately, 300 µl DMEM without additives were mixed with 4 µg plasmid, then 6 µl TurboFect^{TM} were added and mixed by pipetting. After 30 min at room temperature, the cell suspension was added to the transfection mixture and mixed by flicking the tube. After incubation for 6 h in a cell culture incubator, an appropriate amount of culture medium was added and the cells were seeded on cell culture dishes.

2.17 Inhibition of the proteasome

In some experiments, the proteasomal turnover of proteins was inhibited by addition of the proteasome inhibitor MG132. Because MG132 has toxic effects on cells, incubation time must be minimized. Therefore, MG132 was added to the cells at 1 µM 5 h before harvesting or at 10 µM 2.5 h before harvesting of the cells for analysis. Because it was intended to analyze the consequences of proteasome inhibition on HSV-1 induced

downregulation of c-FLIP, which occurs between 10 h and 12 h post infection, MG132 was added to infected cells at 5.25 h or 7.5 h post infection and analysis was done 2.5 h or 5 h later.

2.18 c-FLIP protein degradation assay

A549 cells were transfected with plasmids myc-FLIP$_L$ F23G/F114G (mutated c-FLIP$_L$ which does not aggregate when overexpressed in cells [67]) or FLIP$_S$-EGFP using Turbofect^{TM} and lysed after 48 h in Triton buffer. After 1 h on ice and sedimentation of debris by centrifugation, the lysates were divided into four aliquots. One aliquot was frozen at -20,°C until SDS-PAGE. Another aliquot was incubated at 37 °C for 2 h and then loaded on SDS-PAGE. The two remaining aliquots were each mixed with an equal volume of lysate from HSV-1 infected (strain KOS, MOI 10, lysed at 18 h post infection) but untransfected A549 cells and also incubated at 37 °C before loading on SDS-PAGE. To one of the aliquots mixed with lysates from HSV-1 infected A549 cells, the proteasome inhibitor MG132 (50 μM) was added before incubation at 37 °C. SDS-PAGE and immunoblot for detection of c-FLIP was performed as described above.

2.19 RNA interference in human monocyte-derived dendritic cells

RNA interference in DCs was performed by Juliane Lippmann, a diploma student working under my supervision. Control non-silencing siRNA (siC, target sequence, TTT ATG TGT GCC CGT GTG GAA) and FLIP specific siRNA (siFLIP, target sequence, TTG TGC CGG GAT GTT GCT ATA, targeting both c-FLIP$_L$ and c-FLIP$_S$) were purchased from MWG (Ebersberg, Germany). Monocytes were isolated from buffy coats of healthy donors (DRK, Berlin, Germany) with CD14 MicroBeads after density gradient centrifugation over Ficoll-Paque. Immediately after isolation, monocytes were transfected with 1 μmol siRNA per 2×10^7 cells using Amaxa Nucleofector^{TM} according to the manufacturer's protocol (Human Monocyte Nucleofector^{TM} Kit, Nucleofector^{TM} program Y-001). The transfected cells were then differentiated into iDCs by culture in DC-medium for 3 to 6 days. Before apoptosis assay, 1×10^5 iDCs were stimulated with 0.125 μg/ml agonistic anti-CD95 monoclonal antibody (clone CH-11) for 12 h or were left untreated.

3 Results

Previous studies showed that iDCs die from apoptosis after infection with HSV-1 [23, 133]. Müller *et al.* [115] demonstrated the downregulation of the cellular antiapoptotic protein c-FLIP$_L$ after HSV-1 infection and proposed that the lack of c-FLIP$_L$ could sensitize iDCs to apoptosis. The first experiments in this work were performed to investigate this hypothesis.

3.1 siRNA mediated knockdown of c-FLIP in iDCs

After HSV-1 infection, a multitude of changes occurs in many cellular processes, which influence viability of the cell. To investigate the impact of c-FLIP downregulation on viability of iDCs separate from other HSV-1 induced effects, the amount of c-FLIP in uninfected iDCs was reduced by RNA interference.

Monocytes were isolated from PMBC of healthy blood donors with CD14-microbeads and immediately nucleofected with c-FLIP specific siRNA, control siRNA, or were left untreated. Afterwards, monocytes were differentiated into iDCs for 3 to 6 days. Immunoblot analysis confirmed the specific reduction of c-FLIP$_L$ (figure 3.1A) and c-FLIP$_S$ (data not shown).

Viability was assessed by flow cytometry. One representative experiment out of three is shown in figure 3.1B. Without further treatment, successful reduction of c-FLIP resulted in a prominent loss of viable iDCs (figure 3.1B, upper panel). After nucleofection with control siRNA (siC) 85 % of iDCs were viable (AnnexinV$^-$/PI$^-$), compared to 20 % viable iDCs after nucleofection with c-FLIP specific siRNA (siFLIP). This was associated with an increase in apoptotic (AnnexinV$^+$/PI$^-$) iDCs from 2 % (siC) to 16 % (siFLIP). However, after nucleofection with siFLIP, most AnnexinV$^+$ iDCs were also PI$^+$ (61 %). This cell population likely represents iDCs in the late apoptotic state, because analysis of viability was performed not before 3 to 6 days after nucleofection. Stimulation of the extrinsic apoptosis pathway with an agonistic CD95 (Fas) antibody (figure 3.1B, lower panel) resulted in a 4-fold (85 % to 20 %) reduction of viable iDCs nucleofected with siC and a 20-fold (20 % to 1 %) reduction of viable iDCs nucleofected with siFLIP.

Taken together, reduction of c-FLIP by RNA interference induced apoptosis in the majority of iDCs and sensitized the remaining iDCs to induction of apoptosis via the extrinsic pathway. These data suggest a direct correlation between the amount of c-FLIP and viability of iDCs. Therefore it can be assumed that HSV-1 induced c-FLIP downregulation could also lead to increased apoptosis in iDCs.

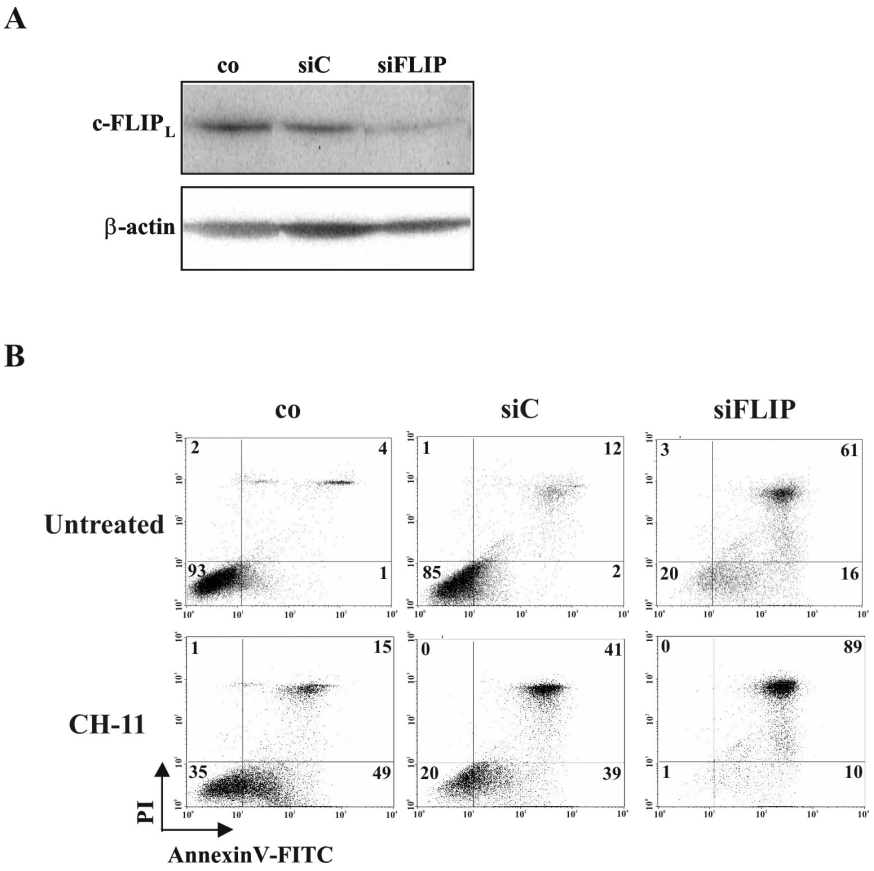

Figure 3.1: **Immunoblot of c-FLIP (A) and flow cytometry analysis of apoptosis (B) in iDCs after siRNA mediated knockdown of c-FLIP.** iDCs were nucleofected with siRNA specifically targeting c-FLIP (siFLIP) or with unspecific control siRNA (siC) or were left untreated (co). **(A)** Specific knockdown of c-FLIP was verified by immunoblot using anti-FLIP antibody (clone NF-6) and antibody against β-actin as loading control. **(B)** Viability of iDCs was analyzed by staining of cells with AnnexinV-FITC and propidium iodide (PI) and subsequent flow cytometry analysis. One aliquot of the cells was treated with anti-CD95 agonistic antibody (clone CH-11) for 12 h before assessment of viability. Data are representative of three independent experiments.

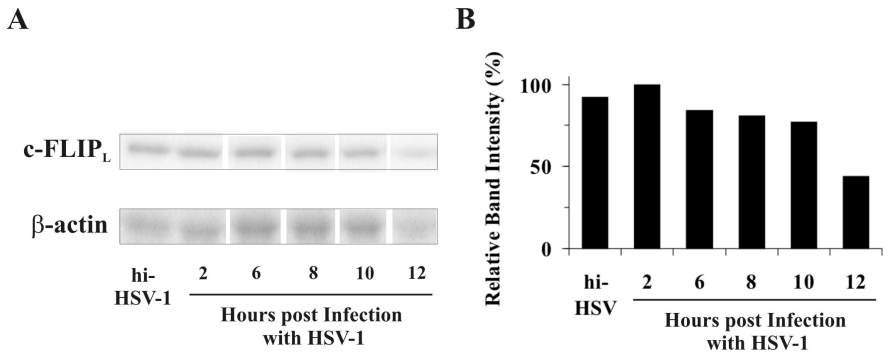

Figure 3.2: **Time course of HSV-1 induced c-FLIP downregulation in iDCs.** iDCs were infected with HSV-1 strain F at MOI 1.5 or with heat-inactivated HSV-1 (hi-HSV). At different time points post infection, cells were harvested and analyzed by immunoblot analysis using anti-FLIP antibody (clone NF-6) and antibody against β-actin as loading control. **(A)** One representative blot of three independent experiments is shown. **(B)** Relative band intensity of c-FLIP$_L$ bands was determined by densitometry and normalized to β-actin. The value obtained with HSV-1 infected iDCs at 2 h p. i. was set to 100 %. For comparison, the relative band intensity obtained at 2 h p. i. with heat-inactivated virus is also depicted.

3.2 Time course of HSV-1 induced c-FLIP reduction and apoptosis in iDCs

In the publication by Müller *et al.* [115] c-FLIP and apoptosis were analyzed exclusively at 18 h post infection (h p. i.) of iDCs with HSV-1. However, at this time point replication of HSV-1 is almost completed. Therefore, the temporal pattern of HSV-1 induced c-FLIP downregulation and apoptosis in iDCs was investigated in more detail.

iDCs were infected with wild type HSV-1 strain F at MOI 1.5 and the amount of c-FLIP was analyzed by immunoblot at different time points post infection. Up to 10 h p. i. no reduction of c-FLIP$_L$ was detected (figure 3.2). However, at 12 h p. i. the amount of c-FLIP$_L$ dropped below 50 % of the amount detected in iDCs treated with heat-inactivated virus. At later time points (18 h p. i.) the amount of c-FLIP$_L$ was further decreased, to about 25 % (figure 3.14A, first panel).

In some experiments presented in this thesis, the short form of c-FLIP, c-FLIP$_S$, which is also expressed in iDCs, was detectable by immunoblot analysis. c-FLIP$_S$ was also downregulated after HSV-1 infection of iDCs, to a comparable extent and at the same time point as c-FLIP$_L$ (figures 3.8 and 3.10).

In different experiments several wild type HSV-1 strains (F, KOS, Patton and 17) were used and all showed a comparable ability to downregulate c-FLIP. Immunoblot data of c-FLIP in iDCs after infection with strain F (figures 3.2, 3.10 and 3.14) and KOS (figures 3.10 and 3.8) are presented in this thesis.

Kinetics of c-FLIP downregulation depended on the MOI used for infection. At

higher MOI (for example MOI 3), reduction of c-FLIP to 40 % occured already at 10 h p. i. (figure 3.8).

Figure 3.3 shows the time course of apoptosis in HSV-1 infected iDCs (HSV-1 strain F, MOI 1.5). The number of apoptotic iDCs was determined by flow cytometry after staining with AnnexinV-FITC and propidium iodide. Flow cytometry diagrams of one representative experiment are shown in figure 3.3A. While in hi-HSV-1 treated iDCs the number of apoptotic cells (AnnexinV$^+$/PI$^-$, lower right quadrant) did not increase between 10 h p. i. (8 %) and 16 h p. i. (6 %), in HSV-1 infected iDCs the number of apoptotic cells increased from 10 % to 20 %. At 20 h p. i. only 10 % of hi-HSV-1 treated iDCs were apoptotic, but 27 % of HSV-1 infected iDCs. However, at 20 h p. i. more HSV-1 infected iDCs were in the late apoptotic stage (AnnexinV$^+$/PI$^+$, upper right quadrant) compared to 16 h p. i. (21 % compared to 8 %). Statistical analysis revealed that up to 12 h p. i. there was no significant difference in the number of apoptotic iDCs (AnnexinV$^+$/PI$^-$) after HSV-1 infection compared to iDCs treated with heat-inactivated virus (hi-HSV-1) (figure 3.3B). However, at 14, 16, and 20 h p. i. a significantly higher number of HSV-1 infected iDCs was apoptotic compared to hi-HSV-1 treated iDCs. In following experiments, analysis of apoptosis in HSV-1 infected cells was done after 16 h p. i.

These data demonstrate that the reduction of c-FLIP at 12 h p. i. precedes apoptosis in HSV-1 infected iDCs, which is first detectable at 14 h p. i. This is another indication for a correlation between the downregulation of antiapoptotic c-FLIP and induction of apoptosis in iDCs after infection with HSV-1. Furthermore, these data indicate that c-FLIP downregulation and apoptosis of iDCs are induced in a late stage of HSV-1 replication.

3.3 Mechanism of c-FLIP reduction by HSV-1

The data presented above strongly indicate that HSV-1 induced downregulation of c-FLIP could contribute to apoptosis after HSV-1 infection of iDCs. Next, experiments were conducted in order to resolve how HSV-1 achieves the reduction of c-FLIP.

3.3.1 c-FLIP mRNA after infection of iDCs with HSV-1

HSV-1 could target c-FLIP either at the level of mRNA transcription and stability or directly at the protein level. As shown by Müller *et al.* [115], the total amount of c-FLIP$_L$ mRNA is increased after infection of iDCs with HSV-1. This result points toward a mechanism operating directly on the protein rather than on mRNA. But it is also possible that HSV-1 impairs the export of c-FLIP mRNA from the nucleus to the cytoplasm. Therefore, the amount of c-FLIP$_L$ mRNA was quantified separately in nuclei and cytoplasm of HSV-1 infected iDCs using quantitative real-time PCR.

As shown in figure 3.4, these experiments confirmed the increase in total c-FLIP$_L$ mRNA after infection of iDCs with HSV-1, which was already published by Müller *et al.* [115]. Although most of the additional transcripts did accumulate in the nucleus (91 ± 23 % in HSV-1 infected iDCs compared to 20 ± 4 % in uninfected cells), the

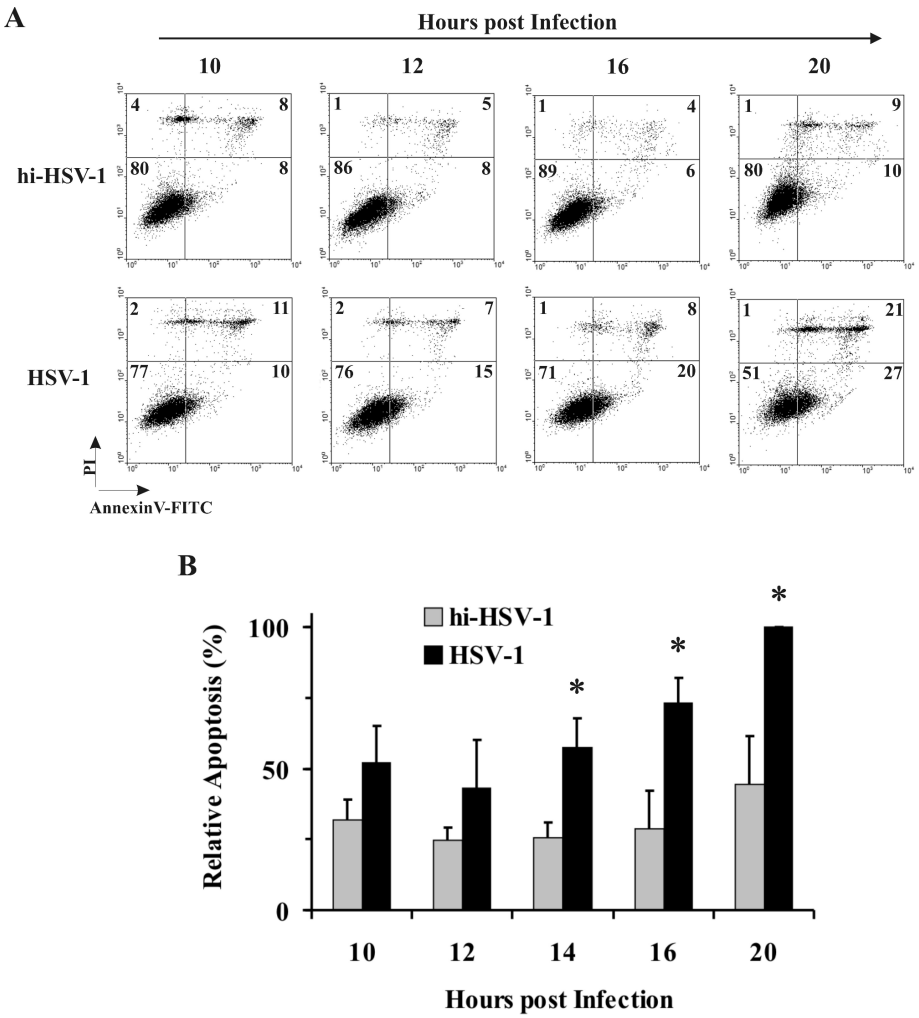

Figure 3.3: **Time course of apoptosis in iDCs infected with HSV-1.** iDCs were infected with HSV-1 strain F at MOI 1.5 or with heat-inactivated HSV-1 (hi-HSV-1). At different time points post infection apoptosis was assessed by staining of iDCs with AnnexinV-FITC and propidium iodide (PI) and subsequent flow cytometry. **(A)** Flow cytometry diagrams are shown for one representative experiment. Numbers in each quadrant indicate percentage of cells contained in this quadrant. **(B)** The number of apoptotic iDCs ($AnnexinV^+/PI^-$) at 20 h p. i. was set to 100 %. Median values ±SD of three independent experiments are shown for different time points post infection with HSV-1 or hi-HSV-1. Asterisks indicate that at this time point apoptosis in HSV-1 infected iDCs is significantly higher than in iDCs treated with hi-HSV-1 (Student's unpaired two-tailed *t* test, $P \leq 0.05$).

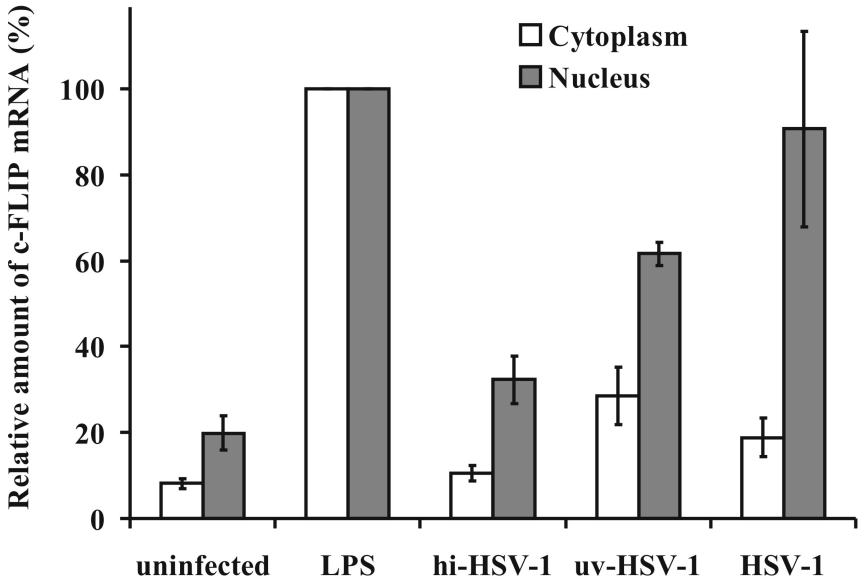

Figure 3.4: **Distribution of c-FLIP$_L$ mRNA in iDCs after infection with HSV-1.** iDCs were infected for 18 h with HSV-1, heat-inactivated HSV-1 (hi-HSV-1) or UV-inactivated HSV-1 (uv-HSV-1) or were left uninfected. Relative copy numbers of c-FLIP$_L$ mRNA in the nucleus and the cytosol were determined separately by quantitative RT-PCR. Values obtained with LPS-treated (24 h) iDCs were set to 100 %. Data shown are mean values $\pm$ SD calculated from three independent experiments (except uv-HSV-1, two experiments).

number of c-FLIP$_L$ mRNA transcripts in the cytoplasm was not decreased after infection (19 ± 5 % in HSV-1 infected iDCs compared to 8 ± 1 % in uninfected cells). UV-inactivated HSV-1 and LPS also increased the amount of c-FLIP$_L$ mRNA in the nucleus and the cytoplasm of iDCs (uv-HSV-1, 62 ± 3 % in the nucleus and 29 ± 7 % in the cytoplasm; LPS, set to 100 % in both cell compartiments). This might be due to induction of maturation of iDCs, which is known to be associated with elevated c-FLIP$_L$ transcription [58]. Heat-inactivated HSV-1 did not increase the amount of c-FLIP$_L$ mRNA (32 ± 6 % in the nucleus and 11 ± 2 % in the cytoplasm) compared to uninfected cells (20 ± 4 % in the nucleus and 8 ± 1 % in the cytoplasm). Because the ratio cytoplasm/nucleus of the amount of c-FLIP$_L$ mRNA was 0.2 in HSV-1 infected cells compared to 0.5 in uv-HSV-1 infected cells and 0.4 in uninfected control cells, there might be some retention of c-FLIP$_L$ mRNA in the nucleus of infected iDCs. However, the amount of c-FLIP$_L$ mRNA in the cytoplasm was not decreased after HSV-1 infection of iDCs compared to uninfected iDCs.

Based on these observations it can be concluded that downregulation of c-FLIP by HSV-1 is not due to disturbances of mRNA-transcription, stability or transport, but rather due to degradation of the protein itself.

3.3.2 Impact of HSV-1 infection on overexpressed c-FLIP

Isolation and differentiation of iDCs is labor-intensive and expensive. Furthermore, flow cytometry of fluorophore-tagged proteins allows a much more direct quantification of the protein amount than immunoblot analysis. Therefore, studies on the mechanism of c-FLIP downregulation by HSV-1 were planned to be performed in c-FLIP transfected cell lines instead of iDCs.

Overexpressed c-FLIP is resistant to HSV-1 induced downregulation

HEp-2 cells were transfected with eucaryotic expression plasmids containing EGFP tagged c-FLIP$_L$ (FLIP$_L$-EGFP) or c-FLIP$_S$ (FLIP$_S$-EGFP) or EGFP alone. After 32 h, cells were infected with HSV-1 (strain KOS, MOI 1 - 3) or left uninfected. 18 h p. i., cells were stained with an antibody against viral glycoprotein gD, which accumulates on the surface of infected cells, and analyzed by flow cytometry. Results are depicted in figure 3.5.

In some experiments, the geo mean fluorescence intensity of FLIP$_L$-EGFP and FLIP$_S$-EGFP after HSV-1 infection was slightly reduced in gD-positive cells (upper right quadrant) compared to gD-negative cells (lower right quadrant) while the geo mean fluorescence intensity of EGFP alone was slightly enhanced (85 compared to 92 for FLIP$_L$-EGFP, 137 compared to 183 for FLIP$_S$-EGFP, 589 compared to 562 for EGFP, figure 3.5A, lower panel). However, when mean values $\pm$ SD were calculated from three independent experiments, no reproducible and significant difference in geo mean fluorescence intensity of FLIP$_L$-EGFP, FLIP$_S$-EGFP, or EGFP was observed between gD positive and gD negative cells, which were set to 100 % (FLIP$_L$-EGFP, 105 ± 23 %; FLIP$_S$-EGFP, 88 ± 19 %; EGFP, 135 ± 43 %; figure 3.5B).

From these data it must be concluded, that overexpressed c-FLIP is to a large extent resistant to downregulation by HSV-1. There are several possible explanations for this result: i) The mechanism of HSV-1 induced c-FLIP downregulation is operative only in iDCs, but not in HEp-2 cells. ii) The EGFP tag protects c-FLIP against degradation by HSV-1. iii) Stable EGFP tagged degradation products of c-FLIP are formed after HSV-1 infection. iv) The amount of c-FLIP in transiently transfected cells exceeds the capacity of the HSV-1 induced degradation mechanism.

Immunoblot analysis would be helpful to elucidate the reason why transfected c-FLIP-EGFP is not downregulated by HSV-1. For example, intermediate degradation products of c-FLIP-EGFP could be detected and smaller non-fluoresce tags could be used. However, efficiency of transfection and infection achieved in the experiment presented above were not sufficient for immunoblot analysis. Transfection efficiency was low and only one third to half of EGFP-positive cells were infected, as determined by staining against HSV-1 gD (FLIP$_L$-EGFP, 8 % EGFP$^+$/gD$^-$ and 6 % EGFP$^+$/gD$^+$; FLIP$_S$-EGFP, 7 % EGFP$^+$/gD$^-$ and 6 % EGFP$^+$/gD$^+$; EGFP, 6 % EGFP$^+$/gD$^-$ and 5 % EGFP$^+$/gD$^+$; figure 3.5A, lower panel). Therefore, transfection and infection had to be optimized.

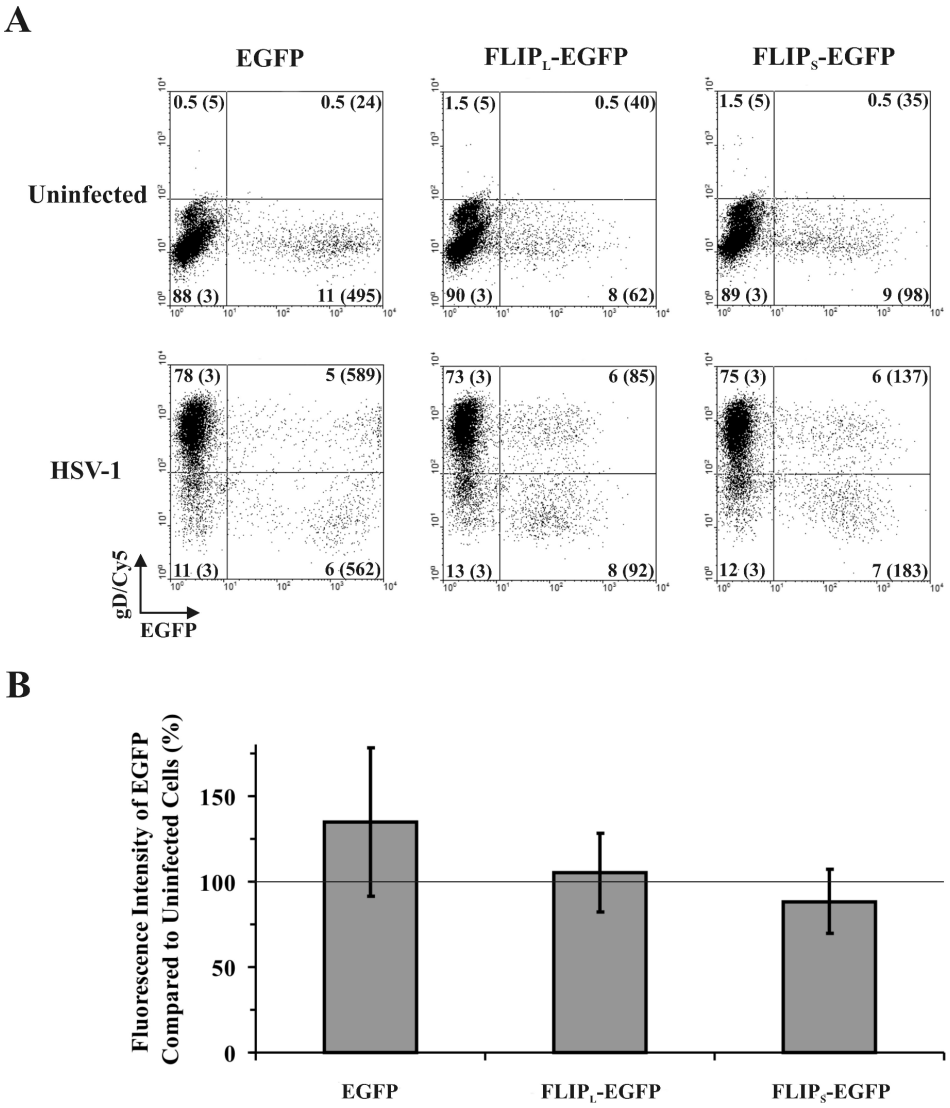

Figure 3.5: **Flow cytometry analysis of EGFP-tagged c-FLIP in HSV-1 infected cells.** HEp-2 cells were transfected with pEGFP-N1 (EGFP), FLIP$_L$-EGFP, or FLIP$_S$-EGFP using ExGen 500 and 32 h later infected with HSV-1 (strain KOS, MOI 1 - 3) or were left uninfected. 18 h p. i., cells were harvested, stained with anti-gD antibody (stains glycoprotein gD of HSV-1 on surface of infected cells) and goat-anti-mouse-Cy5 secondary antibody and immediately analyzed by flow cytometry. **(A)** Dot plots from one representative experiment are shown. Numbers in each quadrant indicate percentage of cells contained in this quadrant and in brackets the geo mean fluorescence intensity of the EGFP signal. **(B)** Mean values ± SD of the geo mean fluorescence intensity of the EGFP signal of gD-positive cells compared to gD-negative cells (set to 100 %) obtained in three independent experiments.

Optimization of transfection and infection

Using immunoblot analysis, detection of the impact of HSV-1 infection on overexpressed c-FLIP could be difficult when efficiency of infection in transfected cells is low. To achieve a higher number of $EGFP^+/gD^+$ cells, different transfection reagents and cell types were tested (figure 3.6) and the MOI was titrated.

HEp-2 cells were transfected with pEGFP-N1 using ExGen 500 and 32 h later infected with HSV-1 (strain KOS, MOI 100) or were left uninfected. Only one third of EGFP-positive cells were also HSV-1 gD positive, as determined by flow cytometry (5.4 % $EGFP^+/gD^-$ and 2.7 % $EGFP^+/gD^+$, figure 3.6A, third diagram). From these data it must be concluded that ExGen 500 transfection can disturb HSV-1 infection, even at high MOI (MOI 100). Therefore, another transfection reagent, FuGENE® 6, was tested. At MOI 100, FuGENE® 6 transfection allowed high infection efficiency. Almost all EGFP positive cells were also gD-positive (0.4 % $EGFP^+/gD^-$ and 10.2 % $EGFP^+/gD^+$, figure 3.6A, fifth diagram). Lipofectamine^{TM} 2000 was also used in some experiments, but it also reduced infectibility of cells (14.6 % $EGFP^+/gD^-$ and 8.6 % $EGFP^+/gD^+$, data not shown).

To improve transfection efficiency, different cell types were transfected with pEGFP-N1 using FuGENE® 6. The highest transfection efficiency was achieved with A549 cells (26.4 % EGFP positive cells, figure 3.6B, second diagram). HeLa, HaCaT and HEK cells were also tested but all showed lower transfection efficiencies (data not shown). Based on these results, all following experiments were conducted in A549 cells, transfected with FuGENE® 6.

In order to find the optimal MOI for efficient infection of transfected cells, a titration of HSV-1 strain KOS was done on pEGFP-N1 transfected A549 cells (figure 3.6C). The experiment revealed that the number of $EGFP^+/gD^+$ cells was still high at MOI 50 and MOI 10, but was decreased at lower MOI ($EGFP^+/gD^+$ cells, 29.3 % at MOI 50, 23.4 % at MOI 10, 21.7 % at MOI 3, 9.8 % at MOI 1). Therefore, following experiments were performed at MOI 10 or MOI 50.

HSV-1 induced downregulation of overexpressed c-FLIP is restored by mutation of the DED

Ishioka and colleagues showed that overexpressed c-$FLIP_L$ forms aggregates and is resistant to degradation by the proteasome [67]. This aggregation is mediated by the death effector domains (DEDs) contained in the c-$FLIP_L$ molecule. By mutation of the DEDs, Ishioka *et al.* could restore the proteasomal turnover of overexpressed c-$FLIP_L$. Figure 1.4 shows the mutants used in this publication and their distribution in transfected cells. The tendency of overexpressed c-$FLIP_L$ to form insoluble aggregates could also contribute to its resistance against HSV-1 induced downregulation observed in the experiments presented above (figure 3.5). In these experiments, similar dot-like aggregates as published by Ishioka *et al.* [67] were observed in $FLIP_L$-EGFP transfected cells when analyzed under a microscope (data not shown). Based on these considerations, it was investigated, whether specific mutation of c-FLIP could also restore the suscep-

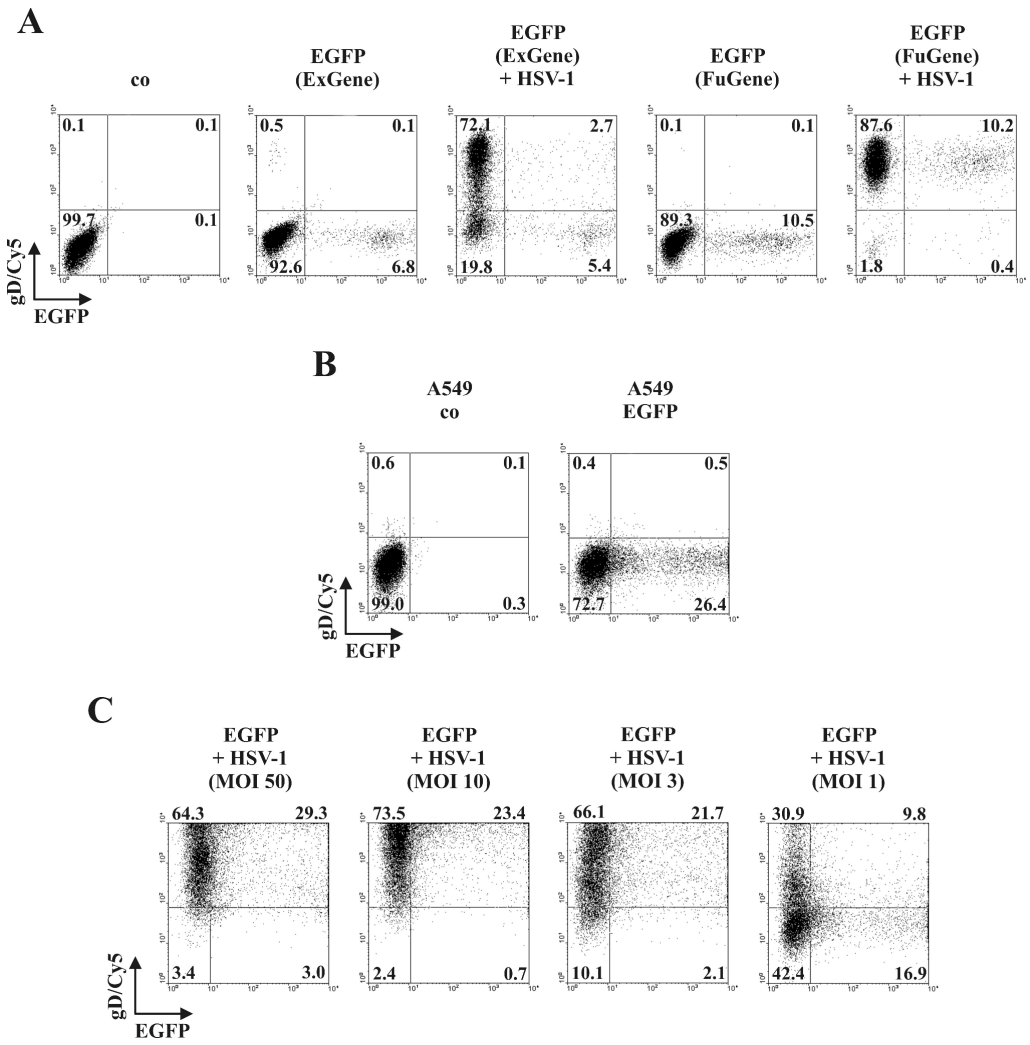

Figure 3.6: **Optimization of transfection and infection.** Cells were transfected with pEGFP-N1 and 32 h later infected with HSV-1 (strain KOS) or were left uninfected. 18 h p. i., cells were harvested, stained with anti-gD-antibody (detects HSV-1 glycoprotein D at surface of infected cells) and goat-anti-mouse-Cy5 secondary antibody and immediately analyzed on a flow cytometer. Numbers in or above each quadrant indicate percentage of cells contained in this quadrant. co, non-transfected and uninfected control cells. **(A)** HEp-2 cells were transfected with two different transfection reagents (ExGen 500 or FuGENE® 6) and infected with HSV-1 (KOS, MOI 100). **(B)** A549 cells were transfected with FuGENE® 6 and left uninfected or were **(C)** infected with HSV-1 strain KOS at different MOI as indicated.

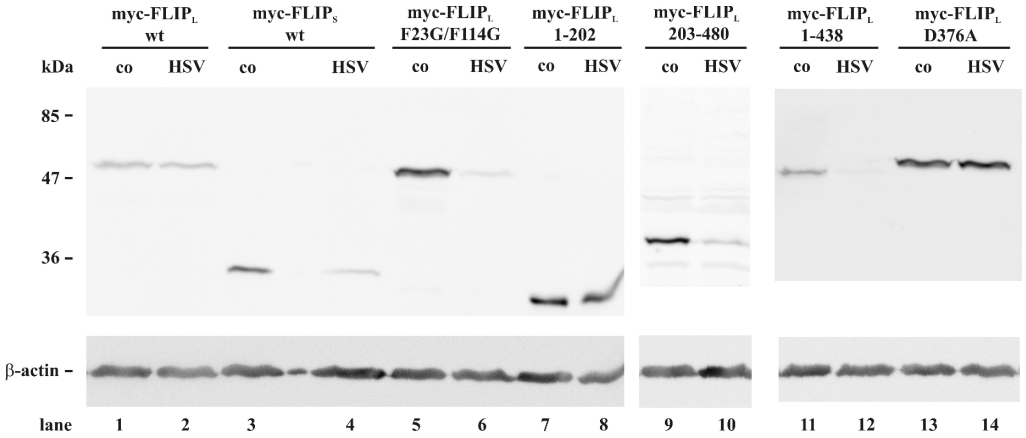

Figure 3.7: **Immunoblot analysis of mutated c-FLIP after HSV-1 infection.** A549 cells were transfected with different expression plasmids encoding myc-tagged wild type (wt) and mutant c-FLIP (described in figure 1.4) using FuGENE® 6 transfection reagent and 17 h later each transfection was split into two petri dishes. 24 h after transfection cells were infected with HSV-1 strain KOS at MOI 50 or were left uninfected (co). Cells were harvested and lysed at 18 h post infection. Lysates were subjected to SDS-PAGE separation with subsequent blotting to PVDF membranes. c-FLIP was detected either with anti-myc-antibody (myc-FLIP$_L$ 203-480) or with anti-FLIP-antibody (clone NF6, all other c-FLIP forms). Subsequent staining of blots with anti-β-actin antibody served as loading control. Blots shown are representative of three independent experiments.

tibility of overexpressed c-FLIP to HSV-1 induced downregulation.

Therefore, the c-FLIP mutants generated by Ishioka *et al.* [67] were transfected into A549 cells. 24 h after transfection, half of the cells were infected with HSV-1 (wild type strain KOS, MOI 50). 18 h p. i., cells were harvested and analyzed by immunoblot. Results are depicted in figure 3.7. In accordance with the results obtained by flow cytometry analysis (figure 3.5), wild type forms of c-FLIP were either not (myc-FLIP$_L$, figure 3.7 lanes 1 and 2) or only weakly (myc-FLIP$_S$, figure 3.7 lanes 3 and 4) downregulated by HSV-1, although the C-terminal EGFP tag was exchanged with a N-terminal myc tag. Furthermore, wild type c-FLIP forms detected in uninfected and HSV-1 infected cells appeared to have the same molecular mass and no stable degradation products were detected. c-FLIP$_L$ with a mutated caspase cleavage site (myc-FLIP$_L$ D376A, figure 3.7 lanes 13 and 14) and truncated c-FLIP$_L$ consisting only of DEDs (myc-FLIP$_L$ 1-202, figure 3.7 lanes 7 and 8) were also resistant to HSV-1 induced downregulation. However, mutation (c-FLIP$_L$ F23G/F114G, figure 3.7 lanes 5 and 6) or removal (c-FLIP$_L$ 203-480, figure 3.7 lanes 9 and 10) of the DEDs restored susceptibility of c-FLIP$_L$ to HSV-1 induced downregulation. Interestingly, certain modifications of the C-terminus also increased the susceptibility of c-FLIP with functional DEDs to downregulation by HSV-1, as was the case for truncated myc-FLIP$_L$ 1-438 (figure 3.7 lanes 11 and 12) and

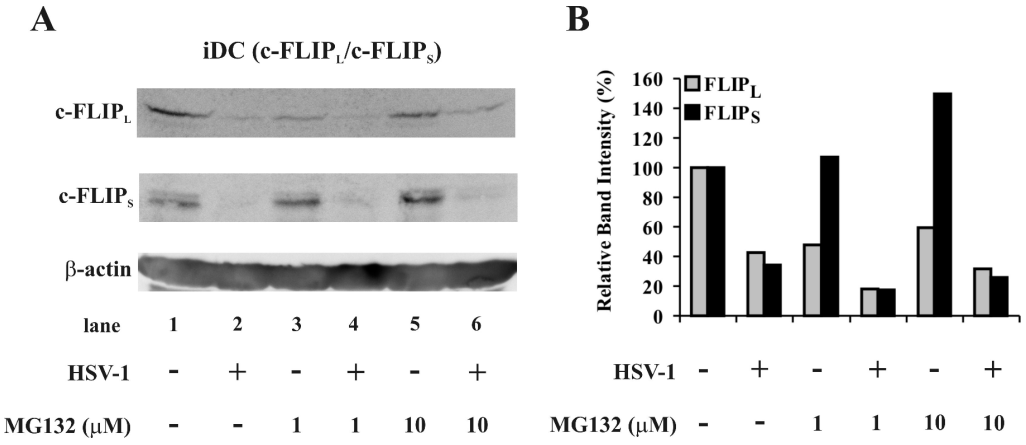

Figure 3.8: **Immunoblot of c-FLIP in HSV-1 infected iDCs treated with the proteasome inhibitor MG132.** iDCs were infected with HSV-1 (KOS, MOI 3) or left uninfected. MG132 was added at 1 μM at 5.25 h p. i. or at 10 μM at 7.5 h p. i. iDCs were lysed at 10 h p. i. and subjected to immunoblot analysis using anti-FLIP-antibody (clone NF-6). Staining of the blots with antibody against β-actin served as a loading control. **(A)** One representative blot out of three experiments is shown. **(B)** Relative band intensity of c-FLIP bands was determined by densitometry and normalized to β-actin. The value obtained with uninfected and untreated iDCs was set to 100 %.

for myc-FLIP$_S$ (figure 3.7 lanes 3 and 4), which contains a unique C-terminus.

From these results a number of conclusions can be drawn: i) HSV-1 can induce downregulation of c-FLIP also when it is overexpressed in cell lines, however, ii) aggregation of overexpressed c-FLIP mediated via DEDs impairs downregulation by HSV-1. ii) Experiments to study the mechanism of HSV-1 induced c-FLIP downregulation in transfected cells should be conducted with mutated forms of c-FLIP, for example c-FLIP$_L$ F23G/F114G, which are susceptible to downregulation because the DED's are mutated. iii) Interference with the ability of c-FLIP to bind to the DISC (by mutation of the DEDs) does not disturb HSV-1 induced downregulation. iv) The mechanism of HSV-1 induced downregulation of c-FLIP is presumably operative directly on the protein.

3.3.3 Effect of inhibition of the proteasome on c-FLIP reduction by HSV-1

c-FLIP has been shown to have a short half-life time. Turnover occurs mainly via proteasomal degradation [41, 89, 128, 135]. Therefore it was analyzed whether HSV-1 induced downregulation of c-FLIP could be mediated by enhanced proteasomal turnover.

To block the function of the proteasome, the inhibitor MG132 was added to infected iDCs (HSV-1 strain KOS, MOI 3) either at 1 μM at 5.25 h p. i. or at 10 μM at 7.5 h p. i. The amount of c-FLIP was determined at 10 h p. i. by immunoblot analysis. Without addition of MG132, the amount of c-FLIP$_L$ (grey column) was decreased to 43 % and the amount of c-FLIP$_S$ (black column) was decreased to 34 % in HSV-1 infected iDCs

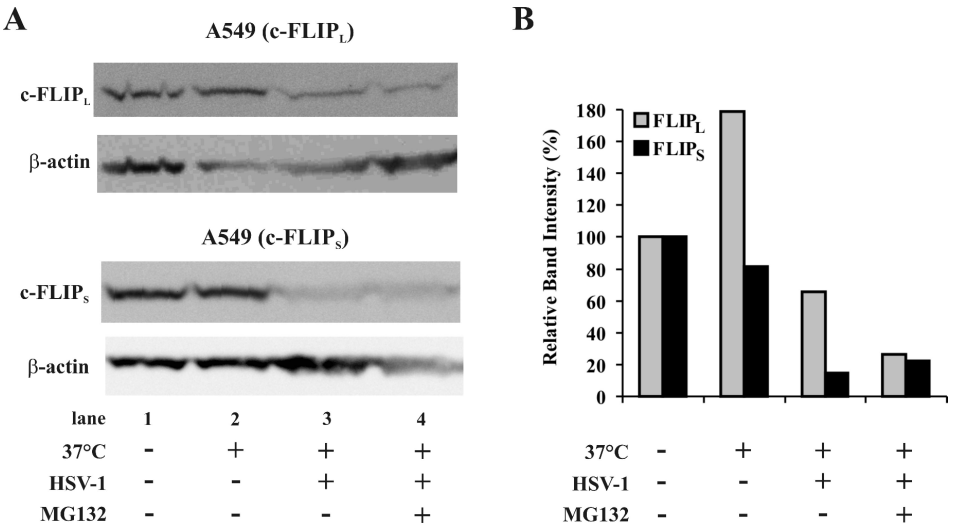

Figure 3.9: **Degradation of c-FLIP by lysates derived from HSV-1 infected cells. (A)** A549 cells were transfected using TurboFect^{TM} with a mutated form of c-FLIP$_L$ (F23G/F114G, upper panel) that does not aggregate when overexpressed in cells [67] or FLIP$_S$-EGFP (lower panel). Lysates were prepared after 48 h and four aliquots were generated. One aliquot was kept at -20 °C until loading on SDS-PAGE, another aliquot was incubated for 2 h at 37 °C and then loaded on SDS-PAGE. The two remaining aliquots were each mixed with lysates of untransfected A549 cells, which were infected with HSV-1 (strain KOS, MOI 10, lysed at 18 h p. i.). The mixed lysates were incubated at 37 °C for 2 h in the presence or absence of proteasome inhibitor MG132 (50 μM) before loading on SDS-PAGE. After blotting to PVDF-membranes, c-FLIP was detected with anti-FLIP antibody (clone NF-6). Staining of the blots with antibody against β-actin served as a loading control. **(B)** Relative band intensity of c-FLIP bands was determined by densitometry and normalized to β-actin. The value obtained with lysates kept at -20 °C was set to 100 %.

(figure 3.8 lane 2) compared to uninfected iDCs (amount of c-FLIP$_L$ and c-FLIP$_S$ set to 100 %, figure 3.8 lane 1). Inhibition of the proteasome did not prevent HSV-1 induced reduction of the amount of c-FLIP$_L$ or c-FLIP$_S$ regardless whether MG132 was added at 1 μM (c-FLIP$_L$, 18 %; c-FLIP$_S$, 17 %; 3.8 lane 4) or at 10 μM (c-FLIP$_L$, 32 %; c-FLIP$_S$, 26 %; 3.8 lane 6).

Interestingly, addition of MG132 to uninfected cells increased the amount of c-FLIP$_S$ (1 μM, 107 %; 10 μM, 150 %; figure 3.8 lanes 3 and 5). This can be explained with the high turnover of c-FLIP$_S$ by the proteasome, which is published to be higher than turnover of c-FLIP$_L$ [135]. So it is expected that c-FLIP$_S$ accumulates in the cells when the proteasome is blocked. Intriguingly, c-FLIP$_L$ behaves completely different. It is reduced in uninfected iDCs treated with MG132 compared to untreated iDCs (1 μM, 48 %; 10 μM, 59 %; figure 3.8 lanes 3 and 5). This observation indicates, that turnover of c-FLIP$_L$ might be mediated by a mechanism other than proteasomal degradation, at least in

iDCs. When the proteasome is blocked in iDCs by addition of MG132, the amount of c-FLIP$_L$ might be decreased because transcription of c-FLIP$_L$ mRNA is dependent on NFκB [93, 111]. Activation of NFκB is mediated by proteasomal degradation of iκB [45].

The results obtained in the experiment presented above indicate that it is unlikely that the downregulation of c-FLIP observed in HSV-1 infected cells is mediated by enhanced proteasomal turnover. Therefore, another experiment was performed to analyze whether lysates of HSV-1 infected cells contain a factor, which could directly attack c-FLIP. To proof this, A549 cells were transfected with myc-FLIP$_L$ (F23G/F114G) or FLIP$_S$-EGFP and lysed after 48 h. Lysates of these cells showed a high expression of transfected c-FLIP in immunoblot analysis, regardless whether lysates were kept at -20 °C (amount of myc-FLIP$_L$ (F23G/F114G) and c-FLIP$_S$-EGFP set to 100 %, figure 3.9 lane 1) or were incubated at 37 °C for 2 h (myc-FLIP$_L$ (F23G/F114G), 179 %; c-FLIP$_S$-EGFP, 82 %; figure 3.9 lane 2). However, when myc-FLIP$_L$ (F23G/F114G) or FLIP$_S$-EGFP containing lysates were mixed with lysates from HSV-1-infected, untransfected A549 cells and incubated for 2 h at 37 °C, the amount of c-FLIP$_L$ (66 %, figure 3.9 lane 3) and c-FLIP$_S$-EGFP (15 %, figure 3.9 lane 3) was strongly decreased. Furthermore, reduction of c-FLIP induced by HSV-1 lysates could not be prevented by addition of the proteasome inhibitor MG132 (myc-FLIP$_L$ (F23G/F114G), 26 %; c-FLIP$_S$-EGFP, 22 %; figure 3.9 lane 4).

Taken together, the data presented in this section hint to a viral or cellular factor, which is expressed in HSV-1 infected cells and directly causes c-FLIP degradation independent from the proteasome.

3.3.4 Amount of c-FLIP after infection of iDCs with replication defective HSV-1

Next it was investigated in which part of the HSV-1 replication cycle the c-FLIP downregulating factor could be expressed. Kinetic data presented in section 3.2 indicate that c-FLIP is downregulated in the late part of HSV-1 replication (12 h p. i.). However, Müller *et al.* [115] showed that HSV-1 induced c-FLIP downregulation is not disturbed if HSV-1 DNA replication and consequently expression of true late viral genes is blocked using aciclovir. Hence, one or several leaky late HSV-1 genes most likely mediate c-FLIP degradation.

Based on these considerations, one experiment was performed with a HSV-1 mutant (ΔICP27 [154]), which is deleted for the essential regulatory immediate early ICP27 protein. ΔICP27 shows impaired expression of some early and most late genes, while immediate early genes are expressed properly or are overexpressed [146, 158].

iDCs were infected with ΔICP27 or wild type HSV-1 strains F or KOS (MOI 1.5). For control, iDCs were incubated with the respective heat-inactivated or UV-inactivated virus or were left uninfected. The amount of c-FLIP was analyzed by immunoblot at 18 h p. i.

As expected, the amount of c-FLIP$_L$ and c-FLIP$_S$ was strongly reduced in iDCs infected with wt HSV-1 strains F or KOS (figure 3.10, lane 3) compared to uninfected control iDCs (figure 3.10, lane 4). After infection of iDCs with ΔICP27, the amount of

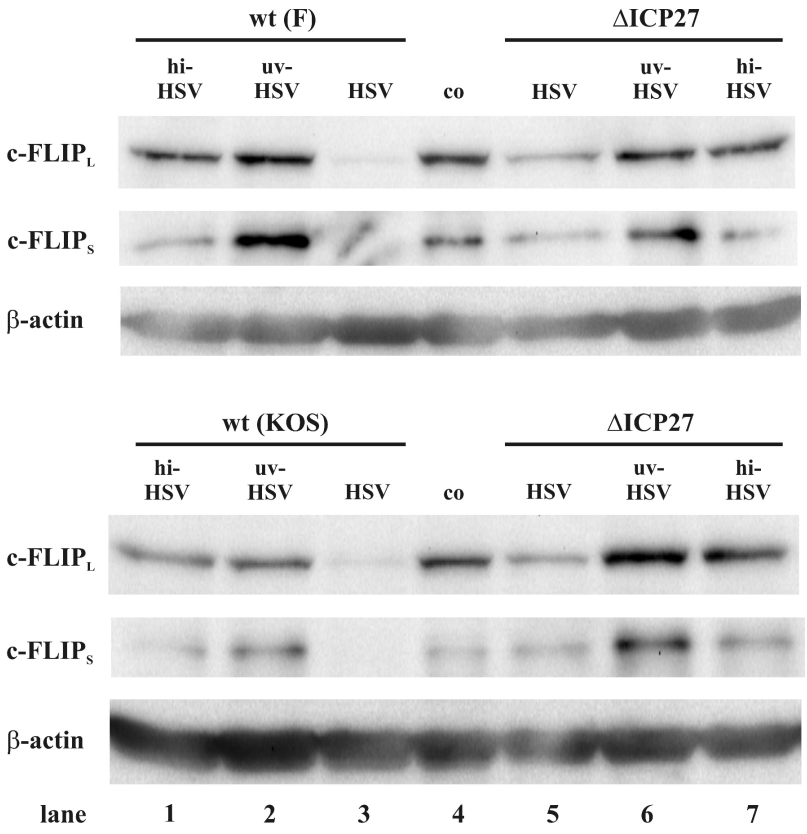

Figure 3.10: **Immunoblot analysis of c-FLIP in ΔICP27 infected iDCs.** iDCs were infected with wt HSV-1 (strain F or KOS as indicated) or a ICP27 knockout mutant of HSV-1 (ΔICP27) at MOI 1.5. For control, iDCs were either left uninfected (co) or were treated with heat-inactivated (hi-HSV) or UV-inactivated (uv-HSV) virus. 18 h p. i. cells were lysed and subjected to immunoblot analysis. FLIP was visualized by staining with anti-FLIP antibody (clone NF6). After stripping, membranes were stained with anti-β-actin-antibody in order to control for equal protein loading. Blots are representative of four experiments.

c-FLIP$_L$ and c-FLIP$_S$ was also reduced (figure 3.10, lane 5), but to a lesser extent compared to wild type HSV-1 infected iDCs (figure 3.10, lane 3). Heat-inactivated (figure 3.10, lanes 1 and 7) and UV-inactivated (figure 3.10, lanes 2 and 6) did not induce downregulation of c-FLIP$_L$ or c-FLIP$_S$.

Attenuated downregulation of c-FLIP after infection of iDCs with ΔICP27 indicates that one early or leaky late gene of HSV-1, which is expressed to a lower extent in this HSV-1 mutant, is involved in c-FLIP downregulation. Furthermore, UV-inactivated HSV-1 was not able to downregulate c-FLIP in iDCs. This shows that c-FLIP downregulation is dependent on transcription of viral genes, while attachment of virus particles and release of viral DNA into the cell are not sufficient to induce c-FLIP downregulation.

3.3.5 Immunofluorescence analysis of c-FLIP in HSV-1 infected cells

In order to further elucidate the factor(s), which cause the degradation of c-FLIP in HSV-1 infected cells, the cellular distribution of c-FLIP was compared in infected and uninfected cells by fluorescence microscopy. However, the amount of c-FLIP in iDCs was too low to be detected with this method. Therefore, experiments were performed in A549 cells transiently transfected with a mutated form of c-FLIP$_L$ (F23G/F114G), which does not form aggregates when overexpressed in cells [67] and is therefore susceptible to HSV-1 induced downregulation (see section 3.3.2).

In uninfected cells, overexpressed c-FLIP$_L$ (F23G/F114G) was evenly distributed (figure 3.11A). 11 h p. i. with HSV-1 (strain KOS, MOI 10) exposure time for detection of c-FLIP$_L$ had to be approximately twice as long as in uninfected cells in order to get the same intensity of the signal. That indicated, that degradation of c-FLIP$_L$ had already started. Furthermore, in the majority of cells c-FLIP$_L$ appeared to form more or less dense accumulations (figure 3.11C and 3.11E). These accumulations were round or oval shaped in cells with a stronger signal and dot-like in cells with a weaker signal. Based on these data it is conceivable that for degradation, c-FLIP$_L$ must accumulate in special structures of HSV-1 infected cells.

Co-staining of the transfected cells with anti-HSV-1 serum did not reveal viral proteins in the observed c-FLIP$_L$ accumulations (figure 3.11D and 3.11F). Due to the fact that the anti-serum might not detect all viral proteins expressed in HSV-1 infected cells, this observation does not exclude the possibility that c-FLIP interacts with a viral factor.

3.3.6 Co-transfection of c-FLIP with HSV-1 proteins US3 and gJ

Based on previous publications, there are two viral proteins, which could directly influence c-FLIP stability: i) HSV-1 protein kinase U$_S$3 can phosphorylate procaspase-3 [18]. Therefore, it could be possible that U$_S$3 also phosphorylates the caspase-homolog c-FLIP. Furthermore, the stability of c-FLIP can be regulated by phosphorylation [86]. ii) HSV-1 glycoprotein gJ induces ROS formation [10] and there is evidence that c-FLIP stability is influenced by ROS [90, 101]. In addition, both U$_S$3 and gJ are leaky late

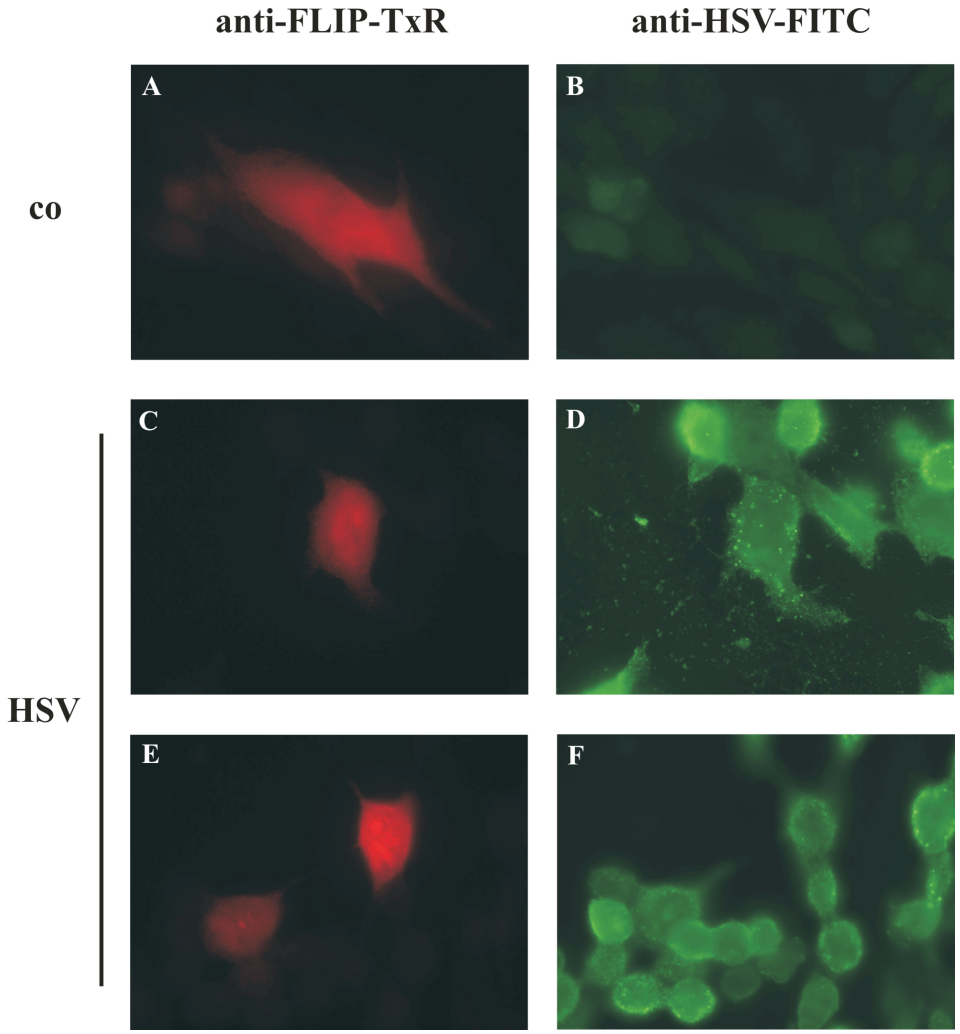

Figure 3.11: **Immunofluorescence analysis of the distribution of c-FLIP in HSV-1 infected cells.** A549 cells were transfected using FuGENE® 6 with a mutated form of c-FLIP$_L$ (F23G/F114G) that does not aggregate when overexpressed in cells [67]. After 14 h cells were seeded on glass slides. 35 h post transfection half of the slides were infected with HSV-1 (strain KOS, MOI 10), the remaining slides were left uninfected (co). 10 μM MG132 was added at 7.5 h p. i. to stop proteasomal degradation of proteins. 11 h p. i. cells were fixed with 3.7 % PFA and stained with anti-FLIP (clone NF6) followed by anti-mouse-TexasRed (TxR) secondary antibody and with anti-HSV rabbit serum followed by anti-rabbit-FITC secondary antibody. Representative analyses out of two experiments are shown (100 x magnification).

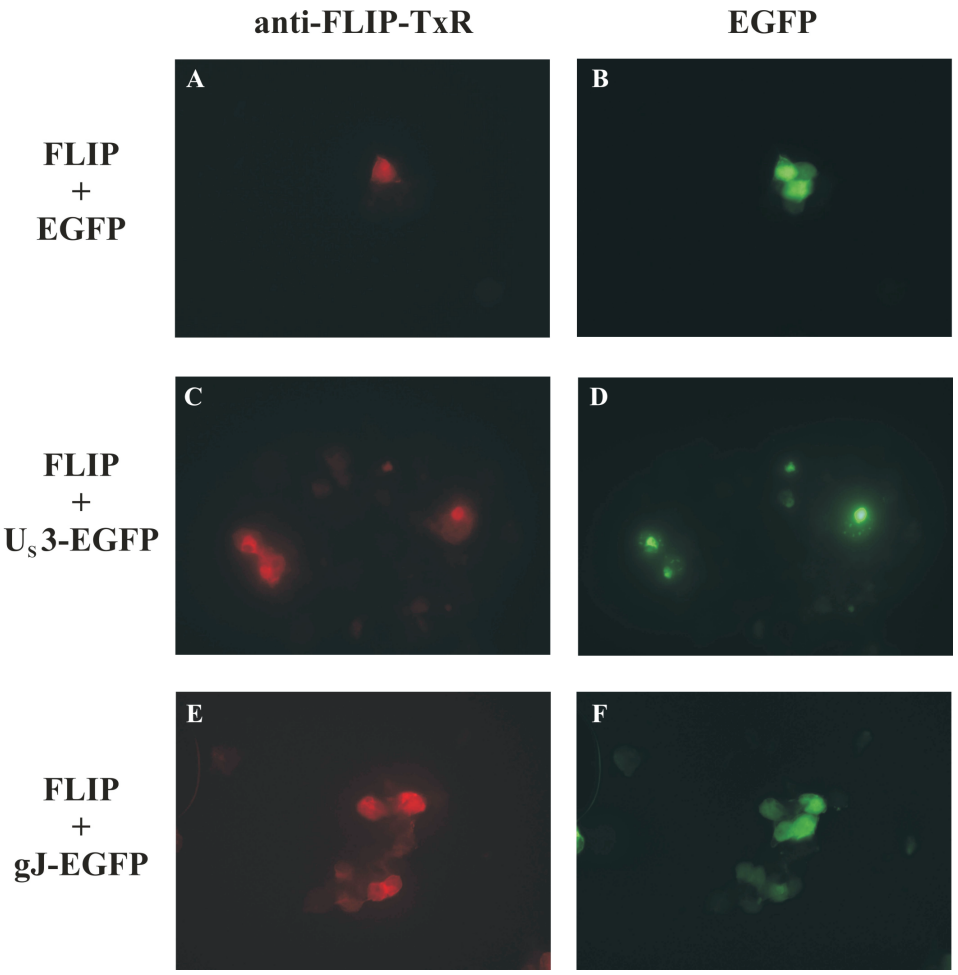

Figure 3.12: **Immunofluorescence analysis of c-FLIP$_L$ co-transfected with EGFP, U$_S$3-EGFP, or gJ-EGFP.** HEK cells were transfected using TurboFect^{TM} with a mutated form of c-FLIP$_L$ (F23G/F114G) that does not aggregate when overexpressed in cells [67] and pEGFP-N1, U$_S$3-EGFP, or gJ-EGFP as indicated. After 30 h cells were plated on poly-L-Lysin coated glass-slides. 48 h post transfection cells were fixed with 3.7 % PFA and stained with anti-FLIP (clone NF6) followed by anti-mouse-TexasRed (TxR) secondary antibody. Representative analyses out of two experiments are shown (60 x magnification).

HSV-1 genes, which show reduced expression by the ΔICP27 HSV-1 mutant. Therefore, in view of the results presented in section 3.3.4, U_S3 and gJ are good candidates for a c-FLIP downregulating factor of HSV-1.

In order to investigate whether U_S3 or gJ could directly downregulate c-FLIP, HEK cells were co-transfected using TurboFect^{TM} with myc-FLIP$_L$ (F23G/F114G) and U_S3-EGFP or gJ-EGFP. For comparison, myc-FLIP$_L$ (F23G/F114G) was co-transfected with EGFP. Expression of the transfected proteins was analysed by immunofluorescence.

None of the three co-transfected proteins reduced the amount of c-FLIP$_L$. All three co-transfections showed a strong c-FLIP$_L$ signal also in EGFP-positive cells (figure 3.12). However, co-localization of U_S3-EGFP and c-FLIP$_L$ was observed. In double-transfected cells, c-FLIP$_L$ accumulated in the same area of the cells where the characteristic dot-like aggregates were localized, which are formed by U_S3-EGFP when overexpressed in HEK cells, see figure 3.12C and 3.12D. Furthermore, these structures were similar to the aggregates of c-FLIP$_L$ observed in HSV-1 infected cells (figure 3.11C,E). In co-transfections of c-FLIP$_L$ with EGFP or gJ-EGFP no such obvious co-localization was observed, see figures 3.12A,B and 3.12E,F.

Taken together, it was demonstrated here that HSV-1 kinase U_S3, but not HSV-1 glycoprotein gJ, co-localizes with c-FLIP when co-transfected into cells. These data indicate that U_S3 might interact with c-FLIP. However, co-transfection of U_S3 in the absence of HSV-1 infection was not sufficient to downregulate c-FLIP.

3.3.7 Mechanism of c-FLIP downregulation by HSV-1: Summary

In this thesis the mechanism of HSV-1 induced c-FLIP downregulation was resolved to a large extent. First it was demonstrated, that the decrease in c-FLIP observed in HSV-1 infected iDCs is not due to reduced availability of mRNA for translation. It was furthermore shown that downregulation of c-FLIP after HSV-1 infection is independent from the proteasome and the ability of c-FLIP to bind to the DISC. Instead, c-FLIP was degraded directly by factor(s) contained in lysates of HSV-1 infected cells. It was found that c-FLIP downregulation occurs in the late stage of viral replication and is dependent on proper expression of early and leaky late HSV-1 genes. Co-localization indicates that the HSV-1 kinase U_S3 interacts with c-FLIP. However, in the absence of HSV-1 infection U_S3 did not downregulate c-FLIP. Therefore, further viral or cellular factors are required for downregulation of c-FLIP after HSV-1 infection of cells.

3.4 c-FLIP amount and apoptosis after HSV-1 infection of different cell types

The experiments presented above demonstrate that HSV-1 can not only downregulate naturally expressed c-FLIP in iDCs, but also c-FLIP which is expressed in cell lines from a transfected vector. Next it was investigated, whether HSV-1 can also induce downregulation of naturally expressed c-FLIP in cells other than iDCs and whether HSV-1 infection induces apoptosis in these cells. The following cells were tested: epithelial

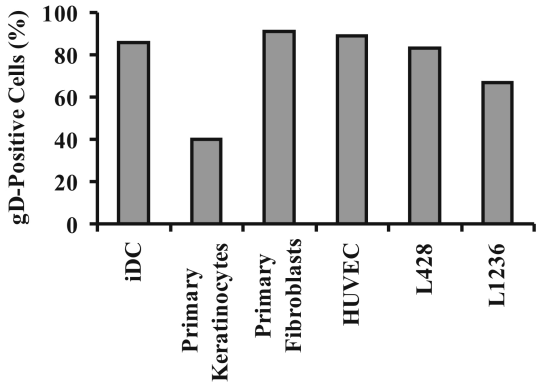

Figure 3.13: **Efficiency of HSV-1 infection in different cell types, determined by staining against gD.** Cells were infected with HSV-1 strain F at MOI 1 (iDCs), MOI 1.5 (fibroblasts, keratinocytes), MOI 3 (HUVEC), or MOI 5 (L428, L1236). 18 h p. i. (fibroblasts, 16.5 h p. i.) cells were harvested and the number of HSV-1 positive cells was determined by flow cytometric analysis after staining against the viral glycoprotein gD (background staining as determined by staining of uninfected cells was subtracted). Data are representative of four experiments (iDCs, HUVEC) or three experiments (primary keratinocytes, L428) or two experiments (primary fibroblasts, L1236).

cells (primary keratinocytes), connective tissue cells (primary fibroblasts), endothelial cells (HUVEC) and hematopoetical cells (Hodgkin/Reed-Sternberg cell lines L428 and L1236). Cells were infected with HSV-1 strain F at MOI 1 (iDCs), MOI 1.5 (fibroblasts, keratinocytes), MOI 3 (HUVEC), or MOI 5 (L428, L1236) and after 16.5 or 18 h, efficiency of infection, amount of c-FLIP, and apoptosis were determined.

Efficiency of infection was assessed by staining of cells with antibody against HSV-1 glycoprotein gD and subsequent flow cytometry, results are shown in figure 3.13. All cell types showed high percentages of gD positive cells after infection with HSV-1 (iDCs, 86 %; keratinocytes, 40 %; fibroblasts, 91 %; HUVECs, 89 %; L428, 83 %; L1236, 67 %).

Figure 3.14A shows immunoblot and densitometry analysis of the amount of c-FLIP$_L$ after HSV-1 infection. The amount of c-FLIP$_L$ was considerably lower in all tested cell types compared to uninfected cells, which were set to 100 % (iDCs 31 %, keratinocytes 36 %, fibroblasts 61 %, HUVECs 27 %, L428 30 %, L1236 22 %). No reduction respectively an increase of the amount of c-FLIP$_L$ was observed in cells treated with heat-inactivated virus (iDCs, 116 %; keratinocytes, 94 %; fibroblasts, 91 %; HUVECs, 125 %; L428, 301 %; L1236, 102 %) or UV-inactivated virus (fibroblasts, 98 %). Most tested cells (iDCs, primary keratinocytes, HUVEC, L428, L1236) also expressed c-FLIP$_S$, which was also downregulated after HSV-1 infection (data not shown).

Apoptosis was analyzed by flow cytometry of AnnexinV-FITC and propidium iodide (PI) stained cells. Figure 3.14B shows representative dot blots of HSV-1 infected,

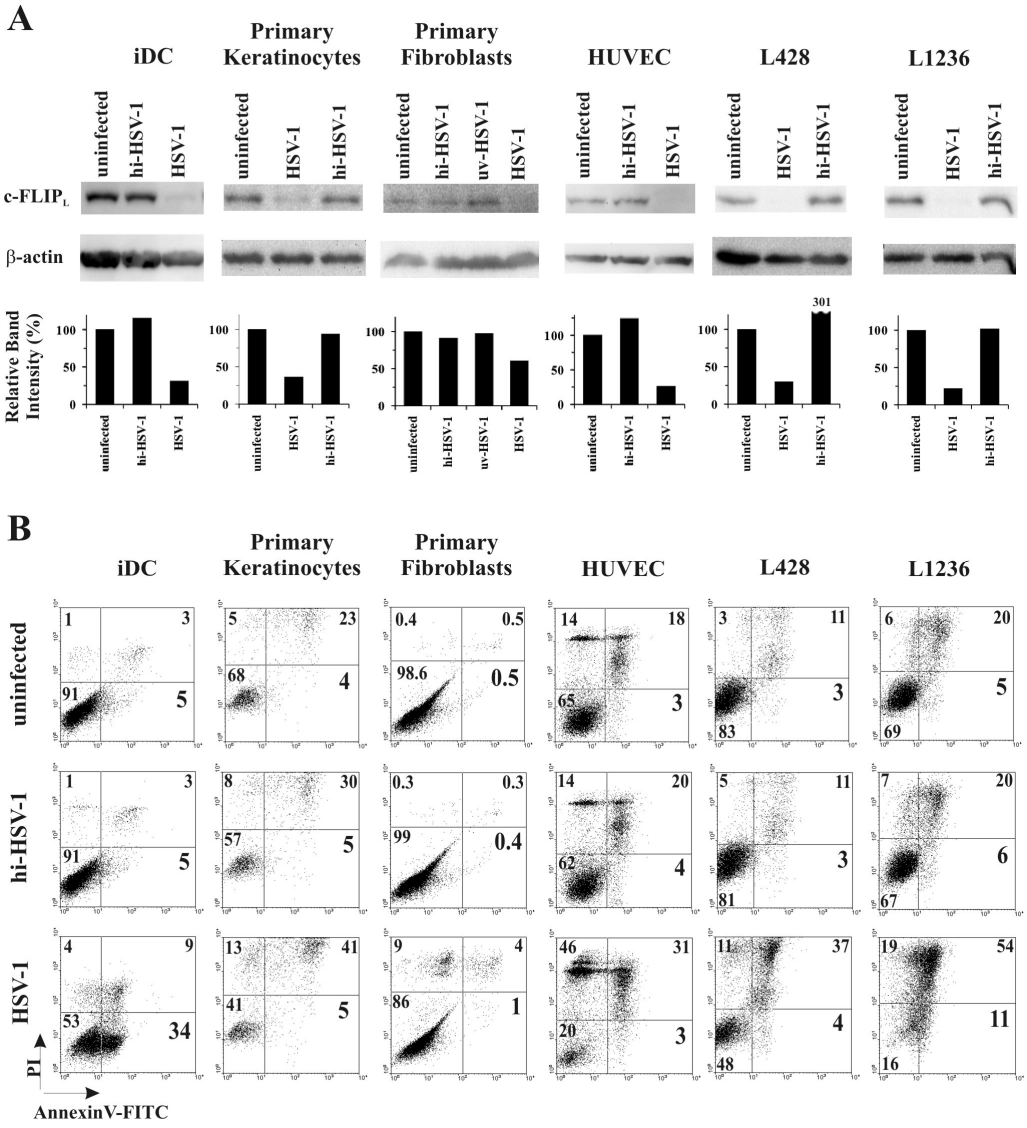

Figure 3.14: **Amount of c-FLIP (A) and extent of apoptosis (B) in different cell types after infection with HSV-1.** Cells were infected with HSV-1 strain F at MOI 1 (iDCs), MOI 1.5 (fibroblasts, keratinocytes), MOI 3 (HUVEC), or MOI 5 (L428, L1236). As a control, cells were either left uninfected or were incubated with heat-inactivated (hi-HSV-1) or UV-inactivated (uv-HSV-1) virus. **(A)** 18 h p. i. (fibroblasts, 16.5 h p. i.) cells were lysed and subjected to immunoblot analysis with c-FLIP specific antibody (clone NF-6) and β-actin specific antibody as a loading control. Below the blots, relative band intensity is depicted, as determined by densitometry of c-FLIP bands, normalized to β-actin. The value obtained with uninfected cells was set to 100 %. **(B)** Before lysis, one aliquot of cells was stained with AnnexinV-FITC/PI and apoptosis was analyzed by flow cytometry. Numbers in each quadrant indicate percentage of cells contained in this quadrant. Data are representative of four experiments (iDCs, HUVEC) or three experiments (primary keratinocytes, L428) or two experiments (primary fibroblasts, L1236).

hi-HSV-1 treated, and uninfected cells. As expected, after HSV-1 infection of iDCs the number of viable cells (AnnexinV$^-$/ PI$^-$, lower left quadrant) was drastically reduced (53 % compared to 91 % in uninfected iDCs or iDCs treated with hi-HSV-1). This reduction was mainly due to an increase in the number of apoptotic (AnnexinV$^+$/PI$^-$, lower right quadrant) iDCs, from 5 % in uninfected or hi-HSV-1 treated iDCs to 34 % after HSV-1 infection. The number of necrotic iDCs (AnnexinV$^-$/PI$^+$ and AnnexinV$^+$/PI$^+$, upper left and upper right quadrant) was only slightly increased (4 % respective 9 % after HSV-1 infection compared to 1 % respective 3 % in hi-HSV-1 treated and uninfected iDCs).

Although in primary keratinocytes, one of the main host cells for HSV-1 replication, c-FLIP$_L$ was also downregulated (figure 3.14A, second panel), the number of apoptotic cells was not increased after HSV-1 infection (5 % compared to 5 % in hi-HSV-1 treated cells and 4 % in uninfected cells, figure 3.14B, second panel). However, there was a reduction in the number of viable keratinocytes after HSV-1 infection (41 % compared to 68 % in uninfected cells and 57 % in hi-HSV-1 treated cells). This reduction was due to an increase of necrotic cells. After HSV-1 infection 13 % of keratinocytes were AnnexinV$^-$/PI$^+$ compared to 5 % in uninfected and 8 % in hi-HSV-1 treated keratinocytes. The number of AnnexinV$^+$/PI$^+$ keratinocytes was 41 % after HSV-1 infection but only 23 % in uninfected and 30 % in hi-HSV-1 treated cells.

Similar to primary keratinocytes, numbers of apoptotic cells were also not increased or only slightly increased after infection of other cells (primary fibroblasts, HUVEC, L428 and L1236). However, there was a certain degree of loss of viable cells due to necrosis (figure 3.14B). This necrotic death was probably a consequence of high viral replication causing exhaustion of these cells.

Collectively, these data indicate that downregulation of antiapoptotic c-FLIP is not sufficient for induction of apoptosis in HSV-1 infected cells and additional events must occur in iDCs.

3.5 Microarray analysis of HSV-1 gene expression in apoptotic iDCs and nonapoptotic epithelial cells

Although the antiapoptotic cellular protein c-FLIP was downregulated in all cell types after HSV-1 infection, apoptosis was only observed in HSV-1 infected iDCs (figure 3.14). In most cell types powerful antiapoptotic viral factors might counteract induction of apoptosis caused by c-FLIP downregulation, as was already demonstrated for other apoptosis inducing events [43, 71, 123]. HSV-1 genes encoding antiapoptotic factors might not be expressed properly in iDCs resulting in susceptibility of iDCs to apoptosis induced by c-FLIP downregulation. Therefore, a HSV-1 microarray [158, 177] was used to globally analyze HSV-1 gene expression in epithelial cells (HeLa and HaCaT), which do not become apoptotic after HSV-1 infection and in iDCs, which become apoptotic after infection with HSV-1.

iDCs, HeLa and HaCaT cells were infected with HSV-1 strain KOS at MOI 1.5 or with heat-inactivated HSV-1 (hi-HSV-1) and at 2-3, 6, 10, and 18 h p. i. aliquots of the infected

gD expression and apoptosis 18 hours after infection with HSV-1 in samples used for microarray-analysis

	gD expressing cells (%)			Apoptotic cells (%)		
	Infection 1	Infection 2	Infection 3	Infection 1	Infection 2	Infection 3
iDC: D1	88	77	86	44	43	53
D2	57	39	74	64	31	30
D3	86	68	81	68	55	71
D4	63	78	91	68	56	64
D5	44	-	-	55	-	-
HaCaT	90	93	94	0	3	-2
HeLa	97	93	94	1	2	2

Table 3.1: iDCs, HaCaT or HeLa cells were infected with HSV-1 strain KOS at MOI 1.5 and aliquots of the cells were taken at 2-3, 6, 10 and 18 h post infection for RNA extraction. At 18 h p. i., one additional aliquot was taken for flow cytometry analysis of gD expression and apoptosis. The number of gD positive cells was determined by staining with anti-gD monoclonal antibody and FITC-conjugated secondary antibody. Background staining was determined by analysis of cells treated with hi-HSV-1 and subtracted. The number of apoptotic cells was determined by staining with AnnexinV-FITC. Propidium iodide positive cells were excluded. Background apoptosis was determined by analysis of cells treated with hi-HSV-1 and subtracted. Microarray analysis was performed with samples from three independent infections. Values are shown for each infection and cell type. For each microarray analysis, RNA of iDCs from 4 or 5 blood donors was pooled.

cells were subjected to Trizol lysis for RNA preparation. Additionally, at 18 h p. i. cells were analyzed by flow cytometry for infection efficiency and apoptosis. Microarray analysis of HSV-1 gene expression in the different cell types was performed three times with RNA obtained from three independent infections. In order to get enough RNA, RNA from iDCs of 4 or 5 different donors was pooled for each microarray analysis.

3.5.1 Efficiency of infection and amount of apoptosis in iDCs, HeLa and HaCaT cells used for microarray analysis

One representative flow cytometry diagram for efficiency of HSV-1 infection (number of gD^+ cells) and apoptosis induction (number of $AnnexinV^+/PI^-$ cells) is shown for each cell type in figures 3.15A and 3.15B, respectively. In this experiment, the number of gD^+ cells after HSV-1 infection was 87 % in iDCs, 99 % in HeLa and 93 % in HaCaT (figure 3.15A). The number of apoptotic ($AnnexinV^+/PI^-$, lower right quadrant) cells was severely increased after HSV-1 infection of iDCs (74.1 % compared to 5.8 % in hi-HSV-1 treated iDCs). In contrast, there was no difference in the number of apoptotic cells between HSV-1 infected and hi-HSV-1 treated HeLa or HaCaT cells (9.4 % compared to 8.5 % in HeLa, 10.5 % compared to 10.5 % in HaCaT, figure 3.15B).

Infection and apoptosis data from all samples used for microarray analysis are shown in table 3.1. Efficiency of infection was generally high, ranging for HeLa and HaCaT

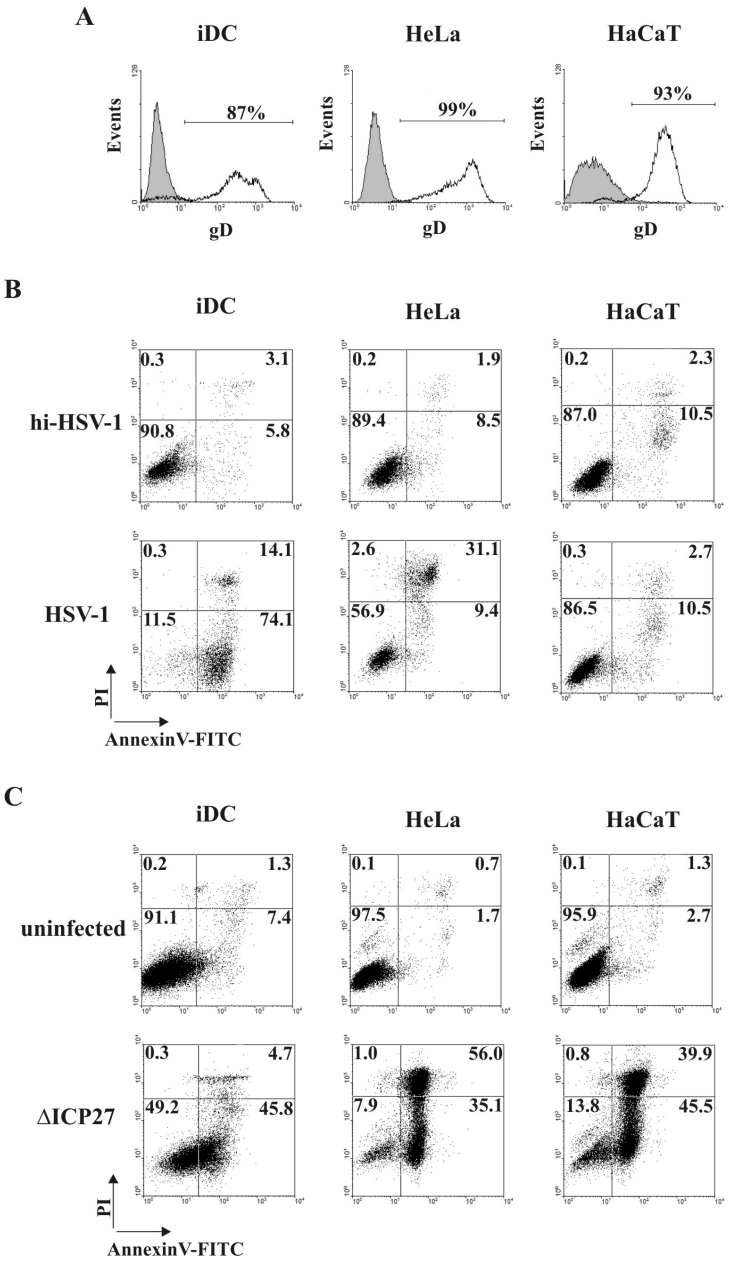

Figure 3.15: **Representative flow cytometry diagrams of the percentage of HSV-1 infected and apoptotic iDCs, HeLa or HaCaT cells used for microarray analysis. (A, B)** Cells were infected with wild type HSV-1 (strain KOS, MOI 1.5, open curve) or heat-inactivated virus (hi-HSV-1, filled curve). Infection **(A)** and apoptosis **(B)** were analyzed 18 h p. i. by flow cytometry after staining of cells with gD/FITC, respectively AnnexinV-FITC/PI. **(C)** Cells were infected with an apoptosis inducing HSV-1 mutant (ΔICP27, MOI 1.5) or left uninfected. Apoptosis was analyzed at 18 h p. i. One representative experiment out of three is shown.

cells between 90 % and 97 % and for iDCs between 39 % and 91 %. While iDCs showed a pronounced increase in apoptotic cells after HSV-1 infection (ranging between 30 % and 71 %), no increase in the number of apoptotic cells was observed after infection of HeLa or HaCaT cells (ranging between -2 % and 2 %). Taken together, iDCs did undergo apoptosis after HSV-1 infection, while epithelial cells (HeLa and HaCaT) were resistent to HSV-1 induced apoptosis. These results are in accordance with observations presented earlier in this thesis (section 3.4) and data published in the literature [8, 9, 43, 116].

In order to demonstrate that HeLa and HaCaT cells used in these experiments are in principle susceptible to HSV-1 induced apoptosis, cells were infected with the HSV-1 mutant ΔICP27 in a separate experiment. As published by others, infection with ΔICP27 induces apoptosis in most cell types [7, 8], because antiapoptotic HSV-1 genes are not sufficiently expressed in this mutant. iDCs, HeLa and HaCaT were infected with the apoptosis-inducing HSV-1 mutant ΔICP27 at MOI 1.5 or left uninfected and 18 h p. i. stained with AnnexinV-FITC/PI. As shown in figure 3.15C, not only the number of apoptotic (AnnexinV$^+$/PI$^-$) iDCs, but also the number of apoptotic HeLa and HaCaT cells was drastically increased after infection with ΔICP27 compared to uninfected cells (iDCs, 45.8 % compared to 7.4 %; HeLa, 35.1 % compared to 1.7 %; HaCaT, 45.5 % compared to 2.7 %). These data indicate, that HSV-1 infection can result in apoptosis also in HeLa and HaCaT cells, if antiapoptotic HSV-1 genes are not expressed properly, as is the case for the HSV-1 mutant ΔICP27.

3.5.2 Pattern of HSV-1 gene expression in iDCs, HeLa and HaCaT cells

Relative abundance of HSV-1 transcripts obtained by microarray analysis of infected iDCs, HeLa and HaCaT are shown in tables 1, 2, 3, and 4.

The first line of the tables shows the median $\pm$ SD of the total viral signal (sum of hybridization values of all probes, corresponds to the accumulation of total HSV-1 transcripts) for each time point and cell type. Median maximum numbers of total viral transcripts reached in the three cell types were comparable: iDCs 640253 ± 123599 (18 h p. i.), HaCaT 618127 ± 293075 (18 h p. i.), HeLa 561168 ± 166110 (10 h p. i.). However, there were some differences in the time course of accumulation of transcripts. While in HaCaT cells the total viral signal increased continuously from 3 to 18 h p. i., in HeLa cells it reached its maximum already at 10 h p. i. and declined thereafter. In iDCs, the total viral signal reached a first maximum at 6 h p. i., was lower at 10 h p. i. and showed the highest value at 18 h p. i. Therefore, the total viral signal was significantly higher in iDCs compared to HeLa cells at 18 h p. i. (640253 ± 123599 compared to 359646 ± 54179, $P = 0.0428$).

In order to allow a fast and convenient overview of differences in the expression of HSV-1 genes between iDCs and HeLa or HaCaT, the $\log_{10}$ of the ratio iDCs/HaCaT or iDCs/HeLa of relative transcript abundances listed in tables 1, 2, 3 and 4 was calculated and is depicted in figures 3.16, 3.17, 3.18 and 3.19.

The data obtained by microarray analysis showed that the timing and extent of transcription of HSV-1 genes was very similar in iDCs, HeLa and HaCaT. There were only

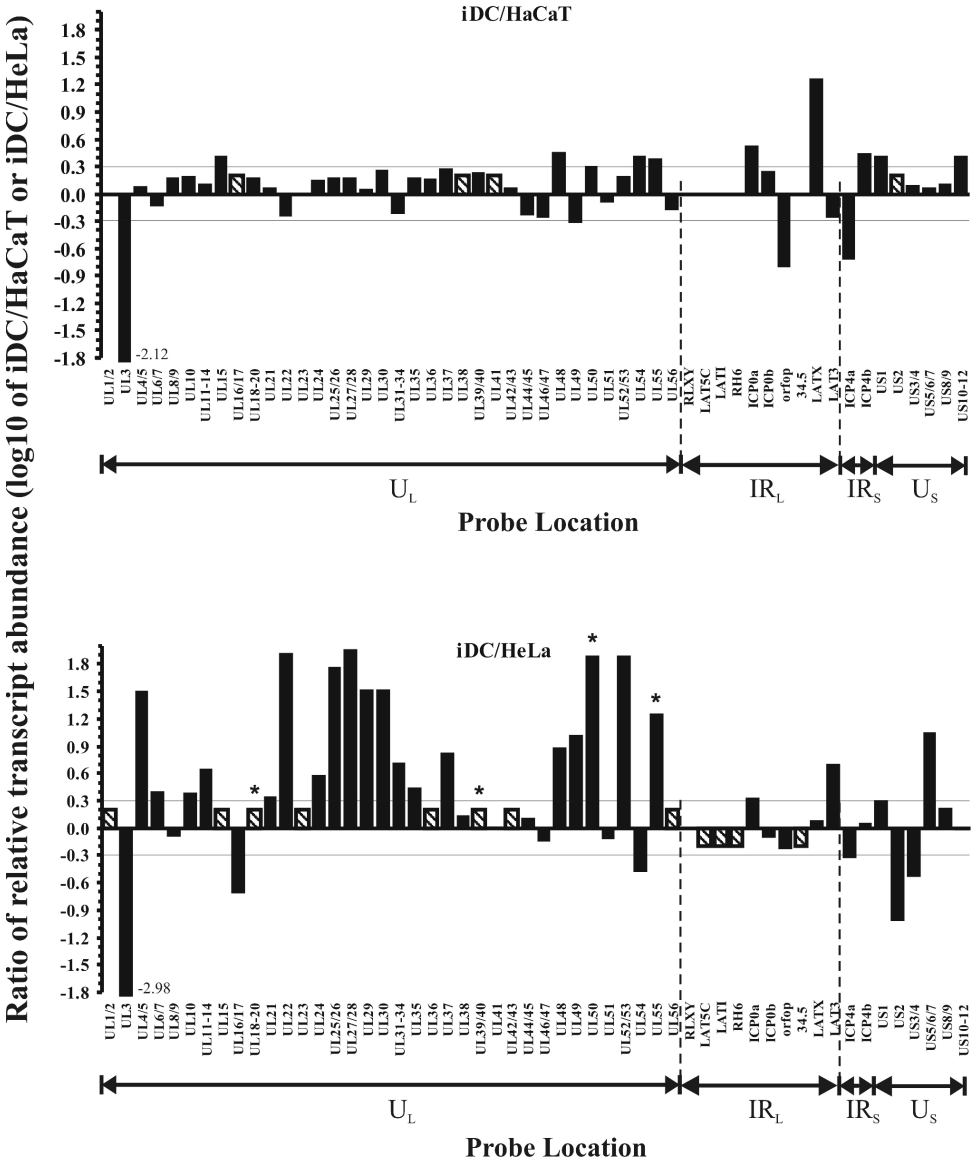

Figure 3.16: **Differential expression of HSV-1 genes in iDCs compared to HaCaT (upper panel) or HeLa (lower panel) at 3 h p. i.** Total RNA was extracted at 3 h p. i. with HSV-1 strain KOS (MOI 1.5) and subjected to HSV-1 microarray analysis. The median relative abundance of each HSV-1 transcript in iDCs was divided by the median relative abundance of the corresponding transcript in HaCaT or HeLa (median relative abundances are listed in table 1). Log_{10} values of the obtained ratios are shown. A log_{10} of 0.3 corresponds to a 2-fold difference in relative abundance. Probes are depicted in the order of the respective genes on the HSV-1 genome. Significant differences (with $P \leq 0.05$) are marked with an asterisk. For some probes, a signal was detected only with RNA from one cell type, while the other cell type showed no signal. Therefore, no ratio could be calculated. This is indicated by hatched columns.

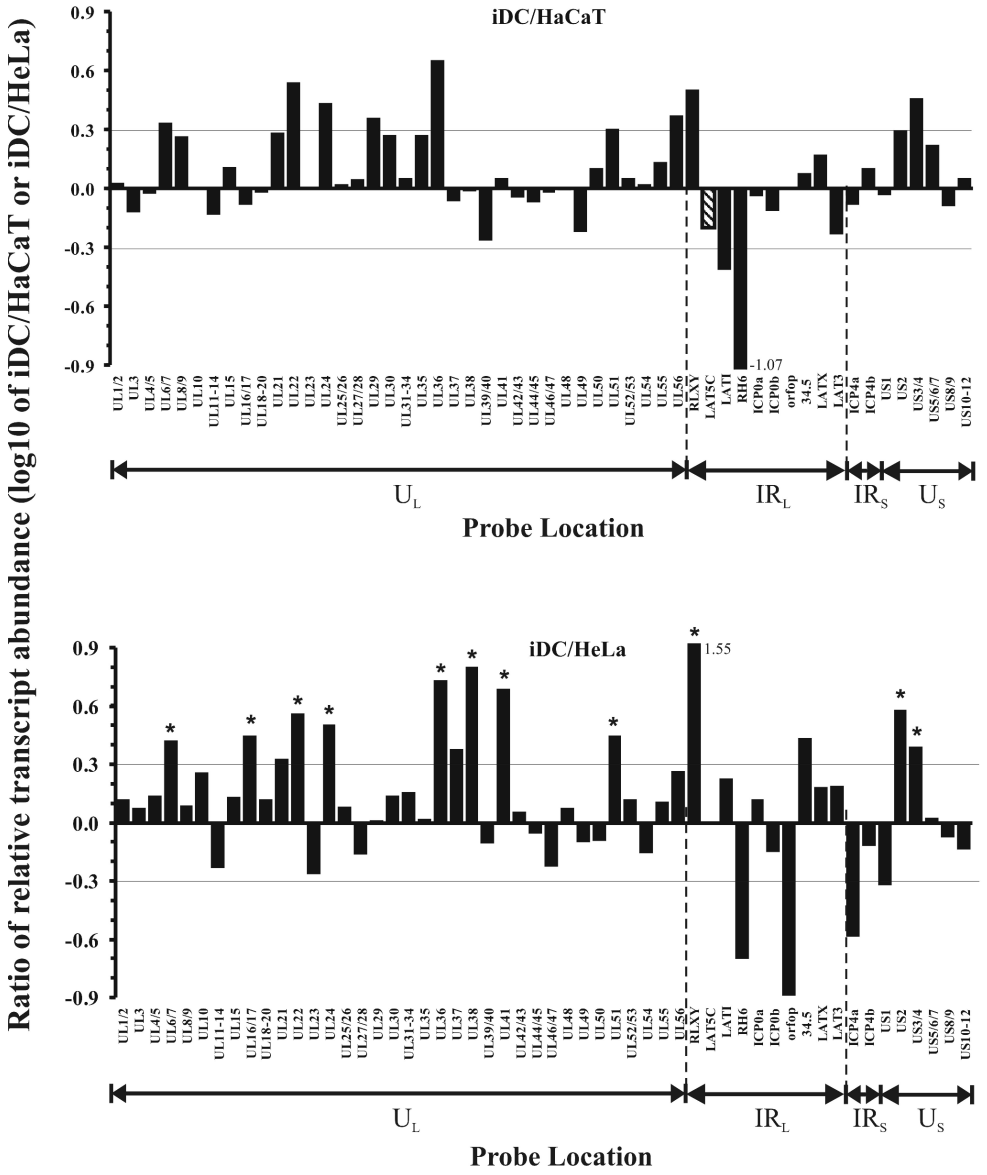

Figure 3.17: **Differential expression of HSV-1 genes in iDCs compared to HaCaT (upper panel) or HeLa (lower panel) at 6 h p. i.** Total RNA was extracted at 6 h p. i. with HSV-1 strain KOS (MOI 1.5) and subjected to HSV-1 microarray analysis. The median relative abundance of each HSV-1 transcript in iDCs was divided by the median relative abundance of the corresponding transcript in HaCaT or HeLa (median relative abundances are listed in table 2). Log_{10} values of the obtained ratios are shown. A log_{10} of 0.3 corresponds to a 2-fold difference in relative abundance. Probes are depicted in the order of the respective genes on the HSV-1 genome. Significant differences (with $P \leq 0.05$) are marked with an asterisk. For some probes, a signal was detected only with RNA from one cell type, while the other cell type showed no signal. Therefore, no ratio could be calculated. This is indicated by hatched columns.

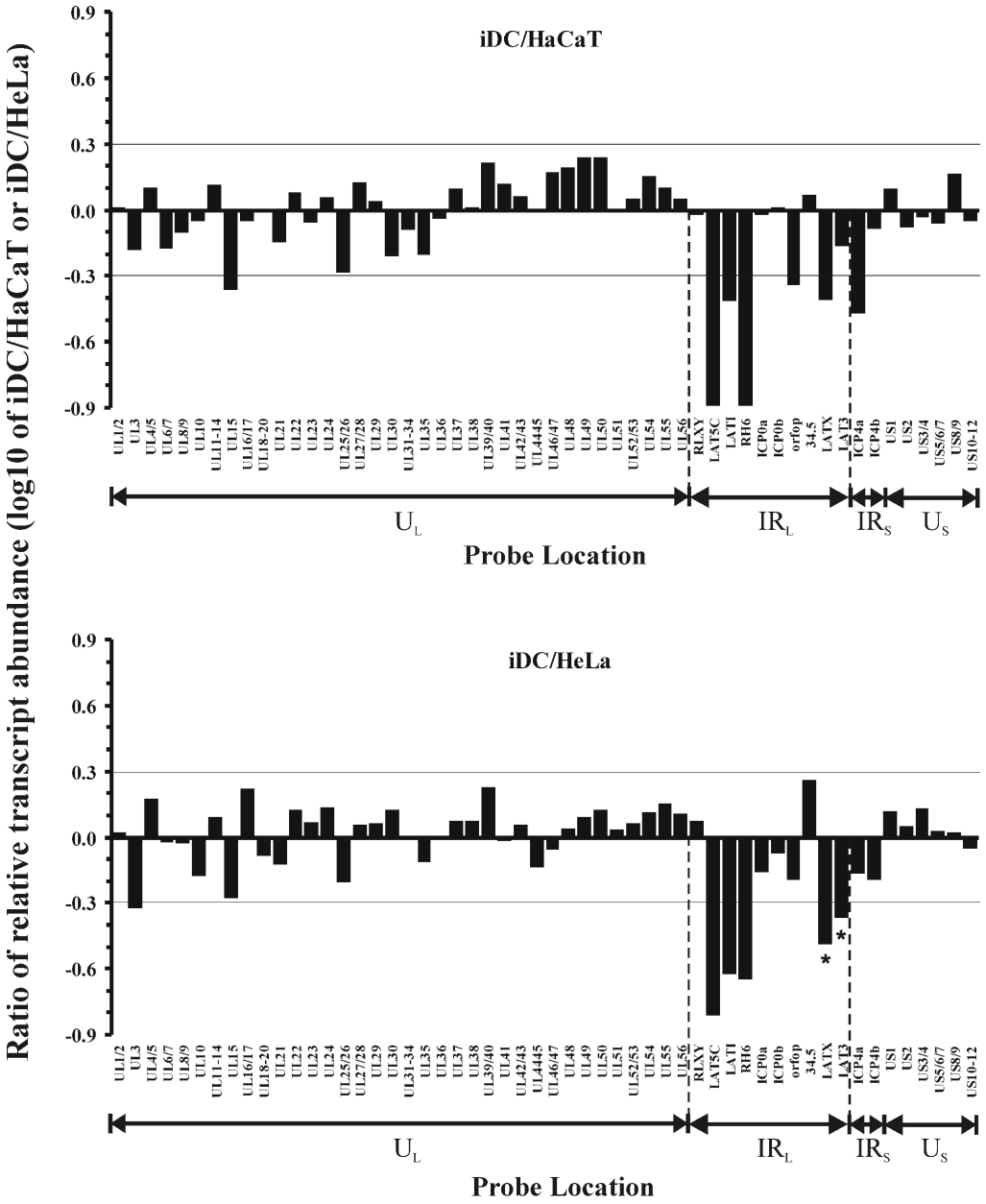

Figure 3.18: **Differential expression of HSV-1 genes in iDCs compared to HaCaT (upper panel) or HeLa (lower panel) at 10 h p. i.** Total RNA was extracted at 10 h p. i. with HSV-1 strain KOS (MOI 1.5) and subjected to HSV-1 microarray analysis. The median relative abundance of each HSV-1 transcript in iDCs was divided by the median relative abundance of the corresponding transcript in HaCaT or HeLa (median relative abundances are listed in table 3). Log_{10} values of the obtained ratios are shown. A log_{10} of 0.3 corresponds to a 2-fold difference in relative abundance. Probes are depicted in the order of the respective genes on the HSV-1 genome. Significant differences (with $P \leq 0.05$) are marked with an asterisk.

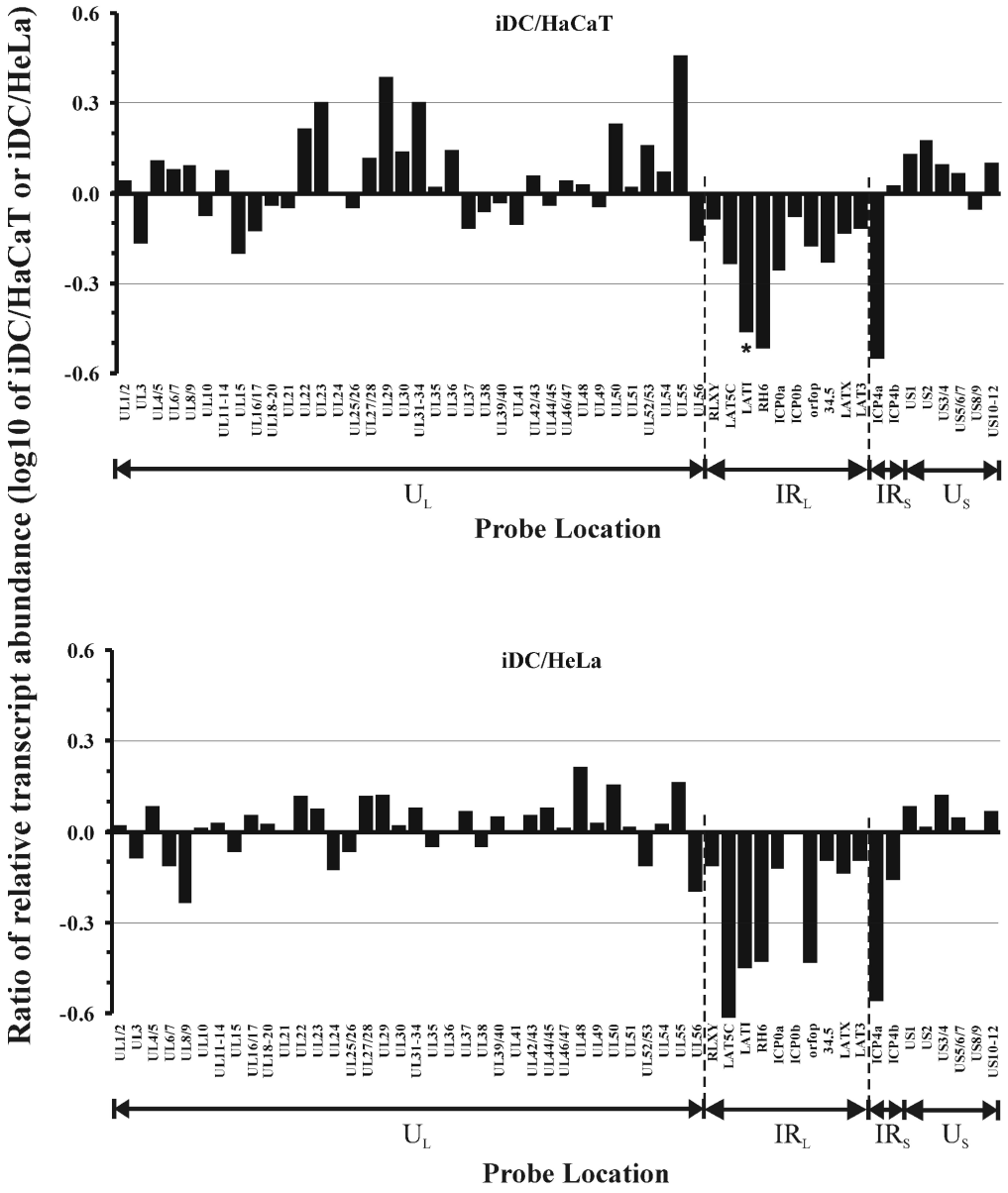

Figure 3.19: **Differential expression of HSV-1 genes in iDCs compared to HaCaT (upper panel) or HeLa (lower panel) at 18 h p. i.** Total RNA was extracted at 18 h p. i. with HSV-1 strain KOS (MOI 1.5) and subjected to HSV-1 microarray analysis. The median relative abundance of each HSV-1 transcript in iDCs was divided by the median relative abundance of the corresponding transcript in HaCaT or HeLa (median relative abundances are listed in table 4). Log_{10} values of the obtained ratios are shown. A $\log_{10}$ of 0.3 corresponds to a 2-fold difference in relative abundance. Probes are depicted in the order of the respective genes on the HSV-1 genome. Significant differences (with $P \leq 0.05$) are marked with an asterisk.

a few significant differences between iDCs and HeLa or HaCaT, which were more than two-fold ($\log_{10}$ ratio > 0.3). At 6 h p. i. (figure 3.17), some late genes showed significantly higher abundances in iDCs compared to HeLa: U_L22 ($\log_{10}$ ratio 0.56, $P = 0.0282$), U_L24 ($\log_{10}$ ratio 0.51, $P = 0.0079$), U_L36 ($\log_{10}$ ratio 0.73, $P = 0.0001$), U_L38 ($\log_{10}$ ratio 0.8, $P = 0.0243$), U_L41 ($\log_{10}$ ratio 0.69, $P = 0.0191$), U_L51 ($\log_{10}$ ratio 0.45, $P = 0.0162$), U_S2 ($\log_{10}$ ratio 0.58, $P = 0.0085$), $U_S3/4$ ($\log_{10}$ ratio 0.39, $P = 0.0125$), and RLXY ($\log_{10}$ ratio 1.55, $P = 0.0317$). Several of these genes were also more than two-fold higher expressed in iDCs compared to HaCaT, although these differences were not significant: U_L22 ($\log_{10}$ ratio 0.54, $P = 0.2655$), U_L24 ($\log_{10}$ ratio 0.43, $P = 0.4471$), U_L36 ($\log_{10}$ ratio 0.65, $P = 0.1627$), $U_S3/4$ ($\log_{10}$ ratio 0.46, $P = 0.0924$), and RLXY ($\log_{10}$ ratio 0.5, $P = 0.2259$). This indicates a faster progression of the viral transcription cascade in iDCs at early time points, as already indicated by the high total viral signal at 6 h p. i. (see above). This could be linked with the observed higher expression of some genes involved in nucleotide metabolism in iDCs compared to HeLa at 3 h p. i. (figure 3.16): $U_L39/40$ (no signal in HeLa, relative abundance $6.4\,\% \pm 0.38\,\%$ in iDCs, $P = 0.0266$), U_L50 ($\log_{10}$ ratio 1.89, $P = 0.0034$). Intriguingly, at later time points (10 and 18 h p. i., figures 3.18 and 3.19) the only significant difference between iDCs and HeLa or HaCaT was the much lower abundance of LATs (described in more detail in section 3.5.3). Importantly, the abundance of the proapoptotic HSV-1 transcript $\alpha 0$ was not significantly different in the three cell types at any time point (figures 3.16, 3.17, 3.18, and 3.19).

3.5.3 Expression of apoptosis-relevant genes in iDCs, HeLa and HaCaT cells

Microarray analysis was performed in order to investigate whether antiapoptotic HSV-1 genes (U_L54, $\alpha 4$, U_S1, U_S3, U_S5, U_S6, U_S11 and LAT [70, 123]) are differentially expressed in iDCs. The time course of their relative abundance is depicted in detail in figures 3.20 and 3.21. The data revealed, that the expression pattern of U_L54 (ICP27), $\alpha 4$ (ICP4), U_S1 (ICP22), $U_S10/11/12$, $U_S3/4$ (Kinase/gG) and $U_S5/6/7$ (gJ/gD/gI) in the three cell types was quite similar. However, $U_S3/4$ had a significantly higher relative abundance in iDCs compared to HeLa at 6 h p. i. ($1.59\,\% \pm 0.06\,\%$ compared to $0.64\,\% \pm 0.09\,\%$, $P = 0.0125$).

Unfortunately, it can not finally be concluded, that U_S3 is higher expressed in iDCs at 6 h p. i., because an unknown proportion of the detected signal originates from the U_S4 transcript. The HSV-1 genome contains only 52 polyadenylation sites, but encodes more than 80 open reading frames. Only approximately half of the viral transcripts are terminated with a unique polyadenylation site, the remaining HSV-1 genes belong to coterminal transcript families. Probes of the microarray are designed to bind immediately adjacent to the polyadenylation sites of transcripts, therefore it is not possible to discriminate between transcripts which belong to a coterminal transcript family. For the same reason, it is still possible that U_S6 is differentially expressed in iDCs compared to HeLa or HaCaT, although there was no significant difference in the signal of the $U_S5/6/7$ probe (figure 3.20). Expression of the antiapoptotic late gene U_S11 can only be detected with the microarray probe $U_S10/11/12$, and as shown in figure 3.20, the signal of this probe is dominated throughout the course of infection by the detec-

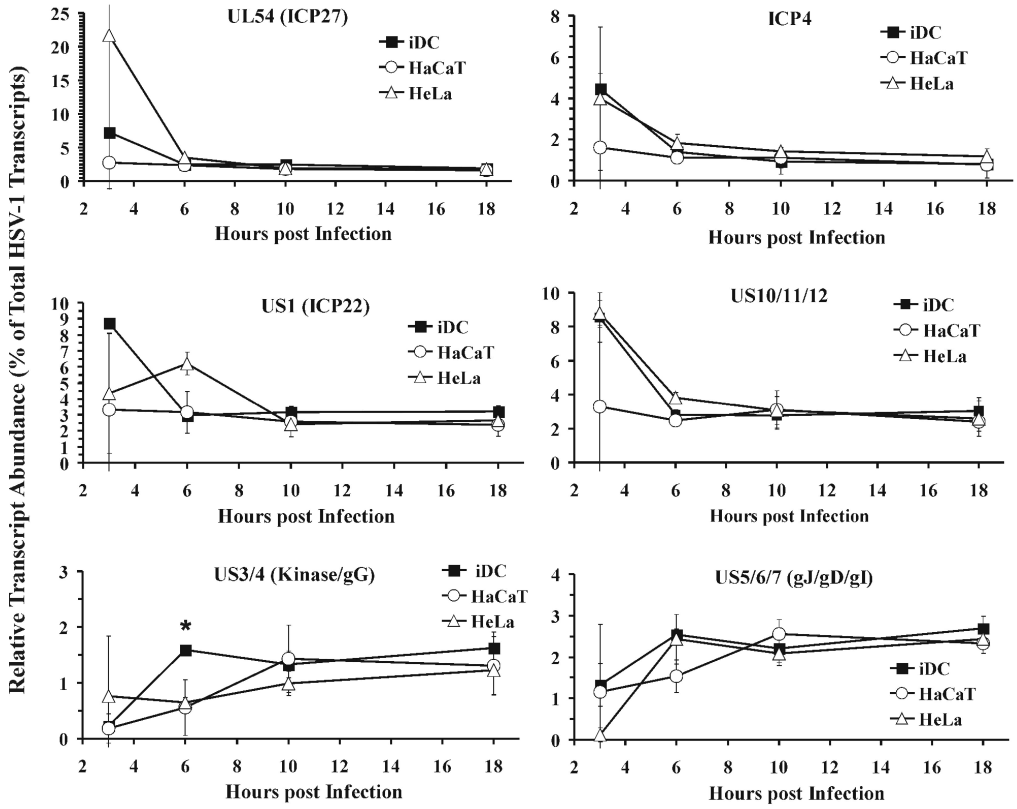

Figure 3.20: **Time course of expression of known apoptosis modulating HSV-1 genes in iDCs in comparison to HaCaT or HeLa cells.** The median relative abundance detected with the HSV-1 microarray for each gene or coterminal transcript family at different time points is shown as percentage of total HSV-1 transcripts (based on data in tables 1-4). Significant differences (with $P \leq 0.05$) in relative abundance of transcripts in iDCs compared to HeLa are marked with an asterisk.

tion of the immediate early transcript U_S12, which shares the polyadenylation site with U_S11 and U_S10.

Interestingly, LATs showed a significantly different expression pattern in iDCs compared to HeLa or HaCaT (figure 3.21). Five different LATs can be discriminated with probes on the microarray (LAT5C, LATI, RH6, LATX and LAT3, see figure 2.1 for location of LAT probes on the HSV-1 genome). In the epithelial HeLa and HaCaT cells, the abundance of latency associated transcripts increased strongly in an exponential manner between 6 and 10 h p. i. and either further increased until 18 h p. i. (LATI and RH6) or remained at the level detected at 10 h p. i. (LAT5C, LATX, and LAT3). In contrast, expression of LATs in iDCs showed only a moderate linear increase in abundance between 6 and 18 h p. i. As a result of this difference in the course of expression, relative abundances of LATs in iDCs were much lower than in HaCaT or HeLa at 10 and

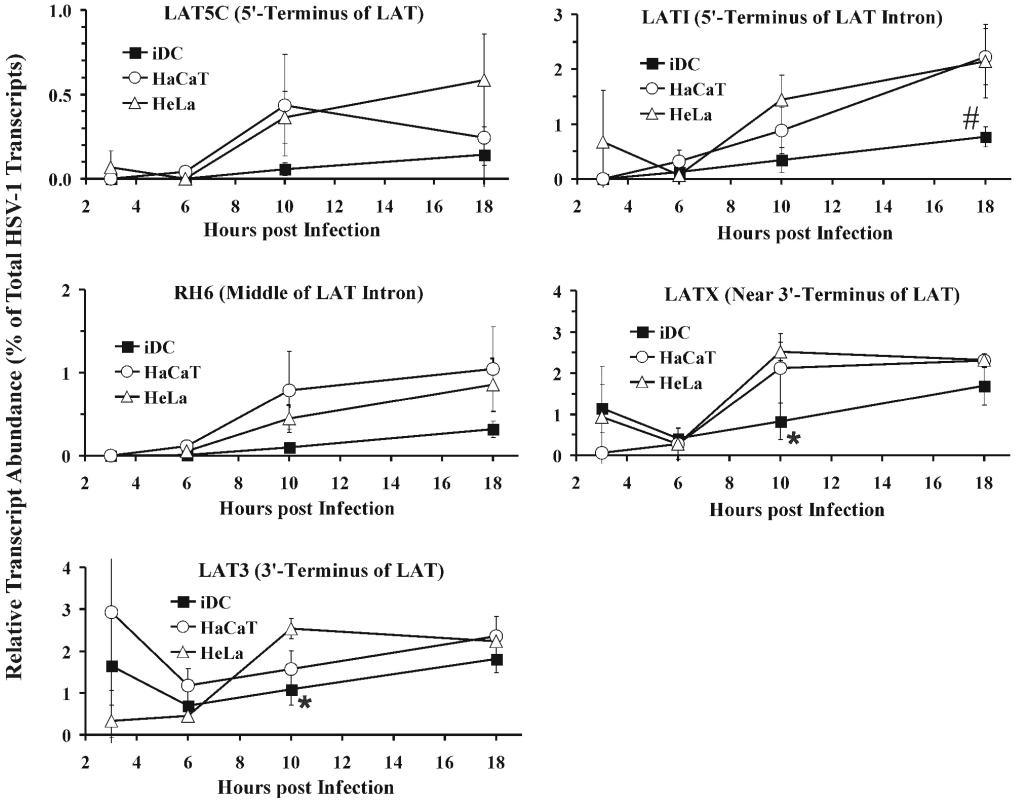

Figure 3.21: **Time course of expression of LATs in iDCs in comparison to HaCaT or HeLa cells.** The median relative abundance detected with the HSV-1 microarray for LATs at different time points is shown as percentage of total HSV-1 transcripts (based on data in tables 1-4). Significant differences (with $P \leq 0.05$) in relative abundance of transcripts in iDCs compared to HeLa are marked with an asterisk and compared to HaCaT with a number sign.

18 h p. i. As can be seen in figure 3.18, at 10 h p. i. LATs were 2.3 fold ($\log_{10}$ ratio -0.37, LAT3) to 6 fold ($\log_{10}$ ratio -0.81, LAT5C) lower abundant in iDCs compared to HeLa and 1.4 fold ($\log_{10}$ ratio -0.16, LAT3) to 7.9 fold ($\log_{10}$ ratio -0.89, RH6) lower abundant compared to HaCaT. Differences reached statistical significance for LAT3 ($\log_{10}$ ratio -0.37, $P = 0.0107$) and LATX ($\log_{10}$ ratio -0.48, $P = 0.0098$) at 10 h p. i. in iDCs compared to HeLa and for LATI ($\log_{10}$ ratio -0.46, $P = 0.0187$) at 18 h p. i. compared to HaCaT.

Taken together, global analysis of HSV-1 gene expression in iDCs compared to epithelial cells (HeLa and HaCaT) revealed no significant differences in expression of most known apoptosis modulating viral genes. However, at late time points post infection with HSV-1, the expression of LATs was significantly lower in iDCs compared to epithelial cells.

A role for LATs in protection against HSV-1 induced apoptosis was not only pub-

lished for latently infected neurons [2, 65, 74, 131], but also for lytically infected cells [2, 75]. Therefore, it is conceivable that the higher susceptibility of iDCs for HSV-1 induced apoptosis could be due to the lower expression of LATs.

3.6 LAT expression and apoptosis of HSV-1 infected iDCs

Next, the impact of LAT expression on HSV-1 induced apoptosis of iDCs was further investigated. As determined by microarray analysis (see section 3.5.3), there was a residual expression of LATs in iDCs after infection with wild type HSV-1. If LAT is further reduced, for example after infection with a LAT knockout mutant of HSV-1, the amount of apoptosis would be expected to be higher compared to wild type HSV-1.

To proof this, iDCs isolated from five different blood donors (D1-D5) were infected with the LAT knockout HSV-1 mutant 17N/H (ΔLAT) [22] or the respective wild type HSV-1 strain 17. LPS was added to some cells immediately after infection, because it has been shown that LPS triggers signaling pathways in DCs, which are involved in regulation of survival [4, 140]. Apoptosis was analyzed at 18 h p. i. by staining of iDCs with AnnexinV-FITC/PI and subsequent flow cytometry.

In four (D1, D2, D4 and D5) out of five donors, ΔLAT induced more apoptosis in iDCs than wild type HSV-1. Figure 3.22A shows flow cytometry diagrams obtained from donor D5. The number of apoptotic iDCs (AnnexinV$^+$/PI$^-$, lower right quadrant), which increased from 4 % after treatment with hi-HSV-1 to 31 % after infection with wild type HSV-1, was further increased to 42 % after infection with ΔLAT. After additional treatment with LPS, 33 % of wild type HSV-1 infected iDCs were apoptotic, but 50 % of ΔLAT infected iDCs. Similar results were obtained after infection of iDCs from all other tested donors (figure 3.22B), except D3, which showed no difference in the number of apoptotic iDCs after infection with ΔLAT (23 %) compared to infection with wild type HSV-1 (23 %). However, when iDCs from donor D3 were treated with LPS after infection, there were more apoptotic iDCs after ΔLAT infection (30 %) compared to infection with wild type HSV-1 (24 %). Increased apoptosis can not be explained by differences in infection efficiency, as flow cytometry analysis of the viral glycoprotein gD on the surface of infected iDCs revealed no difference in the number of infected cells after ΔLAT infection compared to wt HSV-1 (figure 3.22C).

In order to proof whether the knockout in ΔLAT is complete, one aliquot of infected iDCs was lysed after 18 h and subjected to quantitative real time PCR of LAT expression (see figure 2.1 for location of probes in the LAT region). ΔLAT infected iDCs showed no signal for primer pairs LAT-A and LAT-B, as expected (figure 3.23A). However, there was a signal with probe LAT-C in ΔLAT infected iDCs, which was comparable to the signal obtained with extracts from HSV-1 wild type infected iDCs. Probe LAT-C detects aberrant LAT sequences, which are known to be expressed downstream of the deletion in ΔLAT [22]. However, these sequences are located in a region not associated with the antiapoptotic function of LAT [22, 24].

The higher number of apoptotic iDCs after infection with ΔLAT compared to infection with wild type virus could also be caused by differences in the expression of

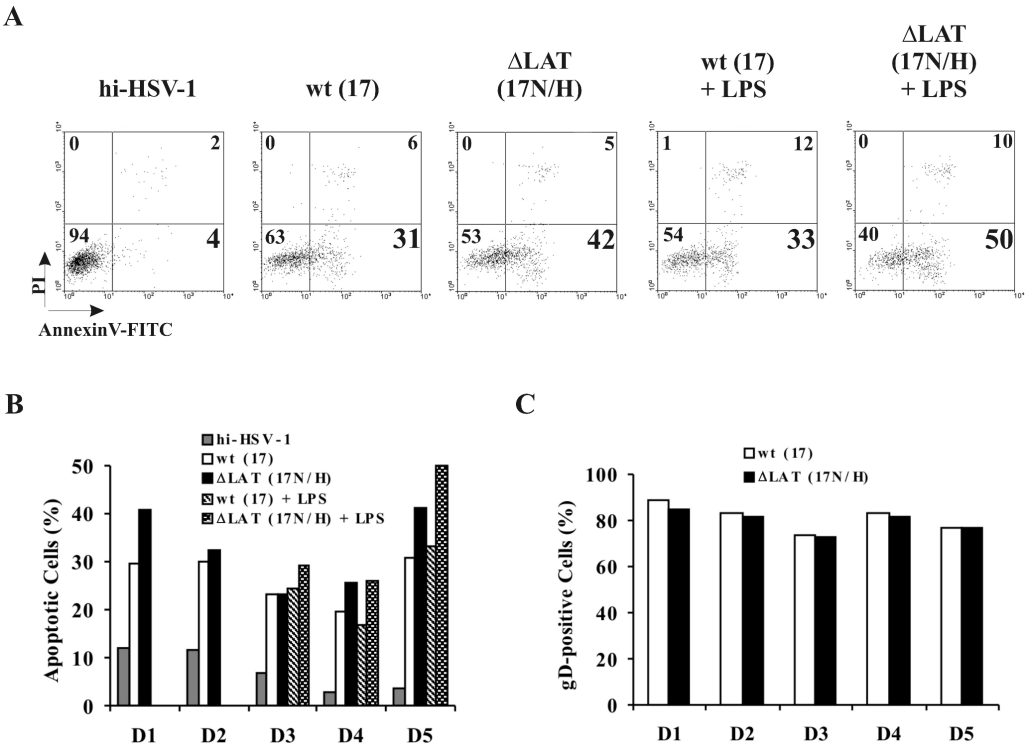

Figure 3.22: **Apoptosis in iDCs infected with a HSV-1 LAT deletion mutant.** iDCs from five different blood donors (D1-D5) were infected with either HSV-1 wild type (wt, strain 17) or a LAT deletion mutant (ΔLAT, 17N/H) at MOI 1.5 or treated with a mix of heat-inactivated wt and mutant virus (hi-HSV-1). LPS (1 μg/ml) was added immediately after infection to some cells as indicated. 18 h p. i. apoptosis was analyzed by flow cytometry after staining of iDCs with AnnexinV-FITC and propidium iodide (PI). **(A)** Flow cytometry diagrams of one representative donor (D5) are shown. Numbers in each quadrant indicate percentage of cells contained in this quadrant. **(B)** The number of apoptotic iDCs (AnnexinV$^+$/PI$^-$) is depicted for all tested donors. **(C)** The number of infected cells was determined by staining with anti-gD antibody (stains HSV-1 glycoprotein gD on surface of infected cells) and subsequent flow cytometry. Unspecific background staining as determined by staining of uninfected cells was subtracted.

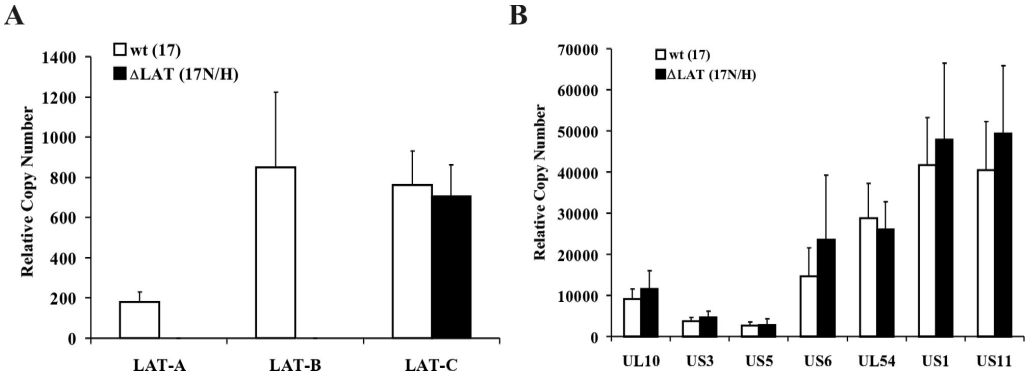

Figure 3.23: **Quantitative RT-PCR of expression of LAT (A) and other antiapoptotic virus genes (B) in iDCs infected with a HSV-1 LAT deletion mutant.** iDCs from five different blood donors (D1-D5) were infected with either HSV-1 wild type (wt, strain 17) or a LAT deletion mutant (ΔLAT, 17N/H) at MOI 1.5. At 18 h p. i., cells were lysed and subjected to quantitative RT-PCR analysis. **(A)** Mean values ± SD of relative copy numbers obtained with three different probes for LAT (LAT-A, LAT-B, LAT-C; see figure 2.1 for location in the LAT region) are shown. **(B)** Mean values ± SD of relative copy numbers of six antiapoptotic HSV-1 genes (U_S3, protein kinase; U_S5, gJ; U_S6, gD; U_L54, ICP27; U_S1, ICP22; U_S11, tegument protein) and for comparison one not apoptosis modulating virus gene (U_L10, gM) were determined.

other apoptosis-regulating HSV-1 genes. Quantitative RT-PCR (figure 3.23B) revealed a slight, but not significant higher expression of some antiapoptotic HSV-1 genes (U_S3, U_S6, U_S1, U_S11) in lysates of ΔLAT infected iDCs, compared to wild type HSV-1 infected iDCs. This was also seen with a probe for one HSV-1 gene not associated with apoptosis (U_L10). There were no differences in the expression of U_S5, while U_L54 was slightly lower expressed in ΔLAT infected iDCs compared to wild type HSV-1 infected iDCs. Based on these results it can be assumed that the higher ability of ΔLAT to induce apoptosis in iDCs compared to wild type HSV-1 is due to the knockout of LAT and not due to reduced expression of other antiapoptotic HSV-1 genes.

Taken together, the absence of LAT expression in HSV-1 infected iDCs resulted in increased apoptosis. Therefore, it can be concluded that LAT has a antiapoptotic function in iDCs. It is conceivable that the antiapoptotic function of LAT can compensate the downregulation of c-FLIP at late time points post infection with HSV-1. Epithelial cells which express high amounts of LATs are protected against apoptosis. In contrast, iDCs express only low amounts of LATs. Therefore, the loss of c-FLIP is not efficiently counter regulated in iDCs and apoptosis can occur. Consequently, the data presented in this thesis indicate that LAT has an important antiapoptotic role not only in latently infected neurons, but also in lytic infection of cells.

4 Discussion

HSV-1 can productively infect iDCs [114, 133], but yield of virus progeny is low. After HSV-1 infection, maturation of iDCs is blocked [133, 143] and a high number of iDCs undergo apoptosis [23, 115, 133]. Because iDCs play a central role in the induction of the antiviral immune response [23, 132, 156], the impairment of their function and viability might be one strategy of HSV-1 to modulate the immune response to its advantage.

The mechanisms underlying induction of apoptosis in iDCs by HSV-1 are still a conundrum, in view of the fact that HSV-1 possesses several strong antiapoptotic factors [43, 123]. In many cell types, such as epithelial cells, antiapoptotic factors dominate and the cells are kept alive until replication of HSV-1 is successfully completed [8, 9, 43].

Müller *et al.* [115] showed that the amount of two proteins of the cellular apoptosis signaling network, p53 and c-FLIP$_L$, is changed after HSV-1 infection of iDCs. However, the mechanism and relevance of these changes was not investigated. Therefore, the mechanism of c-FLIP downregulation after HSV-1 infection of iDCs was studied in detail in the first part of this thesis. Furthermore it was investigated here, whether c-FLIP downregulation could be sufficient for induction of apoptosis in HSV-1 infected iDCs.

Insufficient availability of viral antiapoptotic factors could also contribute to induction of apoptosis in HSV-1 infected iDCs. This hypothesis was not investigated up to now. In the second part of this thesis it was therefore examined, whether antiapoptotic factors of HSV-1 are properly expressed in infected iDCs.

4.1 Correlation between amount of c-FLIP and iDC viability

After infection of iDCs with HSV-1 a strong downregulation of the cellular antiapoptotic protein c-FLIP$_L$ was observed by Müller *et al.* [115]. This result was confirmed by experiments conducted in this thesis. 18 h p. i. with HSV-1, the amount of c-FLIP$_L$ was reduced to 25 % of the amount expressed in uninfected iDCs (figure 3.14A, first panel). In addition, c-FLIP$_S$ was also efficiently downregulated after HSV-1 infection of iDCs (figures 3.8 and 3.10).
Müller *et al.* [115] suggested, that the observed reduction of the amount of c-FLIP could be the direct cause for induction of apoptosis in iDCs after HSV-1 infection. This conclusion is well founded, because a large number of publications have established a direct correlation of the amount of c-FLIP with resistance of cells to death receptor induced apoptosis [66, 96, 148, 169]. In particular, mathematical modeling revealed the amount of c-FLIP as the main switch for the decision of life and death in the extrinsic pathway of apoptosis induction [19, 55].

In iDCs, a publication by Willems *et al.* [179] provided the first indication for a correlation of the amount of c-FLIP$_L$ with resistance to CD95-mediated apoptosis. However, the amount of c-FLIP was reduced by treatment of iDCs with the substances cycloheximide and bisindolylmaleimide. Cycloheximide blocks protein synthesis [37] and bisindolylmaleimide is an inhibitor of protein kinase C [167]. Therefore, many other effects could contribute to apoptosis of iDCs after treatment with these substances.

In this thesis, c-FLIP in iDCs was for the first time specifically knocked down by RNA interference, thereby avoiding side effects of chemical inhibitors. Furthermore, this approach allows assessment of the impact of c-FLIP reduction on viability of iDCs in the absence of viral factors, which could modulate apoptosis. c-FLIP was already successfully reduced by RNA interference in fibroblast, epidermal, and Hodgkin/Reed-Sternberg cell lines, resulting in increased susceptibility to induction of apoptosis [109, 153].

The amount of both c-FLIP$_L$ and c-FLIP$_S$ was successfully reduced in iDCs nucleofected with siRNA specifically targeting c-FLIP (figure 3.1A and data not shown). Interestingly, this was sufficient to dramatically reduce the number of viable iDCs (AnnexinV$^-$/ PI$^-$) in comparison to iDCs nucleofected with control siRNA (from 85 % to 20 %, figure 3.1B). After addition of a CD95 (Fas) agonistic antibody, the number of viable iDCs was reduced to 1 %. Presumably, in a large percentage of iDCs the caspase-8-mediated apoptosis pathway is pre-activated independent from binding of a ligand, as it was published for breast cancer cells [31]. c-FLIP must be expressed in a sufficient amount in these cells in order to block constitutive death signaling and keep the cells alive. c-FLIP specific RNA interference neutralizes this block and apoptosis-inducing signals are transduced into the cell. These findings are in agreement with data presented in the publication by Müller *et al.* [115]. Prevention of binding of the three main death ligands CD95 (Fas) ligand, TRAIL and TNF-α to their receptors could reduce apoptosis after HSV-1 infection of iDCs only in some donors and only partially. Because apoptosis signaling downstream of death receptors is blocked by high amounts of c-FLIP in DCs, activation of these receptors can result in survival, maturation and cytokine release rather than apoptosis, as recently shown for CD95 [53, 54, 141].

The reduction in viability of iDCs after siRNA mediated knockdown of c-FLIP was in part due to an increase in apoptotic cells (AnnexinV$^+$/PI$^-$) compared to control siRNA nucleofected iDCs (16 % compared to 2 %). However, the majority of non-viable iDCs was AnnexinV$^+$/PI$^+$ (61 %). Because analysis of viability was done as late as 3-6 days after nucleofection, it is likely that this population represents cells in the late stage of apoptosis [155].

This is the first time that c-FLIP was specifically reduced in iDCs by RNA interference and the results indicate that c-FLIP is essential for viability of iDCs. This supports the hypothesis that HSV-1 induced c-FLIP downregulation could contribute to induction of apoptosis in iDCs.

4.2 c-FLIP reduction in HSV-1 infected iDCs before onset of apoptosis

In HSV-1 infected iDCs, a reduction of the amount of c-FLIP was not found before 12 h p. i. at MOI 1.5 (figure 3.2). At this time point it was reduced below 50 % of the amount detected in iDCs treated with heat-inactivated HSV-1. At later time points (18 h p. i.) a reduction to 25 % was found (figure 3.14). The time course of HSV-1 induced c-FLIP reduction in iDCs was dependent on the MOI used for infection. At MOI 3 a reduction of the amount of c-FLIP to 40 % was already detectable at 10 h p. i. (figure 3.8). Different HSV-1 strains (F, KOS, 17 and Patton) used in the experiments all showed a comparable extent of c-FLIP reduction in iDCs. Notably, reduction of c-FLIP preceded the occurence of apoptosis after infection of iDCs with HSV-1, as the number of apoptotic iDCs started to increase significantly at 14 h p. i. (figure 3.3). Collectively, these data provide another indication, that reduction of c-FLIP might directly contribute to apoptosis observed in HSV-1 infected iDCs.

Interestingly, reduction of c-FLIP and apoptosis in iDCs occurred at later stages of the HSV-1 replication cycle than the pro- and antiapoptotic events described by other researchers in other cell types. The first proapoptotic event after HSV-1 infection of cells is the expression of the immediate early gene $\alpha 0$, which occurs before 3 h p. i. [25, 145, 147]. Between 3 h and 6 h post infection (apoptosis prevention window), antiapoptotic HSV-1 genes are expressed and prevent execution of apoptosis [8, 92]. Therefore, HSV-1 induced downregulation of c-FLIP in iDCs at 12 h p. i. appears to be a second, independent proapoptotic event.

4.3 Degradation of c-FLIP by viral or virus-induced cellular factor(s)

The results of the experiments discussed above strongly indicate that downregulation of c-FLIP is a crucial event for induction of apoptosis in HSV-1 infected iDCs. Therefore, several experiments were conducted to elucidate the mechanism of HSV-1 induced downregulation of c-FLIP.

Quantitative RT-PCR revealed that after HSV-1 infection of iDCs the number of c-FLIP$_L$ mRNA transcripts was significantly increased (figure 3.4), despite c-FLIP$_L$ downregulation on the protein level. This observation is consistent with data presented by Müller *et al.* [115] and can be explained by induction of maturation processes in iDCs after HSV-1 infection. Although complete maturation of iDCs is prevented after infection with HSV-1, a partial maturation is still induced [134, 133, 143]. This partial maturation is sufficient to activate NFκB [134], which is known to increase the expression of c-FLIP$_L$ [93, 111]. In line with this notion, the amount of c-FLIP$_L$ mRNA was also increased after treatment of iDCs with LPS or UV-inactivated HSV-1 (figure 3.4), both of which induce maturation of iDCs [51]. However, after infection of iDCs with viable HSV-1, c-FLIP$_L$ mRNA transcripts showed a tendency to accumulate in the nucleus, compared to iDCs treated with UV-inactivated HSV-1. This might be due to the abil-

ity of HSV-1 to inhibit splicing of mRNA precursors, which prevents maturation and nuclear export of many cellular mRNAs [56, 57]. Importantly, the amount of c-FLIP$_L$ mRNA detected in the cytoplasm of HSV-1 infected iDCs was not decreased but rather moderately increased compared to uninfected cells (figure 3.4). Because probes used in quantitative RT-PCR are located in the middle of the c-FLIP$_L$ transcript, it is very likely that the transcripts detected in the cytoplasm are intact and suitable for translation. Based on these observations it can be concluded that HSV-1 does not downregulate c-FLIP by impairment of c-FLIP mRNA transcription, transport or stability. This result indicates that HSV-1 downregulates c-FLIP directly on the protein level.

Studies on the mechanism of HSV-1 induced c-FLIP downregulation on the protein level could be conducted much more easily in cell lines overexpressing c-FLIP. iDCs are primary cells, which must be freshly prepared in a time consuming and expensive procedure and yield only low amounts of protein for immunoblot analysis. Furthermore, cell lines could be transfected with tagged or mutated forms of c-FLIP. Therefore, c-FLIP was overexpressed in HEp2 cells from a eucaryotic vector and tested for its susceptibility to HSV-1 induced downregulation. The first experiments were carried out with EGFP-tagged c-FLIP and the amount was analyzed by flow cytometry, which is less time consuming and allows more direct quantification than immunoblot analysis. Surprisingly, neither c-FLIP$_L$-EGFP nor c-FLIP$_S$-EGFP were downregulated after HSV-1 infection of transfected HEp2 cells (figure 3.5). There could be several reasons for this result: i) The mechanism of HSV-1 induced c-FLIP downregulation is operative only in iDCs, but not in HEp2 cells. ii) The EGFP tag protects c-FLIP against degradation by HSV-1. ii) The amount of c-FLIP in transiently transfected cells exceeds the capacity of the HSV-1 induced degradation mechanism.

In order to elucidate the reason why HSV-1 can downregulate naturally expressed c-FLIP in iDCs, but not overexpressed c-FLIP-EGFP in HEp2 cells, it would be helpful to perform immunoblot analysis of untagged c-FLIP or c-FLIP with a smaller tag. However, the effect of HSV-1 on c-FLIP would not be visible in immunoblot analysis if only one third of the transfected cells are infected, as was the case in the experiments described above (figure 3.5). Therefore, an optimization of transfection and infection had to be performed.

To increase infectibility of transfected cells, different transfection reagents were evaluated. Transfection with Lipofectamine^{TM} 2000 (data not shown) did not yield better results compared to transfection with ExGen 500. However, when FuGENE® 6 was used, almost all transfected cells could be infected with HSV-1 (figure 3.6A). Probably these results can be explained by different mechanisms used by different transfection reagents to transport plasmid DNA into cells. All three tested transfection reagents are non-liposomal. It is published that both ExGen 500 and Lipofectamine^{TM} 2000 use the endocytosis pathway and destabilize endosomes [46, 106]. Maybe this impairs entry of HSV-1 into the cell, although endocytosis does not seem to play an important role in entry of HSV-1 [44]. Unfortunately, the mechanism of DNA transfer into cells by FuGENE® 6 is not known. In order to further increase the efficiency of transfection and infection, different cell types and MOIs were tested. The best results were achieved with A549 cells, transfected with FuGENE® 6 and infected with HSV-1 at MOI 10 or

higher (figure 3.6B,C).

Immunoblot analysis of myc-tagged c-FLIP after infection of transfected A549 cells with HSV-1 (strain KOS, MOI 50) confirmed the resistance of c-FLIP$_L$ to downregulation by HSV-1, while c-FLIP$_S$ was partially downregulated (figure 3.7). This result excludes the possibility that the EGFP-tag is responsible for the resistance of overexpressed c-FLIP to downregulation by HSV-1. The position of the tag is not critical, as the EGFP-tag was located on the C-terminus of c-FLIP, while the myc-tag was located on the N-terminus. When transfected cells were analyzed under a microscope, the c-FLIP$_L$-EGFP signal was not evenly distributed in the cells, as observed after transfection with EGFP alone, but was rather aggregated in dot like structures (data not shown). This was also observed by Ishioka *et al.* [67]. In this publication it was demonstrated that overexpressed c-FLIP$_L$ forms insoluble aggregates, which are resistant to proteasomal turnover and block the function of the proteasome in general. This aggregation is mediated by the DEDs contained in the c-FLIP molecule. Mutants of c-FLIP$_L$ constructed by Ishioka *et al.*, which lacked the DED part of the molecule or had mutated DEDs were distributed diffusely in the cells and did no longer block the proteasome. The tendency of c-FLIP$_L$ to form aggregates when overexpressed in cells could also confer resistance to downregulation by HSV-1. Therefore, c-FLIP$_L$ mutants generated by Ishioka *et al.* were transfected in A549 cells and analyzed by immunoblot after infection of the cells with HSV-1.

Indeed, c-FLIP$_L$ with mutated or lacking DEDs (F23G/F114G and 203-480) was efficiently downregulated after infection with HSV-1 (figure 3.7). In contrast, a mutant with intact DEDs but with a mutation in the caspase cleavage site (D376A) was resistant to HSV-1 induced degradation. Interestingly, a mutant with intact DEDs, but with a truncated C-terminus (1-438) was also susceptible to HSV-1 induced degradation. According to the publication by Ishioka *et al.* [67], this mutant still forms aggregates, but they are not as dense as the aggregates formed by wild type c-FLIP$_L$ and they are distributed throughout the cell instead of being condensed in the perinuclear region. A c-FLIP$_L$ mutant (1-202) which consists of both DEDs but lacks the complete caspase-like domain is completely resistant to HSV-1 mediated downregulation. Interestingly, c-FLIP$_L$ 1-202 has the same molecular structure as c-FLIP$_S$, except that c-FLIP$_S$ has a short unique C-terminus in addition. c-FLIP$_S$ is partially downregulated after HSV-1 infection. To summarize these findings, mutation or removal of the DEDs as well as modifications of the C-terminus restore the susceptibility of overexpressed c-FLIP to HSV-1 induced downregulation. This seems to be linked to the density of aggregates formed by c-FLIP mutants after overexpression in cells.

Importantly, susceptibility to HSV-1 induced reduction was not correlated with the ability of c-FLIP mutants to block the function of the proteasome. Ishioka *et al.* found that wild type c-FLIP$_L$ as well as the mutants 1-438 and D376A block the proteasome, while 1-202, 203-480 and F23G/F114G do not. In contrast, HSV-1 downregulation was operative with the c-FLIP$_L$ mutants 1-438, 203-480 and F23G/F114G and with c-FLIP$_S$. An overview of the ability of c-FLIP$_L$ wild type and mutants to form aggregates, to block the proteasome and to resist HSV-1 induced downregulation is shown in figure 4.1. The following conclusions can be drawn from these observations: i) Overexpressed

c-FLIP$_L$ forms aggregates which impair degradation by HSV-1. ii) Mutation or removal of the DEDs and modification of the C-terminus restore susceptibility to HSV-1 mediated downregulation. iii) Resistance to HSV-1 induced downregulation is not correlated with the ability of overexpressed c-FLIP$_L$ to block the function of the proteasome. iv) DEDs and the ability to bind to the DISC are not essential for downregulation of c-FLIP after HSV-1 infection. v) The findings support the hypothesis that HSV-1 directly attacks the protein in order to downregulate c-FLIP. vi) Experiments with overexpressed c-FLIP$_L$ should be performed with a mutant, which does not form aggregates, for example c-FLIP$_L$ F23G/F114G.

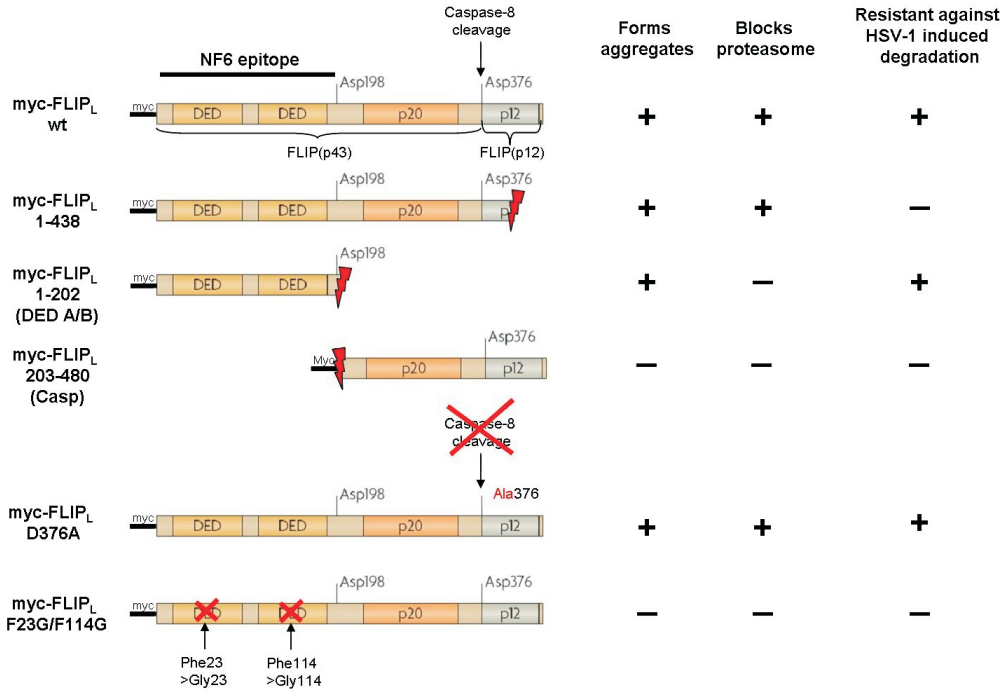

Figure 4.1: **Properties of c-FLIP$_L$ mutants.** The structure of c-FLIP$_L$ wild type and mutants [67] is depicted on the left side. Their ability to form aggregates when overexpressed in cells and to block the proteasome as published by Ishioka *et al.* and their ability to resist HSV-1 induced downregulation is listed on the right side.

In uninfected cells, the c-FLIP amount is mainly determined by proteasomal turnover [41, 89, 128]. Therefore, it had to be investigated whether HSV-1 induced downregulation of c-FLIP is dependent on the proteasome. When the proteasome was blocked by addition of the inhibitor MG132 after infection of iDCs with HSV-1, the loss of c-FLIP$_L$ or c-FLIP$_S$ could not be prevented (figure 3.8). These experiments were difficult to perform, because iDCs turned out to be highly susceptible to the toxic side effects of MG132. Therefore, the earliest time point after infection was chosen, at which downregulation of c-FLIP could be observed. This was the case at 10 h p. i. with HSV-1 strain

KOS at MOI 3. c-FLIP$_L$ and c-FLIP$_S$ were downregulated at this time point in HSV-1 infected iDCs compared to uninfected iDCs no matter if MG132 was added or not.

In summary, the data presented in this thesis indicate that increased proteasomal turnover is not responsible for c-FLIP degradation after HSV-1 infection of iDCs. Therefore, it can be concluded that HSV-1 induced c-FLIP degradation might be mediated directly by a viral factor or a induced cellular factor or a combination of both. To proof this, it was tested whether this factor is introduced into lysates of c-FLIP expressing cells by addition of lysates of HSV-1 infected cells. Therefore, c-FLIP$_L$ F23G/F114G, which is susceptible to HSV-1 induced downregulation when overexpressed in cells (see above) or c-FLIP$_S$-EGFP were transfected into A549 cells. Lysates of the transfected cells were kept at -20°C or incubated for 2 h at 37 °C. Immunoblot analysis showed that c-FLIP$_L$ F23G/F114G and c-FLIP$_S$-EGFP were detectable in comparable amounts in the lysates, independent of the temperature at which the lysates were incubated (figure 3.9). This indicates that lysates of uninfected cells do not contain factors, which can degrade c-FLIP. However, when lysates of untransfected, but HSV-1 infected A549 cells were added to the c-FLIP containing lysates, degradation of both c-FLIP$_L$ F23G/F114G and c-FLIP$_S$-EGFP was observed after incubation for 2 h at 37 °C. This degradation could not be prevented by addition of MG132. These data support the hypothesis that after HSV-1 infection of cells a viral factor is expressed or a cellular factor is induced which directly degrades c-FLIP.

One candidate cellular factor could be the mitochondrial protease HtrA2/Omi. It is released into the cytoplasm after proapoptotic events. HtrA2/Omi can promote or even induce apoptosis by its protease activity [38, 61, 162, 174]. Proapoptotic events after HSV-1 infection of cells might lead to the release of HtrA2/Omi from mitochondria. Though the execution of apoptosis is blocked by viral antiapoptotic proteins [123], HtrA2/Omi might remain in the cytoplasm and could degrade c-FLIP. Although a potential direct interaction of HtrA2/Omi and c-FLIP has not been investigated yet, there are some publications, which consistently show an increase of the amount of c-FLIP when the action of HtrA2/Omi is blocked with a specific inhibitor [21, 159]. In future experiments, the impact of inhibition of HtrA2/Omi on HSV-1 induced c-FLIP downregulation should be investigated.

Candidate viral factors, which could be involved in HSV-1 induced c-FLIP degradation are probably expressed late in the viral replication cycle. This is indicated by several results presented in this thesis and in the literature. As demonstrated by infection of iDCs with UV-inactivated HSV-1, attachment of HSV-1 particles, entry into the cell and release of viral DNA into the nucleus are not sufficient to induce downregulation of c-FLIP (figure 3.10) or apoptosis of iDCs (data not shown). At MOI 1.5, c-FLIP downregulation and apoptosis in HSV-1 infected iDCs occur at 12 and 14 h p. i. (figures 3.2 and 3.3), which corresponds to the late stage of the viral replication cycle. As published by others [177] and confirmed by the microarray analysis presented in this thesis, at 10 h p. i. all HSV-1 genes are expressed, even at MOI 1.5 and also in iDCs (table 3). However, true late genes can be excluded as candidate viral factors, because inhibition of HSV-1 DNA replication and expression of true late genes by aciclovir [36] does not block c-FLIP downregulation and apoptosis in HSV-1 infected iDCs [115].

In this work, some experiments were also carried out with a ICP27 (immediate early regulatory protein) knockout mutant of HSV-1 (ΔICP27) [154]. ΔICP27 is impaired in the expression of some early and many late genes [146, 158], while immediate early genes are expressed properly or are overexpressed. The reduction in the amount of c-FLIP at 18 h p. i. was less pronounced in iDCs infected with ΔICP27 compared to HSV-1 wild type infected iDCs (figure 3.10). Therefore it must be assumed that one or several viral genes, which are lower expressed in ΔICP27 are involved in downregulation of c-FLIP in HSV-1 infected iDCs. It has been shown that ICP27 is involved in the retention of host mRNA in the nucleus at late time points post infection and thereby shuts off expression of some cellular genes [146]. It is unlikely that this function of ΔICP27 is responsible for c-FLIP downregulation, because c-FLIP$_L$ mRNA was found in sufficient amounts in the cytoplasm of HSV-1 infected iDCs (figure 3.4). Moreover, after infection of iDCs with ΔICP27 the distribution of c-FLIP$_L$ mRNA in the nucleus and cytoplasm was not different compared to infection with wild type HSV-1 (data not shown). Unfortunately, it is impossible to make a statement about involvement of virus genes in apoptosis induction after infection of iDCs with ΔICP27, because ΔICP27 induces apoptosis in most cell types anyway [7, 8]. This is due to disturbed expression of antiapoptotic viral genes after infection with this mutant.

In order to get an indication about a potential interaction of c-FLIP with a HSV-1 protein, immunofluorescence analysis was performed with A549 cells, which were transfected with c-FLIP$_L$ F23G/F114G. Consistent with results obtained by immunoblot analysis (figure 3.8), the c-FLIP signal was reduced to approximately 50 % of the signal observed in uninfected cells at 11 h p. i. with HSV-1 strain KOS at MOI 10. As published by Ishioka *et al.* [67], c-FLIP$_L$ F23G/F114G is evenly distributed in uninfected cells (figure 3.11A). In contrast, c-FLIP$_L$ F23G/F114G forms dot like or oval shaped accumulations in many of HSV-1 infected cells (figure 3.11C,E). However, a co-localization with viral proteins stained with anti-HSV-1 rabbit serum could not be detected (figure 3.11D,F). This result does not exclude the possibility that a viral protein does interact with c-FLIP, because the serum does probably not stain all viral proteins expressed after infection of cells. Furthermore, it is possible that the interaction takes place at a different time point.

Based on the literature published so far, a possible impact of two HSV-1 proteins on the stability of c-FLIP is conceivable. First, it has been shown that the stability of some c-FLIP isoforms can be regulated by phosphorylation on serine residues [86]. There is one viral serine/threonine protein kinase, U$_S$3, which is able to phosphorylate procaspase-3 [18]. Because c-FLIP is a caspase homolog, it might be possible that it is also phosphorylated by U$_S$3 and thereby its turnover is increased. Second, reactive oxygen species (ROS) are suspected to influence c-FLIP stability [90, 101]. The viral glycoprotein gJ can induce ROS formation [10] and could thereby destabilize c-FLIP. Both viral proteins are expressed as leaky late genes during HSV-1 replication. Therefore, they would be good candidates for a potential viral factor, which attacks c-FLIP, based on the observations made earlier in this thesis. Surprisingly, when co-transfected with c-FLIP$_L$ F23G/F114G in HEK cells, neither U$_S$3 nor gJ were able to reduce the amount of c-FLIP. However, co-localization of U$_S$3 with c-FLIP$_L$ F23G/F114G was ob-

served (figure 3.12). U_S3 formed dot like aggregates when overexpressed in HEK cells. Co-transfected c-FLIP$_L$ F23G/F114G was in most cells aggregated in the same region as U_S3. Furthermore, the structures formed by c-FLIP$_L$ F23G/F114G when co-transfected with U_S3 were reminiscent of those observed with overexpressed c-FLIP$_L$ F23G/F114G after HSV-1 infection (figure 3.11). A co-localization of U_S3 and c-FLIP$_L$ was confirmed by further experiments performed by Martin J. Raftery (personal communication, Martin J. Raftery, Institute of Virology, Charité Medical School, Berlin, Germany). These observations indicate that U_S3 might play a role in HSV-1 induced c-FLIP downregulation. A contribution of U_S3 to c-FLIP downregulation after HSV-1 infection is supported by the fact, that a ICP27 HSV-1 knockout mutant has a reduced ability to downregulate c-FLIP (figure 3.10) and U_S3 expression in this mutant is five times lower compared to wild type virus [158]. U_S3 might phosphorylate c-FLIP and thereby mark it for degradation by a protease. Because U_S3 alone is not sufficient for downregulation of c-FLIP, the responsible protease must be newly expressed or activated after HSV-1 infection of cells. HSV-1 encodes a protease, U_L26 [142], but up to now it is not investigated whether it also attacks cellular proteins. Further experiments should be performed in order to clarify, whether U_L26 is involved in HSV-1 induced c-FLIP degradation. Peculiarly, U_S3 is almost exclusively discussed as an antiapoptotic factor of HSV-1 [17, 26, 72, 103, 119, 118, 125], but downregulation of c-FLIP would rather induce apoptosis. It is conceivable, that phosphorylation of c-FLIP is a side effect of phosphorylation of caspases by U_S3, which is considered to prevent apoptosis. In most cell types, strong antiapoptotic factors of HSV-1 could compensate for degradation of c-FLIP and the antiapoptotic effect of caspase phosphorylation by U_S3 could dominate. These antiapoptotic factors might not be functional in iDCs.

Taken together, in this thesis the mechanism of HSV-1 induced c-FLIP downregulation was resolved to a great extent. It was shown that HSV-1 does not interfere with c-FLIP mRNA transcription, transport or stability. Instead, c-FLIP is degraded late during HSV-1 infection independent from the proteasome by a newly expressed or activated cellular or viral protease with possible involvement of the viral protein kinase U_S3.

4.4 c-FLIP reduction without apoptosis in HSV-1 infected cell types other than iDCs

Because HSV-1 induced c-FLIP downregulation was operative with overexpressed c-FLIP in A549 cells (figure 3.7), it is likely that it is a general phenomenon occurring also in cell types other than iDCs. Indeed, HSV-1 infection resulted in downregulation of naturally expressed c-FLIP$_L$ (figure 3.14A) and c-FLIP$_S$ (data not shown) in all cell types tested in this work, including epithelial cells (primary keratinocytes), connective tissue cells (primary fibroblasts), endothelial cells (HUVEC), and cells of hematopoietic origin (Hodgkin/Reed-Sternberg cell lines L428 and L1236). The extent of c-FLIP downregulation in these cell types was comparable to iDCs, if a comparable infection rate was achieved.

Although c-FLIP was also downregulated by HSV-1 in primary keratinocytes, primary fibroblasts, HUVECs, and HRS cells, these cell types did not show an increased number of apoptotic (AnnexinV$^+$/PI$^-$) cells after infection, in contrast to iDCs (figure 3.14B). However, in some of these cell types the number of viable cells (AnnexinV$^-$/PI$^-$) was decreased after infection. This was mainly due to an increase in the number of AnnexinV$^+$/PI$^+$ cells. It can be assumed that this cell population represents necrotic cells, as the number of AnnexinV$^-$/PI$^+$ cells is also increased, which is not the case in late stage apoptosis [155], observed for example after siRNA mediated knockdown of c-FLIP in iDCs (figure 3.1). Necrosis observed after HSV-1 infection is probably a consequence of successful viral replication.

These findings are in line with many publications, which report a resistance of HSV-1 infected cells to apoptosis. In most cell types, no apoptosis occurs after infection with wild type HSV-1. However, when protein synthesis and consequently expression of viral proteins is blocked after infection, apoptosis is observed in human epithelial cell lines. Apoptosis is also induced after infection with a ICP27 HSV-1 knock out mutant, which is impaired in expression of early and late genes [7, 8, 92]. From these observations it was concluded that HSV-1 induces apoptosis early in infection, but powerful antiapoptotic viral factors expressed later in infection are able to prevent apoptosis to ensue. Furthermore, dependent on the cell type, these antiapoptotic HSV-1 factors can also protect infected cells from apoptosis induced by different stimuli, such as staurosporine, sorbitol and Fas ligand [8, 43].

Downregulation of c-FLIP after HSV-1 infection is probably an apoptosis inducing event. Because apoptosis after HSV-1 infection is only observed in iDCs, but not in other cell types tested, it must be concluded that antiapoptotic factors of HSV-1 are not sufficiently operative in iDCs.

4.5 Lower expression of LATs in apoptotic iDCs as compared to nonapoptotic epithelial cells

In order to find differences in the expression of antiapoptotic viral genes in apoptotic iDCs compared to nonapoptotic epithelial cells, a global analysis of HSV-1 gene expression was performed using a HSV-1 microarray. Because a high number of cells was necessary to collect sufficient amounts of RNA for microarray analysis, it was not possible to use primary keratinocytes in this set of experiments. It was therefore decided to use the immortalized human keratinocyte cell line HaCaT and the human epithelial tumor cell line HeLa. Consistent with the literature, wild type HSV-1 infection did not induce apoptosis in HaCaT or HeLa, but in iDCs (figure 3.15B). In contrast, infection with an apoptosis inducing ICP27 knockout HSV-1 mutant induced apoptosis in all three cell types (figure 3.15C). These data show that iDCs, HeLa and HaCaT cells are susceptible to HSV-1 induced apoptosis, but HeLa and HaCaT cells are protected against apoptosis after wild type HSV-1 infection by antiapoptotic factors, which do not operate in iDCs.

The results obtained by microarray analysis show that the overall timing and extent of HSV-1 gene transcription is similar in iDCs, HeLa and HaCaT. This is indicated by

the fact that the maximum total number of transcripts and the time course of expression of immediate early, early, leaky late and true late genes was similar in all three cell types and comparable with data published by other groups (figures 3.16-3.19, tables 1-4, and [177]). Interestingly, the HSV-1 transcription cascade proceeded faster in iDCs compared to HeLa or HaCaT at early time points post infection, which resulted in a higher total transcript number in iDCs at 6 h p. i., a higher expression of some early genes at 3 h p. i. and a higher expression of some leaky late genes at 6 h p. i. However, the relative abundance of $\alpha 0$ transcripts, which have been shown to be the apoptosis inducing factor after HSV-1 infection [25, 145, 147], was not different in iDCs compared to HeLa or HaCaT at any time point. Therefore, it is unlikely that the observed faster progression of viral transcription in iDCs is the cause of HSV-1 induced apoptosis.

Expression of antiapoptotic genes of HSV-1, U_L54 (ICP27) [7, 8], $\alpha 4$ (ICP4) [102], U_S1 (ICP22) [8], U_S11 [70], U_S5 (gJ) [72, 73, 188], and U_S6 (gD) [188, 187, 189] was not significantly different in iDCs compared to HeLa or HaCaT (figure 3.20). The antiapoptotic U_S3 kinase [72, 103] even showed a higher transcript abundance in iDCs compared to HeLa or HaCaT at 6 h p. i. However, some of the antiapoptotic genes (U_S11, U_S3, U_S5 and U_S6) are members of coterminal transcript families, which can not be discriminated with the microarray [177]. Therefore, further analyzes, for example by quantitative real time PCR, would be necessary for a final conclusion about a potential differential expression of these genes.

Intriguingly, microarray analysis revealed a lower abundance of LATs in iDCs compared to HeLa or HaCaT at late time points post infection (10 and 18 h p. i., figure 3.21). In HeLa or HaCaT, the time course and extent of expression of LATs detected with the HSV-1 microarray in this thesis confirms data published by others [177]. LATs are the only HSV-1 transcripts abundantly expressed during latent infection of neurons [139, 176]. It has been shown that the first 1.5 kb of the LAT sequence can protect cells against apoptosis and that the antiapoptotic function of LAT is responsible for its ability to increase the spontaneous reactivation of HSV-1 from latency [2, 24, 65, 74, 76, 77, 117, 129, 130, 131]. The LATs species expressed during latency represent mainly two stable introns. In contrast, during lytic replication mostly polyadenylated forms of LATs are detectable [28, 32]. The design of the microarray allows only detection of polyadenylated RNA species [177]. The function of LATs during lytic expression is not fully understood, but LAT knockout HSV-1 mutants induce more apoptosis in productively infected cells compared to wild type HSV-1 [2, 75].

Cell type specific regulation of LAT expression is a well known phenomenon, although the regulation of LAT promoter activity is still not fully resolved. It was soon recognized that LAT is highly and continuously expressed in latently infected neurons but expressed to a lesser extent during lytic infection of other cell types [14, 15, 191]. LAT expression could be influenced by interferons via binding of STAT1 to the LAT promoter [95]. Early growth response (EGR) proteins, which are expressed soon after exposure of cells to stress signals, were also demonstrated to bind to the LAT promoter and repress its activity [164]. Therefore, it is conceivable that iDC specific signaling events reduce the expression of LATs.

The studies presented in this thesis do not exclude the possibility that expression of

some of the antiapoptotic genes of HSV-1 is different on the protein level in iDCs compared to HeLa or HaCaT, for example because of different proteasomal turnover. This might also contribute to apoptosis. Furthermore, differences in expression or function of cellular genes other than c-FLIP could influence sensitivity of iDCs to apoptosis after HSV-1 infection. As indicated by the results presented in figure 3.1, iDCs might also inherently be more sensitive to c-FLIP downregulation than other cell types. However, HSV-1 infection can protect most cell types against various intrinsic and extrinsic apoptosis inducing events [8, 43]. Therefore, it is highly probable that apoptosis of HSV-1 infected iDCs is at least partly caused by a failure of viral antiapoptotic functions.

The following conclusions can be made based on the results obtained with the HSV-1 microarray in iDCs, HeLa and HaCaT: i) The antiapoptotic HSV-1 genes U_L54, $\alpha 4$, U_S1, U_S11, U_S3, U_S5 and U_S6 are properly expressed during infection of iDCs. Still, apoptosis is not prevented. ii) LATs are expressed in apoptotic iDCs to a much lower extent at 10 and 18 h p. i. compared to nonapoptotic epithelial cells. This indicates that LATs play an essential role in prevention of apoptosis late in lytic infection. iii) iDCs might undergo apoptosis because the essential antiapoptotic function of LATs is not sufficiently available.

4.6 Increased apoptosis in iDCs after infection with a LAT knockout HSV-1 mutant

Because expression of LATs was reduced in iDCs compared to HeLa or HaCaT, but not completely abrogated, it is conceivable that a further reduction in the amount of LATs would lead to an increase in apoptosis after HSV-1 infection of iDCs. This was confirmed with a LAT knockout HSV-1 mutant (17N/H). iDCs from four out of five donors showed an increased number of apoptotic cells after infection with 17N/H compared to wild type HSV-1 (figure 3.22A,B). The increase in apoptosis could not be explained by differences in infection efficiency between the mutant and wild type HSV-1 (figure 3.22C). It was also excluded that disturbed expression of other antiapoptotic HSV-1 genes is responsible for the higher apoptosis inducing capability of 17N/H (figure 3.23B). 17N/H lacks the expression of the promoter region and the first 1.66 kb of the coding region of LAT. It has been shown that it does not express any 2 kb or longer forms of LATs, but one aberrant 1.1 kb transcript downstream of the deletion [22]. This transcript was also detected in 17N/H infected iDCs in this work (figure 3.23A). However, this aberrant transcript is located downstream of the region, which was defined to be involved in protection against apoptosis [2, 24, 65, 74, 131]. Therefore it is unlikely that it has influenced the results of the experiments presented here. In conclusion, it was demonstrated that expression of LATs can protect HSV-1 infected iDCs from apoptosis.

Recently it was published that c-FLIP can substitute for LAT in reactivation from latency [77]. This indicates that LATs exert a FLIP-like function in order to facilitate reactivation. It is possible that LATs do not only play a role in protection of latently infected neurons against apoptosis, but also prevent apoptosis late in lytic infection of

productively infected cells. This is supported by data obtained by other groups with 17N/H in lytically infected cells [2, 75]. In this thesis it is shown that LATs are not expressed in sufficient amounts in iDCs and are therefore not able to compensate HSV-1 induced c-FLIP downregulation.

4.7 Apoptosis of HSV-1 infected iDCs as a consequence of altered balance between pro- and antiapoptotic events

This thesis provides a substantial contribution to the understanding of apoptosis in HSV-1 infected iDCs. Although it has been shown that HSV-1 infects iDCs [114], blocks maturation [143] and induces apoptosis [23, 80, 133], little is known about the mechanism of HSV-1 induced apoptosis in this important cell type. Müller *et al.* have demonstrated that HSV-1 downregulates the cellular antiapoptotic protein c-FLIP in infected iDCs [115]. In this thesis it was discovered that c-FLIP is directly attacked by HSV-1 and degraded by a viral or newly induced cellular protease with potential participation of the viral kinase U_S3. Furthermore it was demonstrated that a reduction of the amount of c-FLIP by RNA interference is sufficient to induce apoptosis in iDCs.

Another cellular apoptosis modulating protein is p53. It has been established that p53 can induce apoptosis independent from transcription [30], for example by inhibiting the mitochondrial antiapoptotic proteins Bcl-X_L and Bcl-2 [112]. Müller *et al.* observed an increase of the amount of p53, but not nuclear localization, in HSV-1 infected iDCs [115]. A polymorphism in p53 which is associated with increased susceptibility to cancer might be associated with a different ability of p53 to modulate apoptosis [34, 42]. A set of experiments conducted in the course of this thesis support the hypothesis that p53 might be involved in apoptosis of iDCs, because the extent of apoptosis observed in iDCs after infection with wild type HSV-1 turned out to be associated with the p53 polymorphism of the donor (diploma thesis of Stefan Kohl).

Bcl-2 is a mitochondrial antiapoptotic protein [1] which has been shown to be downregulated after infection of cells with apoptosis inducing HSV-1 deletion mutants. Restoration of Bcl-2 levels lead to a reduction of the amount of apoptosis observed after infection with HSV-1 deletion mutants [186]. Furthermore, it was found that Bcl-2 might protect iDCs against apoptosis [58]. However, apoptosis of iDCs after infection with wild type HSV-1 is not associated with a reduction of the amount of Bcl-2 [115]. Therefore it is unlikely that Bcl-2 could play a role in HSV-1 induced apoptosis of iDCs.

NFκB is another cellular factor which is discussed to be involved in modulation of apoptosis in HSV-1 infected cells. However, there has been some controversy whether NFκB activation is involved in induction [163] or prevention [50] of apoptosis after HSV-1 infection of cells. Activation of NFκB was also found after HSV-1 infection of iDCs [134]. The results presented in this work also indicate the activation of NFκB after infection of iDCs with HSV-1, because the observed increase of c-FLIP mRNA (figure 3.4) is likely mediated by NFκB [93, 111]. In iDCs, activation of NFκB is associated with maturation and increased resistance to apoptosis [94, 122]. Based on these considerations it is not likely that NFκB could be involved in apoptosis induction by HSV-1 in

iDCs.

It is well established that HSV-1 first induces apoptosis in infected cells, probably by transcription of $\alpha 0$ [25, 145, 147]. However, viral antiapoptotic proteins, such as US3, gJ, gD and US11, are expressed during the apoptosis prevention window 3 - 6 h p. i. and apoptosis is prevented [8, 92]. Surprisingly, no study was undertaken up to now to investigate whether impaired expression of antiapoptotic HSV-1 genes might contribute to apoptosis of infected iDCs. Using a HSV-1 microarray it was shown in this work that almost all antiapoptotic HSV-1 genes are expressed in iDCs to the same extent as in epithelial cells, which are resistant to apoptosis after HSV-1 infection. However, there was one remarkable exception: LATs were 1.4 to 7.9 fold less abundant in iDCs compared to epithelial cells at 10 h p. i. Lower expression of LATs in iDCs was still detectable at 18 h p. i., but was not seen at earlier time points (3 h or 6 h p. i.). Further experiments in this thesis showed that a LAT knockout HSV-1 mutant induced more apoptosis in iDCs compared to wild type HSV-1, which shows a residual expression of LAT. This indicates that the observed lower expression of LAT in iDCs could have an significant impact on susceptibility of iDCs to apoptosis after HSV-1 infection. This is the first time that expression of HSV-1 antiapoptotic genes was studied after infection of iDCs and these studies define a new role for LAT during productive infection. A first indication that LAT might play a role in prevention of apoptosis also during lytic infection was obtained in studies with LAT knockout HSV-1 mutants which induced more apoptosis compared to wild type HSV-1 in HeLa and Neuro2A cells [2, 75].

Based on the results obtained in this work a new model of HSV-1 induced apoptosis can be proposed (figure 4.2). Like in other cell types, HSV-1 induces apoptosis early in infection of iDCs, which can be counterbalanced by HSV-1 antiapoptotic proteins expressed in the apoptosis prevention window between 3 h and 6 h p. i. A second apoptosis inducing event occurs after 10 h p. i. in all cells, which is downregulation of c-FLIP. Lytic LAT expression can counterbalance this event in most cell types, but not in iDCs, which express only minor amounts of LATs. Therefore, a second apoptosis prevention window could be defined post 10 h p. i. This conclusion is supported by two observations, i) c-FLIP can substitute for LAT to enhance reactivation of HSV-1 [77] and ii) a LAT knockout HSV-1 mutant is less effective in protection of HeLa cells against apoptosis induced by Fas Ligand than the respective wild type virus [2].

The data presented in this work indicate that HSV-1 precisely regulates apoptosis in different cell types in order to optimize virus spread, replication and establishment of latency. Epithelial cells, which serve as host for productive replication are protected against apoptosis throughout infection until high numbers of progeny virions are released [8, 43, 92]. Latently infected neurons are also protected against apoptosis to ensure that HSV-1 persists in the organism [131]. In contrast, infection of iDCs probably serves different needs of HSV-1. First, HSV-1 might use iDCs as a vehicle to spread within the organism. Therefore, iDCs are kept alive in the early stage of infection, but antigen presentation and activation of T cells is blocked by U_L47 [185] and by interference of HSV-1 with maturation of iDCs [143]. At late times after infection, apoptosis of iDCs is induced. The destruction of infected iDCs at the site of virus replication might lead to a delay in the antiviral immune response [23, 115, 133]. Thereby, the virus gains

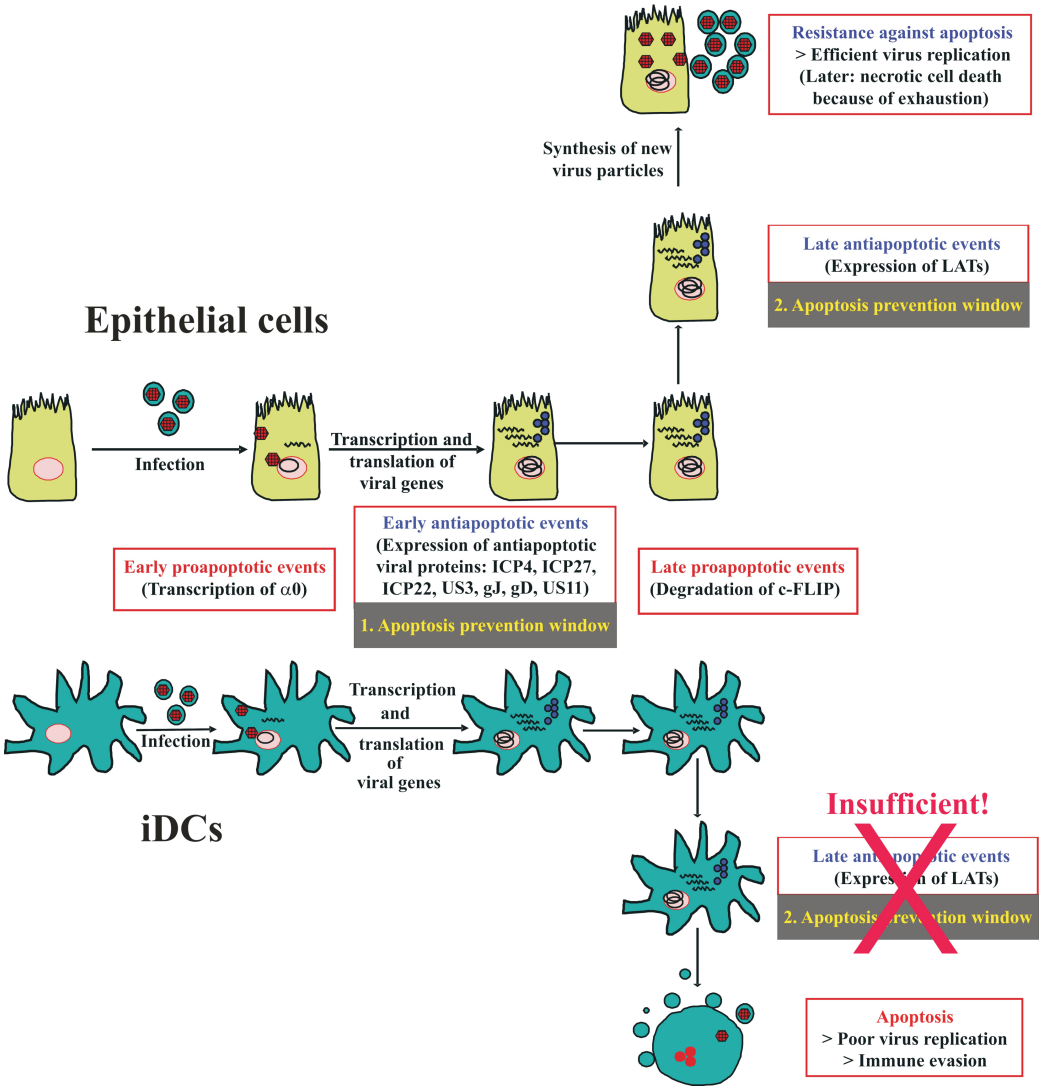

Figure 4.2: **Model of apoptosis modulation by HSV-1.** In addition to the known pro- and antiapoptotic events early after infection, a second proapoptotic event, degradation of c-FLIP, occurs in all cell types late after infection. Lytically expressed LATs can protect most infected cell types from apoptosis. Therefore, a second apoptosis prevention window can be defined late in the lytic HSV-1 replication cycle, which is defined by expression of LATs. In iDCs, LATs are insufficiently expressed and can not counterbalance apoptosis.

time which is needed for infection of neurons and efficient establishment of latency. Finally, bystander iDCs which are not infected take up debris of infected cells and present HSV-1 antigens to T cells [23]. This leads to an immune response which is sufficient to stop replication of the virus and keeps the host alive until reactivation of HSV-1 occurs and the virus can be transmitted to other individuals. This is another intriguing example how a long co-evolution of pathogen and host leads to a complex interaction which ensures maximum dissemination of the pathogen while minimizing damage of the host.

Tables listing the relative abundance of HSV-1 transcripts in iDC, HeLa and HaCaT analyzed with the HSV-1 microarray

Relative abundance of HSV-1 transcripts in iDC compared to HaCaT or HeLa 3 hours after infection

Kinetic class	Transcript(s)	iDC		HaCaT		*P* iDC vs HaCaT	HeLa		*P* iDC vs HeLa
		Median	SD	Median	SD		Median	SD	
	total viral signal	136109	64355	100798	122673	0.7624	25019	14244	0.2347
IE	ICP0a	4.14	0.87	1.24	1.75	0.2146	1.97	2.79	0.4608
IE	ICP0b	7.77	0.81	4.40	2.94	0.3381	9.80	13.86	0.8702
IE	ICP4a	3.71	3.28	19.53	26.32	0.5505	7.76	6.60	0.5432
IE	ICP4b	4.45	0.74	1.61	2.27	0.3076	3.97	3.47	0.8769
IE	UL54	7.24	0.63	2.77	3.91	0.3473	21.68	25.91	0.5749
IE	US1	8.72	0.01	3.34	4.72	0.3529	4.36	3.76	0.3482
L/L/IE	US10-12	8.53	1.46	3.28	4.64	0.3391	8.81	0.73	0.8374
E	UL23	2.51	0.51	2.44	3.45	0.9799	0.00	0.00	0.0899
E	UL29	0.83	0.50	0.73	1.03	0.9137	0.03	0.04	0.2601
E	UL30	0.46	0.16	0.25	0.36	0.5541	0.01	0.02	0.1568
E	UL39/40	**6.40**	**0.38**	3.74	5.29	0.6060	**0.00**	**0.00**	**0.0266**
E	UL50	**2.22**	**0.08**	1.11	1.57	0.5015	**0.03**	**0.04**	**0.0034**
L/E	UL1/2	1.73	0.60	1.80	2.55	0.9751	0.00	0.00	0.1534
L/E	UL4/5	1.15	0.21	0.97	1.37	0.8808	0.04	0.05	0.0716
E(L)	UL8/9	0.40	0.06	0.27	0.38	0.6994	0.50	0.70	0.8814
L/E/L/L	UL11-14	3.80	1.43	2.99	1.27	0.6134	0.85	1.16	0.1569
E/L	UL42/43	0.70	0.09	0.61	0.86	0.9068	0.00	0.00	0.0579
E/L	UL52/53	1.65	0.83	1.07	1.51	0.6912	0.02	0.03	0.2205
L	34.5	0.00	0.00	0	0		0.18	0.25	0.5000
L	UL10	0.69	0.13	0.45	0.36	0.5134	0.28	0.39	0.3642
L	UL15	0.28	0.39	0.11	0.15	0.6503	0.00	0.00	0.5000
L	UL18-20	**1.04**	**0.02**	0.69	0.98	0.7034	**0.00**	**0.00**	**0.0090**
L	UL21	0.10	0.04	0.08	0.12	0.9006	0.04	0.06	0.4258
L	UL22	0.12	0.17	0.21	0.29	0.7560	0.00	0.00	0.5024
L	UL24	0.44	0.37	0.31	0.43	0.7768	0.12	0.16	0.4151
L	UL25/26	1.33	0.84	0.88	1.25	0.7190	0.02	0.03	0.2699
L	UL27/28	3.47	0.77	2.29	3.24	0.6961	0.04	0.05	0.0981
L	UL35	0.75	0.18	0.50	0.70	0.6989	0.27	0.39	0.3016
L	UL36	0.36	0.25	0.25	0.36	0.7566	0.00	0.00	0.2926
L	UL37	1.20	0.04	0.63	0.89	0.5301	0.18	0.25	0.1028
L	UL38	0.01	0.02	0.00	0.00	0.5000	0.01	0.01	0.8482
L	UL41	0.04	0.06	0.00	0.00	0.5000	0.04	0.06	0.9818
L	UL44/45	0.35	0.04	0.58	0.83	0.7578	0.28	0.39	0.8316
L	UL46/47	6.65	0.87	11.81	7.69	0.5157	9.28	13.00	0.8222
L	UL48	2.31	0.01	0.82	1.16	0.3201	0.31	0.43	0.0970
L	UL49	1.36	0.48	2.79	1.69	0.4330	0.13	0.18	0.1364
L	UL51	0.74	0.17	0.92	0.32	0.5835	0.97	0.95	0.7965
L	UL55	**1.08**	**0.18**	0.44	0.63	0.3737	**0.06**	**0.09**	**0.0426**
L	UL56	0.37	0.15	0.56	0.79	0.7963	0.00	0.00	0.1770
L	US2	0.01	0.02	0.00	0.00	0.5000	0.14	0.20	0.5314
L	US3/4	0.23	0.05	0.18	0.26	0.8594	0.76	1.08	0.6097
L	US5/6/7	1.32	0.51	1.15	1.63	0.9085	0.12	0.17	0.1592
L	US8/9	3.33	0.76	2.59	3.67	0.8248	2.01	2.81	0.6262
?	UL3	0.00	0.00	0.07	0.10	0.5024	0.53	0.75	0.5003
?	UL6/7	0.36	0.19	0.48	0.69	0.8422	0.14	0.20	0.3807
?/L	UL16/17	0.17	0.03	0.00	0.00	0.0722	0.86	0.97	0.4979
L/L/?/L	UL31-34	0.15	0.09	0.25	0.18	0.5927	0.03	0.04	0.2773
Latency	LAT5C	0.00	0.00	0.00	0.00		0.07	0.10	0.5000
Latency	LATI	0.00	0.00	0.00	0.00		0.67	0.95	0.5000
Latency	RH6	0.00	0.00	0.00	0.00		17.13	24.22	0.5000
Latency	LATX	1.14	0.59	0.06	0.09	0.2276	0.94	1.24	0.8603
Latency	LAT3	1.65	0.59	2.93	3.81	0.7182	0.33	0.39	0.1366
L	RLXY	0.00	0.00	0.00	0.00		0.00	0.00	
?	orfop	2.51	3.12	15.82	21.82	0.5456	4.25	5.67	0.7504

Table 1: Relative abundance of HSV-1 transcripts in iDCs compared to HaCaT or HeLa 3 h p. i. with HSV-1 strain KOS at MOI 1.5. Kinetic class of transcripts or coterminal transcript families is assigned according to Roizman *et al.* [142]: IE, immediate early; E, early; L, Late; ?, unknown kinetics. U_L8 and U_L9 have early kinetics, but $U_L8.5$ and $U_L9.5$ have late kinetics. Median values of two replicates (infection 2 and 3 as indicated in table 3.1) are shown. Relative abundance is given in % (probe signal expressed as proportion of the total viral signal given in line one). Bold face; relative abundance of this HSV-1 transcript is more than two fold different in iDCs compared to the respective control cell ($P \leq 0.05$).

Relative abundance of HSV-1 transcripts in iDC compared to HaCaT or HeLa 6 hours after infection

Kinetic class	Transcript(s)	iDC		HaCaT		*P* iDC vs HaCaT	HeLa		*P* iDC vs HeLa
		Median	SD	Median	SD		Median	SD	
	total viral signal	601530	166509	327876	392774	0.7302	188306	35960	0.0609
IE	ICP0a	1.25	0.44	1.37	0.71	0.6961	0.95	0.54	0.4471
IE	ICP0b	2.18	0.20	2.84	0.43	0.1395	3.08	0.97	0.4069
IE	ICP4a	0.96	0.39	1.16	3.82	0.4451	3.70	4.34	0.5349
IE	ICP4b	1.39	0.39	1.11	0.21	0.4150	1.83	0.43	0.3913
IE	UL54	2.45	0.49	2.35	0.72	0.9880	3.48	0.32	0.0746
IE	US1	2.96	0.31	3.17	1.30	0.5702	6.21	0.69	0.0686
L/L/IE	US10-12	2.79	0.31	2.48	0.28	0.1019	3.83	0.28	0.0500
E	UL23	2.08	0.20	2.08	0.70	0.6836	3.81	0.42	0.0781
E	UL29	0.94	0.49	0.41	0.20	0.1238	0.91	0.65	0.6810
E	UL30	0.88	0.13	0.48	0.20	0.0884	0.65	0.03	0.0595
E	UL39/40	3.87	0.32	7.10	3.13	0.2972	4.94	0.63	0.2224
E	UL50	3.19	0.07	2.53	0.70	0.2401	3.96	0.57	0.3078
L/E	UL1/2	2.29	0.34	2.15	0.70	0.3319	1.75	1.24	0.5774
L/E	UL4/5	2.30	0.20	2.44	0.10	0.4434	1.68	0.53	0.3209
E(L)	UL8/9	1.08	0.29	0.59	0.49	0.2423	0.88	0.34	0.3768
L/E/L/L	UL11-14	2.85	0.19	3.87	1.18	0.2729	4.82	0.23	0.0111
E/L	UL42/43	2.76	0.19	3.07	1.71	0.8386	2.45	0.64	0.6518
E/L	UL52/53	2.24	0.20	1.99	0.76	0.2552	1.71	0.09	0.0218
L	34.5	0.24	0.08	0.20	0.13	0.4092	0.09	0.07	0.0887
L	UL10	2.39	0.48	2.38	0.08	0.5668	1.33	0.31	0.0844
L	UL15	0.64	0.13	0.50	0.53	0.9984	0.47	0.27	0.5738
L	UL18-20	2.64	0.29	2.75	0.77	0.7234	2.03	0.48	0.3198
L	UL21	1.39	0.22	0.73	0.71	0.3374	0.65	0.29	0.1081
L	UL22	**2.14**	**0.42**	0.62	0.92	0.2655	**0.59**	**0.07**	**0.0282**
L	UL24	**1.51**	**0.13**	0.56	0.85	0.4471	**0.47**	**0.13**	**0.0079**
L	UL25/26	1.93	0.42	1.85	0.82	0.5759	1.61	0.57	0.3959
L	UL27/28	2.52	0.28	2.30	0.12	0.2156	3.67	0.35	0.0801
L	UL35	2.15	0.19	1.16	0.79	0.2680	2.06	0.33	0.6366
L	UL36	**1.39**	**0.02**	0.31	0.61	0.1627	**0.26**	**0.00**	**0.0001**
L	UL37	2.06	0.12	2.38	1.14	0.8247	0.87	0.57	0.1970
L	UL38	**1.65**	**0.37**	1.69	1.11	0.6910	**0.26**	**0.02**	**0.0243**
L	UL41	**1.59**	**0.36**	1.42	0.99	0.4945	**0.33**	**0.06**	**0.0191**
L	UL44/45	2.43	0.18	2.86	1.03	0.8259	2.77	0.47	0.5942
L	UL46/47	3.42	0.04	3.59	3.48	0.4384	5.73	0.84	0.1581
L	UL48	3.65	0.06	3.68	1.13	0.6679	3.11	0.04	0.0015
L	UL49	3.98	0.19	6.60	2.54	0.2832	4.98	0.15	0.0080
L	UL51	**2.43**	**0.37**	1.22	0.87	0.2255	**0.87**	**0.05**	**0.0162**
L	UL55	2.40	0.25	1.77	0.43	0.3858	1.88	0.16	0.1261
L	UL56	1.94	0.20	0.83	0.63	0.1595	1.06	0.37	0.1469
L	US2	**1.21**	**0.16**	0.62	0.70	0.3284	**0.32**	**0.02**	**0.0085**
L	US3/4	**1.59**	**0.06**	0.56	0.50	0.0924	**0.64**	**0.09**	**0.0125**
L	US5/6/7	2.54	0.14	1.53	0.40	0.0451	2.43	0.60	0.9384
L	US8/9	3.18	0.25	3.89	0.59	0.2185	3.77	0.33	0.2185
?	UL3	1.50	0.51	1.98	1.25	0.8411	1.26	0.18	0.7159
?	UL6/7	**1.69**	**0.14**	0.79	0.60	0.2148	**0.64**	**0.08**	**0.0017**
?/L	UL16/17	**1.01**	**0.10**	1.22	0.63	0.8547	**0.36**	**0.04**	**0.0021**
L/L/?/L	UL31-34	0.80	0.42	0.71	0.31	0.5025	0.56	0.16	0.1968
Latency	LAT5C	0.00	0.01	0.04	0.02	0.3160	0.00	0.00	0.4226
Latency	LATI	0.12	0.08	0.32	0.21	0.1903	0.07	0.10	0.8500
Latency	RH6	0.01	0.02	0.12	0.05	0.0865	0.05	0.07	0.6375
Latency	LATX	0.42	0.26	0.28	0.37	0.8865	0.27	0.08	0.2580
Latency	LAT3	0.69	0.20	1.18	0.40	0.2344	0.45	0.10	0.3343
L	RLXY	**0.60**	**0.17**	0.19	0.28	0.2259	**0.02**	**0.02**	**0.0317**
?	orfop	0.44	0.61	0.45	3.59	0.4816	3.44	4.54	0.5494

Table 2: Relative abundance of HSV-1 transcripts in iDCs compared to HaCaT or HeLa 6 h p. i. with HSV-1 strain KOS at MOI 1.5. Kinetic class of transcripts or coterminal transcript families is assigned according to Roizman *et al.* [142]: IE, immediate early; E, early; L, Late; ?, unknown kinetics. U_L8 and U_L9 have early kinetics, but $U_L8.5$ and $U_L9.5$ have late kinetics. Median values were calculated out of three replicates (for iDCs and HaCaT, infection 1-3 as indicated in table 3.1) or two replicates (for HeLa, infection 2 and 3 as indicated in table 3.1). Relative abundance is given in % (probe signal expressed as proportion of the total viral signal given in line one). Bold face; relative abundance of this HSV-1 transcript is more than two fold different in iDCs compared to the respective control cell ($P \leq 0.05$).

Relative abundance of HSV-1 transcripts in iDC compared to HaCaT or HeLa 10 hours after infection

Kinetic class	Transcript(s)	iDC		HaCaT		*P* iDC vs HaCaT	HeLa		*P* iDC vs HeLa
		Median	SD	Median	SD		Median	SD	
	total viral signal	390963	211457	456252	339622	0.5467	561168	166110	0.6961
IE	ICP0a	0.99	0.28	1.03	0.69	0.6512	1.42	0.32	0.3045
IE	ICP0b	2.09	0.33	2.05	0.33	0.5553	2.46	0.29	0.3505
IE	ICP4a	0.35	1.36	1.03	0.48	0.8948	0.51	0.04	0.5349
IE	ICP4b	0.92	0.62	1.11	0.50	0.9453	1.42	0.09	0.5666
IE	UL54	2.49	0.27	1.76	0.22	0.0266	1.92	0.20	0.0956
IE	US1	3.17	0.32	2.56	0.96	0.8746	2.43	0.13	0.0652
L/L/IE	US10-12	2.76	0.73	3.09	1.14	0.6628	3.07	0.83	0.7048
E	UL23	1.57	0.59	1.79	0.31	0.9524	1.35	0.29	0.2731
E	UL29	1.10	0.39	1.00	0.21	0.5448	0.96	0.42	0.7569
E	UL30	0.68	0.07	1.09	0.38	0.2838	0.51	0.42	0.6678
E	UL39/40	4.50	1.25	2.77	0.69	0.0946	2.69	0.63	0.1339
E	UL50	3.27	0.88	1.91	0.33	0.0745	2.47	0.49	0.1866
L/E	UL1/2	2.12	0.49	2.09	0.46	0.7918	2.02	0.07	0.8928
L/E	UL4/5	2.31	0.64	1.84	0.25	0.2193	1.54	0.38	0.1750
E(L)	UL8/9	0.85	0.21	1.07	0.55	0.6559	0.90	0.55	0.9792
L/E/L/L	UL11-14	2.95	1.30	2.28	1.36	0.7390	2.41	0.18	0.3572
E/L	UL42/43	2.65	0.30	2.30	0.32	0.0902	2.35	0.04	0.1583
E/L	UL52/53	2.11	0.46	1.89	0.65	0.8197	1.83	0.03	0.3526
L	34.5	0.19	0.04	0.16	0.25	0.5687	0.10	0.04	0.1409
L	UL10	1.97	0.52	2.21	0.20	0.8552	2.92	0.56	0.3044
L	UL15	0.59	0.20	1.36	0.61	0.2854	1.11	0.83	0.5472
L	UL18-20	2.31	0.34	2.30	0.63	0.4774	2.78	0.31	0.2454
L	UL21	1.35	0.47	1.88	0.65	0.4051	1.77	0.07	0.1773
L	UL22	2.21	0.78	1.84	0.59	0.7276	1.67	0.12	0.6839
L	UL24	1.61	0.37	1.43	1.11	0.4969	1.19	0.10	0.3024
L	UL25/26	1.78	0.91	3.42	0.95	0.3004	2.84	1.26	0.6085
L	UL27/28	3.09	0.61	2.32	0.53	0.7179	2.73	0.81	0.9746
L	UL35	1.82	0.79	2.92	0.87	0.4951	2.36	0.46	0.8893
L	UL36	1.22	0.33	1.33	1.34	0.6279	1.23	0.05	0.9216
L	UL37	1.72	0.15	1.38	0.79	0.5531	1.45	0.29	0.3284
L	UL38	1.62	0.79	1.58	0.66	0.9974	1.36	0.03	0.8221
L	UL41	1.79	0.95	1.36	0.70	0.6106	1.84	0.08	0.9580
L	UL4445	2.43	0.54	2.44	1.06	0.7911	3.30	0.50	0.2330
L	UL46/47	3.66	1.10	2.50	2.53	0.9794	4.12	0.76	0.6720
L	UL48	3.95	0.44	2.55	0.81	0.0752	3.61	0.46	0.4414
L	UL49	4.70	0.62	2.73	1.51	0.3266	3.85	0.30	0.2534
L	UL51	2.28	0.86	2.28	0.90	0.8316	2.14	0.14	0.7891
L	UL55	2.33	0.33	1.84	0.37	0.1804	1.65	0.11	0.0967
L	UL56	1.94	0.53	1.74	0.78	0.7624	1.52	0.17	0.3232
L	US2	1.46	0.53	1.74	0.60	0.4275	1.31	0.20	0.6737
L	US3/4	1.33	0.24	1.43	0.61	0.8128	0.99	0.21	0.2790
L	US5/6/7	2.21	0.41	2.55	0.36	0.8065	2.09	0.22	0.4771
L	US8/9	3.64	0.46	2.51	1.68	0.6754	3.46	0.84	0.8388
?	UL3	1.31	1.10	1.97	0.66	0.5227	2.75	0.03	0.2059
?	UL6/7	1.36	0.12	2.03	0.60	0.3129	1.43	0.38	0.7798
?/L	UL16/17	0.78	0.12	0.87	0.67	0.6251	0.47	0.15	0.1847
L/L/?/L	UL31-34	1.18	0.47	1.46	0.68	0.3569	1.21	0.36	0.5070
Latency	LAT5C	0.06	0.04	0.44	0.30	0.2187	0.36	0.15	0.1959
Latency	LATI	0.34	0.23	0.88	0.42	0.1155	1.44	0.45	0.1312
Latency	RH6	0.10	0.06	0.79	0.47	0.1981	0.45	0.17	0.1795
Latency	LATX	**0.83**	**0.44**	2.11	0.84	0.1814	**2.52**	**0.22**	**0.0098**
Latency	LAT3	**1.09**	**0.37**	1.57	0.44	0.0729	**2.54**	**0.25**	**0.0107**
L	RLXY	0.72	0.58	0.75	0.59	0.8073	0.61	0.19	0.9067
?	orfop	0.34	1.13	0.75	0.55	0.9370	0.53	0.03	0.5619

Table 3: Relative abundance of HSV-1 transcripts in iDCs compared to HaCaT or HeLa 10 h p. i. with HSV-1 strain KOS at MOI 1.5. Kinetic class of transcripts or coterminal transcript families is assigned according to Roizman *et al.* [142]: IE, immediate early; E, early; L, Late; ?, unknown kinetics. U_L8 and U_L9 have early kinetics, but $U_L8.5$ and $U_L9.5$ have late kinetics. Median values were calculated out of three replicates (for iDCs and HaCaT, infection 1-3 as indicated in table 3.1) or two replicates (for HeLa, infection 1 and 3 as indicated in table 3.1). Relative abundance is given in % (probe signal expressed as proportion of the total viral signal given in line one). Bold face; relative abundance of this HSV-1 transcript is more than two fold different in iDCs compared to the respective control cell ($P \leq 0.05$).

Relative abundance of HSV-1 transcripts in iDC compared to HaCaT or HeLa 18 hours after infection

Kinetic class	Transcript(s)	iDC		HaCaT		*P* iDC vs HaCaT	HeLa		*P* iDC vs HeLa
		Median	SD	Median	SD		Median	SD	
	total viral signal	640253	123599	618127	293075	0.8463	359646	54179	0.0428
IE	ICP0a	0.92	0.06	1.64	0.39	0.1230	1.21	0.23	0.3468
IE	ICP0b	1.85	0.04	2.20	0.71	0.3567	1.88	0.07	0.7261
IE	ICP4a	0.32	0.55	1.13	0.34	0.4303	1.15	0.91	0.5635
IE	ICP4b	0.82	0.23	0.78	0.64	0.4846	1.17	0.38	0.3418
IE	UL54	1.85	0.21	1.58	0.66	0.4340	1.75	0.09	0.8614
IE	US1	3.20	0.35	2.38	0.73	0.1274	2.64	0.25	0.0794
L/L/IE	US10-12	3.02	0.80	2.39	0.56	0.2849	2.59	1.04	0.4839
E	UL23	1.22	0.33	0.61	0.44	0.3292	1.03	0.38	0.9374
E	UL29	1.07	0.36	0.44	0.16	0.1645	0.81	0.35	0.7101
E	UL30	0.66	0.08	0.48	0.15	0.1990	0.63	0.27	0.8226
E	UL39/40	2.60	0.45	2.80	0.16	0.6198	2.32	0.57	0.6738
E	UL50	2.49	0.42	1.47	0.27	0.0513	1.74	0.40	0.1714
L/E	UL1/2	2.22	0.63	2.02	0.73	0.8819	2.13	0.54	0.5161
L/E	UL4/5	1.64	0.47	1.28	0.33	0.7134	1.36	0.35	0.6513
E(L)	UL8/9	0.61	0.12	0.49	0.67	0.6446	1.04	0.45	0.4001
L/E/L/L	UL11-14	2.62	0.40	2.20	0.41	0.2818	2.45	0.14	0.4974
E/L	UL42/43	2.67	0.28	2.33	0.31	0.3647	2.36	0.15	0.1300
E/L	UL52/53	1.83	0.23	1.27	0.25	0.0236	2.37	0.07	0.0476
L	34.5	0.10	0.04	0.18	0.20	0.4339	0.13	0.04	0.8728
L	UL10	2.31	0.32	2.73	0.39	0.1733	2.25	0.04	0.9584
L	UL15	0.66	0.08	1.05	0.49	0.3868	0.77	0.28	0.7698
L	UL18-20	2.88	0.15	3.15	0.61	0.9540	2.73	0.40	0.8454
L	UL21	1.66	0.25	1.86	0.43	0.9591	1.69	0.04	0.6381
L	UL22	2.17	0.19	1.32	0.42	0.0874	1.66	0.40	0.2696
L	UL24	1.44	0.16	1.42	0.34	0.5094	1.91	0.60	0.4818
L	UL25/26	2.33	0.69	2.59	0.26	0.9557	2.71	0.42	0.8918
L	UL27/28	3.25	0.36	2.50	0.22	0.0667	2.50	0.84	0.4802
L	UL35	2.67	0.40	2.56	0.23	0.5826	2.98	0.30	0.5925
L	UL36	1.53	0.16	1.10	0.74	0.7178	1.53	0.53	0.9902
L	UL37	1.50	0.14	1.97	0.85	0.9395	1.29	0.27	0.3506
L	UL38	1.68	0.41	1.95	0.72	0.6548	1.88	0.66	0.6242
L	UL41	1.69	0.06	2.14	0.55	0.5697	1.69	0.34	0.9373
L	UL44/45	3.29	0.24	3.62	0.72	0.9464	2.75	0.85	0.5463
L	UL46/47	3.59	0.41	3.29	1.08	0.9038	3.49	0.71	0.8592
L	UL48	3.79	0.39	3.57	1.19	0.9890	2.33	0.81	0.2379
L	UL49	3.40	0.49	3.78	1.47	0.8512	3.20	0.13	0.2442
L	UL51	2.68	0.59	2.57	0.19	0.3915	2.59	0.09	0.4758
L	UL55	2.37	0.11	0.83	0.61	0.0724	1.63	0.24	0.1243
L	UL56	1.54	0.29	2.21	0.64	0.1481	2.43	0.24	0.0401
L	US2	1.74	0.14	1.16	0.60	0.4539	1.68	0.20	0.8100
L	US3/4	1.62	0.29	1.31	0.52	0.4790	1.23	0.44	0.4859
L	US5/6/7	2.70	0.28	2.33	0.24	0.1019	2.43	0.15	0.2929
L	US8/9	3.14	0.47	3.53	0.50	0.4980	3.14	0.60	0.9306
?	UL3	2.37	0.26	3.46	1.09	0.1918	2.88	0.38	0.2746
?	UL6/7	1.17	0.16	0.97	0.32	0.4807	1.52	0.48	0.5017
?/L	UL16/17	0.72	0.11	0.95	0.48	0.6776	0.64	0.31	0.8084
L/L/?/L	UL31-34	1.65	0.23	0.82	0.53	0.2371	1.38	0.39	0.7131
Latency	LAT5C	0.14	0.06	0.24	0.34	0.3255	0.58	0.28	0.2453
Latency	LATI	**0.77**	**0.18**	**2.23**	**0.51**	**0.0187**	2.14	0.67	0.1843
Latency	RH6	0.32	0.10	1.04	0.51	0.1204	0.85	0.32	0.2198
Latency	LATX	1.70	0.47	2.30	0.17	0.0746	2.32	0.08	0.0918
Latency	LAT3	1.80	0.32	2.35	0.47	0.1109	2.24	0.01	0.1317
L	RLXY	0.75	0.26	0.92	0.33	0.5906	0.97	0.40	0.8371
?	orfop	0.46	0.50	0.68	0.51	0.7765	1.23	0.88	0.5262

Table 4: Relative abundance of HSV-1 transcripts in iDCs compared to HaCaT or HeLa 18 h p. i. with HSV-1 strain KOS at MOI 1.5. Kinetic class of transcripts or coterminal transcript families is assigned according to Roizman *et al.* [142]: IE, immediate early; E, early; L, Late; ?, unknown kinetics. U_L8 and U_L9 have early kinetics, but $U_L8.5$ and $U_L9.5$ have late kinetics. Median values were calculated out of three replicates (for iDCs and HaCaT, infection 1-3 as indicated in table 3.1) or two replicates (for HeLa, infection 2 and 3 as indicated in table 3.1). Relative abundance is given in % (probe signal expressed as proportion of the total viral signal given in line one). Bold face; relative abundance of this HSV-1 transcript is more than two fold different in iDCs compared to the respective control cell ($P \leq 0.05$).

Bibliography

[1] J. M. Adams. Ways of dying: multiple pathways to apoptosis. *Genes Dev*, 17(20): 2481–2495, Oct 2003. doi: 10.1101/gad.1126903. URL http://dx.doi.org/10.1101/gad.1126903.

[2] M. Ahmed, M. Lock, C. G. Miller, and N. W. Fraser. Regions of the herpes simplex virus type 1 latency-associated transcript that protect cells from apoptosis in vitro and protect neuronal cells in vivo. *J Virol*, 76(2):717–729, Jan 2002.

[3] G. Andrei, J. van den Oord, P. Fiten, G. Opdenakker, C. D. Wolf-Peeters, E. D. Clercq, and R. Snoeck. Organotypic epithelial raft cultures as a model for evaluating compounds against alphaherpesviruses. *Antimicrob Agents Chemother*, 49 (11):4671–4680, Nov 2005. doi: 10.1128/AAC.49.11.4671-4680.2005. URL http://dx.doi.org/10.1128/AAC.49.11.4671-4680.2005.

[4] K. Ardeshna, A. Pizzey, S. Devereux, and A. Khwaja. The PI3 kinase, p38 SAP kinase, and NF-kappaB signal transduction pathways are involved in the survival and maturation of lipopolysaccharide-stimulated human monocyte-derived dendritic cells. *Blood*, 96(3):1039–46, Aug 2000.

[5] J. Arii, H. Goto, T. Suenaga, M. Oyama, H. Kozuka-Hata, T. Imai, A. Minowa, H. Akashi, H. Arase, Y. Kawaoka, and Y. Kawaguchi. Non-muscle myosin iia is a functional entry receptor for herpes simplex virus-1. *Nature*, 467(7317):859–862, Oct 2010. doi: 10.1038/nature09420. URL http://dx.doi.org/10.1038/nature09420.

[6] H. L. Attrill, S. A. Cumming, J. B. Clements, and S. V. Graham. The herpes simplex virus type 1 us11 protein binds the coterminal ul12, ul13, and ul14 rnas and regulates ul13 expression in vivo. *J Virol*, 76(16):8090–8100, Aug 2002.

[7] M. Aubert and J. A. Blaho. The herpes simplex virus type 1 regulatory protein icp27 is required for the prevention of apoptosis in infected human cells. *J Virol*, 73(4):2803–2813, Apr 1999.

[8] M. Aubert, J. O'Toole, and J. Blaho. Induction and prevention of apoptosis in human HEp-2 cells by herpes simplex virus type 1. *J Virol*, 73(12):10359–70, Dec 1999.

[9] M. Aubert, S. A. Rice, and J. A. Blaho. Accumulation of herpes simplex virus type 1 early and leaky-late proteins correlates with apoptosis prevention in infected human hep-2 cells. *J Virol*, 75(2):1013–1030, Jan 2001. doi:

10.1128/JVI.75.2.1013-1030.2001. URL http://dx.doi.org/10.1128/JVI.75.2.1013-1030.2001.

[10] M. Aubert, Z. Chen, R. Lang, C. H. Dang, C. Fowler, D. D. Sloan, and K. R. Jerome. The antiapoptotic herpes simplex virus glycoprotein j localizes to multiple cellular organelles and induces reactive oxygen species formation. *J Virol*, 82(2): 617–629, Jan 2008. doi: 10.1128/JVI.01341-07. URL http://dx.doi.org/10.1128/JVI.01341-07.

[11] S. Balachandran, P. C. Roberts, T. Kipperman, K. N. Bhalla, R. W. Compans, D. R. Archer, and G. N. Barber. Alpha/beta interferons potentiate virus-induced apoptosis through activation of the fadd/caspase-8 death signaling pathway. *J Virol*, 74(3):1513–1523, Feb 2000.

[12] J. Banchereau and R. M. Steinman. Dendritic cells and the control of immunity. *Nature*, 392(6673):245–252, Mar 1998. doi: 10.1038/32588. URL http://dx.doi.org/10.1038/32588.

[13] J. Banchereau, F. Briere, C. Caux, J. Davoust, S. Lebecque, Y. J. Liu, B. Pulendran, and K. Palucka. Immunobiology of dendritic cells. *Annu Rev Immunol*, 18:767–811, 2000. doi: 10.1146/annurev.immunol.18.1.767. URL http://dx.doi.org/10.1146/annurev.immunol.18.1.767.

[14] A. H. Batchelor and P. O'Hare. Regulation and cell-type-specific activity of a promoter located upstream of the latency-associated transcript of herpes simplex virus type 1. *J Virol*, 64(7):3269–3279, Jul 1990.

[15] A. H. Batchelor and P. O'Hare. Localization of cis-acting sequence requirements in the promoter of the latency-associated transcript of herpes simplex virus type 1 required for cell-type-specific activity. *J Virol*, 66(6):3573–3582, Jun 1992.

[16] Y. Becker, H. Dym, and I. Sarov. Herpes simplex virus dna. *Virology*, 36(2):184–192, Oct 1968.

[17] L. Benetti and B. Roizman. Herpes simplex virus protein kinase us3 activates and functionally overlaps protein kinase a to block apoptosis. *Proc Natl Acad Sci U S A*, 101(25):9411–9416, Jun 2004. doi: 10.1073/pnas.0403160101. URL http://dx.doi.org/10.1073/pnas.0403160101.

[18] L. Benetti and B. Roizman. In transduced cells, the us3 protein kinase of herpes simplex virus 1 precludes activation and induction of apoptosis by transfected procaspase 3. *J Virol*, 81(19):10242–10248, Oct 2007. doi: 10.1128/JVI.00820-07. URL http://dx.doi.org/10.1128/JVI.00820-07.

[19] M. Bentele, I. Lavrik, M. Ulrich, S. Stösser, D. W. Heermann, H. Kalthoff, P. H. Krammer, and R. Eils. Mathematical modeling reveals threshold mechanism in cd95-induced apoptosis. *J Cell Biol*, 166(6):839–851, Sep 2004. doi: 10.1083/jcb.200404158. URL http://dx.doi.org/10.1083/jcb.200404158.

[20] S. M. Best. Viral subversion of apoptotic enzymes: escape from death row. *Annu Rev Microbiol*, 62:171–192, 2008. doi: 10.1146/annurev.micro.62.081307.163009. URL http://dx.doi.org/10.1146/annurev.micro.62.081307.163009.

[21] M. S. Bhuiyan and K. Fukunaga. Inhibition of htra2/omi ameliorates heart dysfunction following ischemia/reperfusion injury in rat heart in vivo. *Eur J Pharmacol*, 557(2-3):168–177, Feb 2007. doi: 10.1016/j.ejphar.2006.10.067. URL http://dx.doi.org/10.1016/j.ejphar.2006.10.067.

[22] T. M. Block, S. Deshmane, J. Masonis, J. Maggioncalda, T. Valyi-Nagi, and N. W. Fraser. An hsv lat null mutant reactivates slowly from latent infection and makes small plaques on cv-1 monolayers. *Virology*, 192(2):618–630, Feb 1993. doi: 10.1006/viro.1993.1078. URL http://dx.doi.org/10.1006/viro.1993.1078.

[23] L. Bosnjak, M. Miranda-Saksena, D. M. Koelle, R. A. Boadle, C. A. Jones, and A. L. Cunningham. Herpes simplex virus infection of human dendritic cells induces apoptosis and allows cross-presentation via uninfected dendritic cells. *J Immunol*, 174(4):2220–7, Feb 2005.

[24] F. J. Branco and N. W. Fraser. Herpes simplex virus type 1 latency-associated transcript expression protects trigeminal ganglion neurons from apoptosis. *J Virol*, 79(14):9019–9025, Jul 2005. doi: 10.1128/JVI.79.14.9019-9025.2005. URL http://dx.doi.org/10.1128/JVI.79.14.9019-9025.2005.

[25] W. Cai and P. A. Schaffer. Herpes simplex virus type 1 icp0 regulates expression of immediate-early, early, and late genes in productively infected cells. *J Virol*, 66 (5):2904–2915, May 1992.

[26] A. Cartier, T. Komai, and M. G. Masucci. The Us3 protein kinase of herpes simplex virus 1 blocks apoptosis and induces phosporylation of the Bcl-2 family member Bad. *Exp Cell Res*, 291(1):242–50, Nov 2003.

[27] K. A. Cassady and M. Gross. The herpes simplex virus type 1 u(s)11 protein interacts with protein kinase r in infected cells and requires a 30-amino-acid sequence adjacent to a kinase substrate domain. *J Virol*, 76(5):2029–2035, Mar 2002.

[28] X. Chen, M. C. Schmidt, W. F. Goins, and J. C. Glorioso. Two herpes simplex virus type 1 latency-active promoters differ in their contributions to latency-associated transcript expression during lytic and latent infections. *J Virol*, 69(12):7899–7908, Dec 1995.

[29] S. K. Chiou, C. C. Tseng, L. Rao, and E. White. Functional complementation of the adenovirus e1b 19-kilodalton protein with bcl-2 in the inhibition of apoptosis in infected cells. *J Virol*, 68(10):6553–6566, Oct 1994.

[30] J. E. Chipuk, U. Maurer, D. R. Green, and M. Schuler. Pharmacologic activation of p53 elicits Bax-dependent apoptosis in the absence of transcription. *Cancer Cell*, 4 (5):371–81, Nov 2003.

[31] T. W. Day, S. Huang, and A. R. Safa. c-flip knockdown induces ligand-independent dr5-, fadd-, caspase-8-, and caspase-9-dependent apoptosis in breast cancer cells. *Biochem Pharmacol*, 76(12):1694–1704, Dec 2008. doi: 10.1016/j.bcp.2008.09.007. URL `http://dx.doi.org/10.1016/j.bcp.2008.09.007`.

[32] G. B. Devi-Rao, S. A. Goodart, L. M. Hecht, R. Rochford, M. K. Rice, and E. K. Wagner. Relationship between polyadenylated and nonpolyadenylated herpes simplex virus type 1 latency-associated transcripts. *J Virol*, 65(5):2179–2190, May 1991.

[33] A. Dolan, F. E. Jamieson, C. Cunningham, B. C. Barnett, and D. J. McGeoch. The genome sequence of herpes simplex virus type 2. *J Virol*, 72(3):2010–2021, Mar 1998.

[34] P. Dumont, J. I.-J. Leu, A. C. D. Pietra, D. L. George, and M. Murphy. The codon 72 polymorphic variants of p53 have markedly different apoptotic potential. *Nat Genet*, 33(3):357–65, Mar 2003. doi: 10.1038/ng1093. URL `http://dx.doi.org/10.1038/ng1093`.

[35] C. R. e Sousa. Dendritic cells in a mature age. *Nat Rev Immunol*, 6(6):476–483, Jun 2006. doi: 10.1038/nri1845. URL `http://dx.doi.org/10.1038/nri1845`.

[36] G. B. Elion, P. A. Furman, J. A. Fyfe, P. de Miranda, L. Beauchamp, and H. J. Schaeffer. Selectivity of action of an antiherpetic agent, 9-(2-hydroxyethoxymethyl) guanine. *Proc Natl Acad Sci U S A*, 74(12):5716–5720, Dec 1977.

[37] H. L. ENNIS and M. LUBIN. Cycloheximide: Aspects of inhibition of protein synthesis in mammalian cells. *Science*, 146:1474–1476, Dec 1964.

[38] L. Faccio, C. Fusco, A. Chen, S. Martinotti, J. V. Bonventre, and A. S. Zervos. Characterization of a novel human serine protease that has extensive homology to bacterial heat shock endoprotease htra and is regulated by kidney ischemia. *J Biol Chem*, 275(4):2581–2588, Jan 2000.

[39] M. C. Frame, F. C. Purves, D. J. McGeoch, H. S. Marsden, and D. P. Leader. Identification of the herpes simplex virus protein kinase as the product of viral gene us3. *J Gen Virol*, 68 (Pt 10):2699–2704, Oct 1987.

[40] L. Frasca, C. Scottà, G. Lombardi, and E. Piccolella. Human anergic cd4+ t cells can act as suppressor cells by affecting autologous dendritic cell conditioning and survival. *J Immunol*, 168(3):1060–1068, Feb 2002.

[41] T. Fukazawa, T. Fujiwara, F. Uno, F. Teraishi, Y. Kadowaki, T. Itoshima, Y. Takata, S. Kagawa, J. Roth, J. Tschopp, and N. Tanaka. Accelerated degradation of cellular

FLIP protein through the ubiquitin-proteasome pathway in p53-mediated apoptosis of human cancer cells. *Oncogene*, 20(37):5225–31, Aug 2001. doi: 10.1038/sj/onc/1204673. URL http://dx.doi.org/10.1038/sj/onc/1204673.

[42] M. Furihata, T. Takeuchi, M. Matsumoto, A. Kurabayashi, Y. Ohtsuki, N. Terao, M. Kuwahara, and T. Shuin. p53 mutation arising in arg72 allele in the tumorigenesis and development of carcinoma of the urinary tract. *Clin Cancer Res*, 8(5): 1192–1195, May 2002.

[43] V. Galvan and B. Roizman. Herpes simplex virus 1 induces and blocks apoptosis at multiple steps during infection and protects cells from exogenous inducers in a cell-type-dependent manner. *Proc Natl Acad Sci U S A*, 95(7):3931–6, Mar 1998.

[44] J. A. Garner. Herpes simplex virion entry into and intracellular transport within mammalian cells. *Adv Drug Deliv Rev*, 55(11):1497–1513, Nov 2003.

[45] A. V. Gasparian, O. A. Guryanova, D. V. Chebotaev, A. A. Shishkin, A. Y. Yemelyanov, and I. V. Budunova. Targeting transcription factor nfkappab: comparative analysis of proteasome and ikk inhibitors. *Cell Cycle*, 8(10):1559–1566, May 2009.

[46] W. T. Godbey, K. K. Wu, and A. G. Mikos. Tracking the intracellular path of poly(ethylenimine)/dna complexes for gene delivery. *Proc Natl Acad Sci U S A*, 96(9):5177–5181, Apr 1999.

[47] P. J. Godowski and D. M. Knipe. Transcriptional control of herpesvirus gene expression: gene functions required for positive and negative regulation. *Proc Natl Acad Sci U S A*, 83(2):256–260, Jan 1986.

[48] A. Golks, D. Brenner, C. Fritsch, P. H. Krammer, and I. N. Lavrik. c-flipr, a new regulator of death receptor-induced apoptosis. *J Biol Chem*, 280(15):14507–14513, Apr 2005. doi: 10.1074/jbc.M414425200. URL http://dx.doi.org/10.1074/jbc.M414425200.

[49] Y. Gong, K. M. Raj, C. A. Luscombe, I. Gadawski, T. Tam, J. Chu, D. Gibson, R. Carlson, and S. L. Sacks. The synergistic effects of betulin with acyclovir against herpes simplex viruses. *Antiviral Res*, 64(2):127–130, Nov 2004. doi: 10.1016/j.antiviral.2004.05.006. URL http://dx.doi.org/10.1016/j.antiviral.2004.05.006.

[50] M. L. Goodkin, A. T. Ting, and J. A. Blaho. NF-kappaB is required for apoptosis prevention during herpes simplex virus type 1 infection. *J Virol*, 77(13):7261–7280, Jul 2003.

[51] F. Granucci, E. Ferrero, M. Foti, D. Aggujaro, K. Vettoretto, and P. Ricciardi-Castagnoli. Early events in dendritic cell maturation induced by lps. *Microbes Infect*, 1(13):1079–1084, Nov 1999.

[52] B. Grubor-Bauk, A. Simmons, G. Mayrhofer, and P. G. Speck. Impaired clearance of herpes simplex virus type 1 from mice lacking cd1d or nkt cells expressing the semivariant v alpha 14-j alpha 281 tcr. *J Immunol*, 170(3):1430–1434, Feb 2003.

[53] Z. Guo, M. Zhang, H. An, W. Chen, S. Liu, J. Guo, Y. Yu, and X. Cao. Fas ligation induces il-1beta-dependent maturation and il-1beta-independent survival of dendritic cells: different roles of erk and nf-kappab signaling pathways. *Blood*, 102(13):4441–4447, Dec 2003. doi: 10.1182/blood-2002-11-3420. URL `http://dx.doi.org/10.1182/blood-2002-11-3420`.

[54] Z. Guo, M. Zhang, H. Tang, and X. Cao. Fas signal links innate and adaptive immunity by promoting dendritic-cell secretion of cc and cxc chemokines. *Blood*, 106(6):2033–2041, Sep 2005. doi: 10.1182/blood-2004-12-4831. URL `http://dx.doi.org/10.1182/blood-2004-12-4831`.

[55] L. Han, Y. Zhao, and X. Jia. Mathematical modeling identified c-flip as an apoptotic switch in death receptor induced apoptosis. *Apoptosis*, 13(10):1198–1204, Oct 2008. doi: 10.1007/s10495-008-0252-3. URL `http://dx.doi.org/10.1007/s10495-008-0252-3`.

[56] M. A. Hardwicke and R. M. Sandri-Goldin. The herpes simplex virus regulatory protein icp27 contributes to the decrease in cellular mrna levels during infection. *J Virol*, 68(8):4797–4810, Aug 1994.

[57] W. R. Hardy and R. M. Sandri-Goldin. Herpes simplex virus inhibits host cell splicing, and regulatory protein icp27 is required for this effect. *J Virol*, 68(12):7790–7799, Dec 1994.

[58] H. Hasebe, K. Sato, H. Yanagie, Y. Takeda, Y. Nonaka, T. Takahashi, M. Eriguchi, and H. Nagawa. Bcl-2, Bcl-xL and c-FLIP(L) potentially regulate the susceptibility of human peripheral blood monocyte-derived dendritic cells to cell death at different developmental stages. *Biomed Pharmacother*, 56(3):144–51, May 2002.

[59] D. Hawiger, K. Inaba, Y. Dorsett, M. Guo, K. Mahnke, M. Rivera, J. V. Ravetch, R. M. Steinman, and M. C. Nussenzweig. Dendritic cells induce peripheral t cell unresponsiveness under steady state conditions in vivo. *J Exp Med*, 194(6):769–779, Sep 2001.

[60] B. He, M. Gross, and B. Roizman. The gamma134.5 protein of herpes simplex virus 1 has the structural and functional attributes of a protein phosphatase 1 regulatory subunit and is present in a high molecular weight complex with the enzyme in infected cells. *J Biol Chem*, 273(33):20737–20743, Aug 1998.

[61] R. Hegde, S. M. Srinivasula, Z. Zhang, R. Wassell, R. Mukattash, L. Cilenti, G. DuBois, Y. Lazebnik, A. S. Zervos, T. Fernandes-Alnemri, and E. S. Alnemri.

Identification of omi/htra2 as a mitochondrial apoptotic serine protease that disrupts inhibitor of apoptosis protein-caspase interaction. *J Biol Chem*, 277(1):432–438, Jan 2002. doi: 10.1074/jbc.M109721200. URL http://dx.doi.org/10.1074/jbc.M109721200.

[62] G. Henderson, W. Peng, L. Jin, G.-C. Perng, A. B. Nesburn, S. L. Wechsler, and C. Jones. Regulation of caspase 8- and caspase 9-induced apoptosis by the herpes simplex virus type 1 latency-associated transcript. *J Neurovirol*, 8 Suppl 2:103–111, Dec 2002. doi: 10.1080/13550280290101085. URL http://dx.doi.org/10.1080/13550280290101085.

[63] S. Henderson, D. Huen, M. Rowe, C. Dawson, G. Johnson, and A. Rickinson. Epstein-barr virus-coded bhrf1 protein, a viral homologue of bcl-2, protects human b cells from programmed cell death. *Proc Natl Acad Sci U S A*, 90(18):8479–8483, Sep 1993.

[64] H. Higuchi, J.-H. Yoon, A. Grambihler, N. Werneburg, S. F. Bronk, and G. J. Gores. Bile acids stimulate cflip phosphorylation enhancing trail-mediated apoptosis. *J Biol Chem*, 278(1):454–461, Jan 2003. doi: 10.1074/jbc.M209387200. URL http://dx.doi.org/10.1074/jbc.M209387200.

[65] M. Inman, G. C. Perng, G. Henderson, H. Ghiasi, A. B. Nesburn, S. L. Wechsler, and C. Jones. Region of herpes simplex virus type 1 latency-associated transcript sufficient for wild-type spontaneous reactivation promotes cell survival in tissue culture. *J Virol*, 75(8):3636–3646, Apr 2001. doi: 10.1128/JVI.75.8.3636-3646.2001. URL http://dx.doi.org/10.1128/JVI.75.8.3636-3646.2001.

[66] M. Irmler, M. Thome, M. Hahne, P. Schneider, K. Hofmann, V. Steiner, J. Bodmer, M. Schröter, K. Burns, C. Mattmann, D. Rimoldi, L. French, and J. Tschopp. Inhibition of death receptor signals by cellular FLIP. *Nature*, 388(6638):190–5, Jul 1997. doi: 10.1038/40657. URL http://dx.doi.org/10.1038/40657.

[67] T. Ishioka, R. Katayama, R. Kikuchi, M. Nishimoto, S. Takada, R. Takada, S. ichi Matsuzawa, J. C. Reed, T. Tsuruo, and M. Naito. Impairment of the ubiquitin-proteasome system by cellular flip. *Genes Cells*, 12(6):735–744, Jun 2007. doi: 10.1111/j.1365-2443.2007.01087.x. URL http://dx.doi.org/10.1111/j.1365-2443.2007.01087.x.

[68] E. A. Jaffe, R. L. Nachman, C. G. Becker, and C. R. Minick. Culture of human endothelial cells derived from umbilical veins. identification by morphologic and immunologic criteria. *J Clin Invest*, 52(11):2745–2756, Nov 1973. doi: 10.1172/JCI107470. URL http://dx.doi.org/10.1172/JCI107470.

[69] C. A. Janeway, P. Travers, M. Walport, and M. J. Shlomchik. *Immunobiology, 5th edition, The Immune System in Health and Disease*. Garland Science, New York, 2001.

[70] E. Javouhey, B. Gibert, A.-P. Arrigo, J. J. Diaz, and C. Diaz-Latoud. Protection against heat and staurosporine mediated apoptosis by the hsv-1 us11 protein. *Virology*, 376(1):31–41, Jun 2008. doi: 10.1016/j.virol.2008.02.031. URL `http://dx.doi.org/10.1016/j.virol.2008.02.031`.

[71] K. Jerome, J. Tait, D. Koelle, and L. Corey. Herpes simplex virus type 1 renders infected cells resistant to cytotoxic T-lymphocyte-induced apoptosis. *J Virol*, 72 (1):436–41, Jan 1998.

[72] K. Jerome, R. Fox, Z. Chen, A. Sears, H. Lee, and L. Corey. Herpes simplex virus inhibits apoptosis through the action of two genes, Us5 and Us3. *J Virol*, 73(11): 8950–7, Nov 1999.

[73] K. Jerome, Z. Chen, R. Lang, M. Torres, J. Hofmeister, S. Smith, R. Fox, C. Froelich, and L. Corey. HSV and glycoprotein J inhibit caspase activation and apoptosis induced by granzyme B or Fas. *J Immunol*, 167(7):3928–35, Oct 2001.

[74] L. Jin, W. Peng, G.-C. Perng, D. J. Brick, A. B. Nesburn, C. Jones, and S. L. Wechsler. Identification of herpes simplex virus type 1 latency-associated transcript sequences that both inhibit apoptosis and enhance the spontaneous reactivation phenotype. *J Virol*, 77(11):6556–6561, Jun 2003.

[75] L. Jin, G.-C. Perng, D. J. Brick, J. Naito, A. B. Nesburn, C. Jones, and S. L. Wechsler. Methods for detecting the hsv-1 lat anti-apoptosis activity in virus infected tissue culture cells. *J Virol Methods*, 118(1):9–13, Jun 2004. doi: 10.1016/j.jviromet.2004.01.011. URL `http://dx.doi.org/10.1016/j.jviromet.2004.01.011`.

[76] L. Jin, G.-C. Perng, K. R. Mott, N. Osorio, J. Naito, D. J. Brick, D. Carpenter, C. Jones, and S. L. Wechsler. A herpes simplex virus type 1 mutant expressing a baculovirus inhibitor of apoptosis gene in place of latency-associated transcript has a wild-type reactivation phenotype in the mouse. *J Virol*, 79(19): 12286–12295, Oct 2005. doi: 10.1128/JVI.79.19.12286-12295.2005. URL `http://dx.doi.org/10.1128/JVI.79.19.12286-12295.2005`.

[77] L. Jin, D. Carpenter, M. Moerdyk-Schauwecker, A. L. Vanarsdall, N. Osorio, C. Hsiang, C. Jones, and S. L. Wechsler. Cellular flip can substitute for the herpes simplex virus type 1 latency-associated transcript gene to support a wild-type virus reactivation phenotype in mice. *J Neurovirol*, 14(5):389–400, Oct 2008. doi: 10.1080/13550280802216510. URL `http://dx.doi.org/10.1080/13550280802216510`.

[78] C. Johnen, B. Hartmann, I. Steffen, K. Bräutigam, T. Witascheck, N. Toman, M. V. Küntscher, and J. C. Gerlach. Skin cell isolation and expansion for cell transplantation is limited in patients using tobacco, alcohol, or are exhibiting diabetes mellitus. *Burns*, 32(2):194–200, Mar 2006. doi: 10.1016/j.burns.2005.10.001. URL `http://dx.doi.org/10.1016/j.burns.2005.10.001`.

[79] L. A. Johnson and R. M. Sandri-Goldin. Efficient nuclear export of herpes simplex virus 1 transcripts requires both rna binding by icp27 and icp27 interaction with tap/nxf1. *J Virol*, 83(3):1184–1192, Feb 2009. doi: 10.1128/JVI.02010-08. URL http://dx.doi.org/10.1128/JVI.02010-08.

[80] C. Jones, M. Fernandez, K. Herc, L. Bosnjak, M. Miranda-Saksena, R. Boadle, and A. Cunningham. Herpes simplex virus type 2 induces rapid cell death and functional impairment of murine dendritic cells in vitro. *J Virol*, 77(20):11139–49, Oct 2003.

[81] R. Josien, H. L. Li, E. Ingulli, S. Sarma, B. R. Wong, M. Vologodskaia, R. M. Steinman, and Y. Choi. Trance, a tumor necrosis factor family member, enhances the longevity and adjuvant properties of dendritic cells in vivo. *J Exp Med*, 191(3): 495–502, Feb 2000.

[82] I. Jurak, U. Schumacher, H. Simic, S. Voigt, and W. Brune. Murine cytomegalovirus m38.5 protein inhibits bax-mediated cell death. *J Virol*, 82(10): 4812–4822, May 2008. doi: 10.1128/JVI.02570-07. URL http://dx.doi.org/10.1128/JVI.02570-07.

[83] G. Karaca, D. Hargett, T. I. McLean, J. S. Aguilar, P. Ghazal, E. K. Wagner, and S. L. Bachenheimer. Inhibition of the stress-activated kinase, p38, does not affect the virus transcriptional program of herpes simplex virus type 1. *Virology*, 329 (1):142–156, Nov 2004. doi: 10.1016/j.virol.2004.08.020. URL http://dx.doi.org/10.1016/j.virol.2004.08.020.

[84] T. Kataoka. The caspase-8 modulator c-flip. *Crit Rev Immunol*, 25(1):31–58, 2005.

[85] T. Kataoka and J. Tschopp. N-terminal fragment of c-FLIP(L) processed by caspase 8 specifically interacts with TRAF2 and induces activation of the NF-kappaB signaling pathway. *Mol Cell Biol*, 24(7):2627–36, Apr 2004.

[86] A. Kaunisto, V. Kochin, T. Asaoka, A. Mikhailov, M. Poukkula, A. Meinander, and J. E. Eriksson. Pkc-mediated phosphorylation regulates c-flip ubiquitylation and stability. *Cell Death Differ*, 16(9):1215–1226, Sep 2009. doi: 10.1038/cdd.2009.35. URL http://dx.doi.org/10.1038/cdd.2009.35.

[87] D. Khoo, C. Perez, and I. Mohr. Characterization of rna determinants recognized by the arginine- and proline-rich region of us11, a herpes simplex virus type 1-encoded double-stranded rna binding protein that prevents pkr activation. *J Virol*, 76(23):11971–11981, Dec 2002.

[88] S. Kim, J. Carew, D. Kooby, J. Shields, C. Entwisle, S. Patel, J. Shah, and Y. Fong. Combination gene therapy using multiple immunomodulatory genes transferred by a defective infectious single-cycle herpes virus in squamous cell cancer. *Cancer Gene Ther*, 7(9):1279–85, Sep 2000. doi: 10.1038/sj.cgt.7700231. URL http://dx.doi.org/10.1038/sj.cgt.7700231.

[89] Y. Kim, N. Suh, M. Sporn, and J. C. Reed. An inducible pathway for degradation of FLIP protein sensitizes tumor cells to TRAIL-induced apoptosis. *J Biol Chem*, 277(25):22320–9, Jun 2002. doi: 10.1074/jbc.M202458200. URL http://dx.doi.org/10.1074/jbc.M202458200.

[90] Y. H. Kim, E. M. Jung, T.-J. Lee, S. H. Kim, Y. H. Choi, J. W. Park, J.-W. Park, K. S. Choi, and T. K. Kwon. Rosiglitazone promotes tumor necrosis factor-related apoptosis-inducing ligand-induced apoptosis by reactive oxygen species-mediated up-regulation of death receptor 5 and down-regulation of c-flip. *Free Radic Biol Med*, 44(6):1055–1068, Mar 2008. doi: 10.1016/j.freeradbiomed.2007.12.001. URL http://dx.doi.org/10.1016/j.freeradbiomed.2007.12.001.

[91] D. M. Koelle and L. Corey. Recent progress in herpes simplex virus immunobiology and vaccine research. *Clin Microbiol Rev*, 16(1):96–113, Jan 2003.

[92] A. H. Koyama and A. Adachi. Induction of apoptosis by herpes simplex virus type 1. *J Gen Virol*, 78 (Pt 11):2909–2912, Nov 1997.

[93] S. Kreuz, D. Siegmund, P. Scheurich, and H. Wajant. Nf-kappab inducers upregulate cflip, a cycloheximide-sensitive inhibitor of death receptor signaling. *Mol Cell Biol*, 21(12):3964–3973, Jun 2001. doi: 10.1128/MCB.21.12.3964-3973.2001. URL http://dx.doi.org/10.1128/MCB.21.12.3964-3973.2001.

[94] E. Kriehuber, W. Bauer, A.-S. Charbonnier, D. Winter, S. Amatschek, D. Tamandl, N. Schweifer, G. Stingl, and D. Maurer. Balance between nf-kappab and jnk/ap-1 activity controls dendritic cell life and death. *Blood*, 106(1):175–183, Jul 2005. doi: 10.1182/blood-2004-08-3072. URL http://dx.doi.org/10.1182/blood-2004-08-3072.

[95] J. D. Kriesel, B. B. Jones, K. M. Dahms, and S. L. Spruance. Stat1 binds to the herpes simplex virus type 1 latency-associated transcript promoter. *J Neurovirol*, 10(1):12–20, Feb 2004.

[96] A. Krueger, I. Schmitz, S. Baumann, P. Krammer, and S. Kirchhoff. Cellular FLICE-inhibitory protein splice variants inhibit different steps of caspase-8 activation at the CD95 death-inducing signaling complex. *J Biol Chem*, 276(23):20633–40, Jun 2001. doi: 10.1074/jbc.M101780200. URL http://dx.doi.org/10.1074/jbc.M101780200.

[97] M. Kruse, O. Rosorius, F. Krätzer, G. Stelz, C. Kuhnt, G. Schuler, J. Hauber, and A. Steinkasserer. Mature dendritic cells infected with herpes simplex virus type 1 exhibit inhibited T-cell stimulatory capacity. *J Virol*, 74(15):7127–36, Aug 2000.

[98] A. D. Kwong, J. A. Kruper, and N. Frenkel. Herpes simplex virus virion host shutoff function. *J Virol*, 62(3):912–921, Mar 1988.

[99] H. Lauterbach, K. M. Kerksiek, D. H. Busch, E. Berto, A. Bozac, P. Mavromara, R. Manservigi, A. L. Epstein, P. Marconi, and T. Brocker. Protection from bacterial infection by a single vaccination with replication-deficient mutant herpes simplex virus type 1. *J Virol*, 78(8):4020–8, Apr 2004.

[100] A. Lawen. Apoptosis-an introduction. *Bioessays*, 25(9):888–896, Sep 2003. doi: 10.1002/bies.10329. URL `http://dx.doi.org/10.1002/bies.10329`.

[101] T.-J. Lee, H. J. Um, D. S. Min, J.-W. Park, K. S. Choi, and T. K. Kwon. Withaferin a sensitizes trail-induced apoptosis through reactive oxygen species-mediated up-regulation of death receptor 5 and down-regulation of c-flip. *Free Radic Biol Med*, 46(12):1639–1649, Jun 2009. doi: 10.1016/j.freeradbiomed.2009.03.022. URL `http://dx.doi.org/10.1016/j.freeradbiomed.2009.03.022`.

[102] R. Leopardi and B. Roizman. The herpes simplex virus major regulatory protein icp4 blocks apoptosis induced by the virus or by hyperthermia. *Proc Natl Acad Sci U S A*, 93(18):9583–9587, Sep 1996.

[103] R. Leopardi, C. V. Sant, and B. Roizman. The herpes simplex virus 1 protein kinase us3 is required for protection from apoptosis induced by the virus. *Proc Natl Acad Sci U S A*, 94(15):7891–7896, Jul 1997.

[104] M. Leverkus, H. Walczak, A. McLellan, H. Fries, G. Terbeck, E. Bröcker, and E. Kämpgen. Maturation of dendritic cells leads to up-regulation of cellular FLICE-inhibitory protein and concomitant down-regulation of death ligand-mediated apoptosis. *Blood*, 96(7):2628–31, Oct 2000.

[105] D. L. Lichtenstein, K. Toth, K. Doronin, A. E. Tollefson, and W. S. M. Wold. Functions and mechanisms of action of the adenovirus e3 proteins. *Int Rev Immunol*, 23(1-2):75–111, 2004.

[106] D. Liu, T. Ren, and X. Gao. Cationic transfection lipids. *Curr Med Chem*, 10(14): 1307–1315, Jul 2003.

[107] X. Luo, K. V. Tarbell, H. Yang, K. Pothoven, S. L. Bailey, R. Ding, R. M. Steinman, and M. Suthanthiran. Dendritic cells with tgf-beta1 differentiate naive cd4+cd25- t cells into islet-protective foxp3+ regulatory t cells. *Proc Natl Acad Sci U S A*, 104 (8):2821–2826, Feb 2007. doi: 10.1073/pnas.0611646104. URL `http://dx.doi.org/10.1073/pnas.0611646104`.

[108] A. Macagno, G. Napolitani, A. Lanzavecchia, and F. Sallusto. Duration, combination and timing: the signal integration model of dendritic cell activation. *Trends Immunol*, 28(5):227–233, May 2007. doi: 10.1016/j.it.2007.03.008. URL `http://dx.doi.org/10.1016/j.it.2007.03.008`.

[109] S. Mathas, A. Lietz, I. Anagnostopoulos, F. Hummel, B. Wiesner, M. Janz, F. Jundt, B. Hirsch, K. Jöhrens-Leder, H.-P. Vornlocher, K. Bommert, H. Stein,

and B. Dörken. c-FLIP Mediates Resistance of Hodgkin/Reed-Sternberg Cells to Death Receptor-induced Apoptosis. *J Exp Med*, 199(8):1041–52, Apr 2004. doi: 10.1084/jem.20031080. URL http://dx.doi.org/10.1084/jem.20031080.

[110] A. Mehling, K. Loser, G. Varga, D. Metze, T. A. Luger, T. Schwarz, S. Grabbe, and S. Beissert. Overexpression of cd40 ligand in murine epidermis results in chronic skin inflammation and systemic autoimmunity. *J Exp Med*, 194(5):615–628, Sep 2001.

[111] O. Micheau, S. Lens, O. Gaide, K. Alevizopoulos, and J. Tschopp. Nf-kappab signals induce the expression of c-flip. *Mol Cell Biol*, 21(16):5299–5305, Aug 2001. doi: 10.1128/MCB.21.16.5299-5305.2001. URL http://dx.doi.org/10.1128/MCB.21.16.5299-5305.2001.

[112] M. Mihara, S. Erster, A. Zaika, O. Petrenko, T. Chittenden, P. Pancoska, and U. M. Moll. p53 has a direct apoptogenic role at the mitochondria. *Mol Cell*, 11(3):577–90, Mar 2003.

[113] Z. Mikloska, P. P. Sanna, and A. L. Cunningham. Neutralizing antibodies inhibit axonal spread of herpes simplex virus type 1 to epidermal cells in vitro. *J Virol*, 73(7):5934–5944, Jul 1999.

[114] Z. Mikloska, L. Bosnjak, and A. Cunningham. Immature monocyte-derived dendritic cells are productively infected with herpes simplex virus type 1. *J Virol*, 75(13):5958–64, Jul 2001. doi: 10.1128/JVI.75.13.5958-5964.2001. URL http://dx.doi.org/10.1128/JVI.75.13.5958-5964.2001.

[115] D. B. Müller, M. J. Raftery, A. Kather, T. Giese, and G. Schönrich. Frontline: Induction of apoptosis and modulation of c-FLIPL and p53 in immature dendritic cells infected with herpes simplex virus. *Eur J Immunol*, 34(4):941–51, Apr 2004. doi: 10.1002/eji.200324509. URL http://dx.doi.org/10.1002/eji.200324509.

[116] E. R. Morton and J. A. Blaho. Herpes simplex virus blocks fas-mediated apoptosis independent of viral activation of nf-kappab in human epithelial hep-2 cells. *J Interferon Cytokine Res*, 27(5):365–376, May 2007. doi: 10.1089/jir.2006.0143. URL http://dx.doi.org/10.1089/jir.2006.0143.

[117] K. R. Mott, N. Osorio, L. Jin, D. J. Brick, J. Naito, J. Cooper, G. Henderson, M. Inman, C. Jones, S. L. Wechsler, and G.-C. Perng. The bovine herpesvirus-1 lr orf2 is critical for this gene's ability to restore the high wild-type reactivation phenotype to a herpes simplex virus-1 lat null mutant. *J Gen Virol*, 84(Pt 11):2975–2985, Nov 2003.

[118] J. Munger and B. Roizman. The us3 protein kinase of herpes simplex virus 1 mediates the posttranslational modification of bad and prevents bad-induced programmed cell death in the absence of other viral proteins. *Proc Natl Acad Sci U S A*, 98(18):10410–10415, Aug 2001. doi: 10.1073/pnas.181344498. URL http://dx.doi.org/10.1073/pnas.181344498.

[119] J. Munger, A. V. Chee, and B. Roizman. The u(s)3 protein kinase blocks apoptosis induced by the d120 mutant of herpes simplex virus 1 at a premitochondrial stage. *J Virol*, 75(12):5491–5497, Jun 2001. doi: 10.1128/JVI.75.12.5491-5497.2001. URL http://dx.doi.org/10.1128/JVI.75.12.5491-5497.2001.

[120] A. J. Nahmias and W. R. Dowdle. Antigenic and biologic differences in herpesvirus hominis. *Prog Med Virol*, 10:110–159, 1968.

[121] M. Naito, R. Katayama, T. Ishioka, A. Suga, K. Takubo, M. Nanjo, C. Hashimoto, M. Taira, S. Takada, R. Takada, M. Kitagawa, S.-I. Matsuzawa, J. C. Reed, and T. Tsuruo. Cellular flip inhibits beta-catenin ubiquitylation and enhances wnt signaling. *Mol Cell Biol*, 24(19):8418–8427, Oct 2004. doi: 10.1128/MCB.24.19.8418-8427.2004. URL http://dx.doi.org/10.1128/MCB.24.19.8418-8427.2004.

[122] M. Neumann, H. Fries, C. Scheicher, P. Keikavoussi, A. Kolb-Mäurer, E. Bröcker, E. Serfling, and E. Kämpgen. Differential expression of rel/nf-kappab and octamer factors is a hallmark of the generation and maturation of dendritic cells. *Blood*, 95(1):277–285, Jan 2000.

[123] M. L. Nguyen and J. A. Blaho. Apoptosis during herpes simplex virus infection. *Adv Virus Res*, 69:67–97, 2007. doi: 10.1016/S0065-3527(06)69002-7. URL http://dx.doi.org/10.1016/S0065-3527(06)69002-7.

[124] V. O'Brien. Viruses and apoptosis. *J Gen Virol*, 79 (Pt 8):1833–45, Aug 1998.

[125] P. D. Ogg, P. J. McDonell, B. J. Ryckman, C. M. Knudson, and R. J. Roller. The hsv-1 us3 protein kinase is sufficient to block apoptosis induced by overexpression of a variety of bcl-2 family members. *Virology*, 319(2):212–224, Feb 2004. doi: 10.1016/j.virol.2003.10.019. URL http://dx.doi.org/10.1016/j.virol.2003.10.019.

[126] A. A. Oroskar and G. S. Read. A mutant of herpes simplex virus type 1 exhibits increased stability of immediate-early (alpha) mrnas. *J Virol*, 61(2):604–606, Feb 1987.

[127] R. A. Pereira, A. Scalzo, and A. Simmons. Cutting edge: a nk complex-linked locus governs acute versus latent herpes simplex virus infection of neurons. *J Immunol*, 166(10):5869–5873, May 2001.

[128] D. Perez and E. White. E1A sensitizes cells to tumor necrosis factor alpha by downregulating c-FLIP S. *J Virol*, 77(4):2651–62, Feb 2003.

[129] G. C. Perng, E. C. Dunkel, P. A. Geary, S. M. Slanina, H. Ghiasi, R. Kaiwar, A. B. Nesburn, and S. L. Wechsler. The latency-associated transcript gene of herpes simplex virus type 1 (hsv-1) is required for efficient in vivo spontaneous reactivation of hsv-1 from latency. *J Virol*, 68(12):8045–8055, Dec 1994.

[130] G. C. Perng, H. Ghiasi, S. M. Slanina, A. B. Nesburn, and S. L. Wechsler. The spontaneous reactivation function of the herpes simplex virus type 1 lat gene resides completely within the first 1.5 kilobases of the 8.3-kilobase primary transcript. *J Virol*, 70(2):976–984, Feb 1996.

[131] G. C. Perng, C. Jones, J. Ciacci-Zanella, M. Stone, G. Henderson, A. Yukht, S. M. Slanina, F. M. Hofman, H. Ghiasi, A. B. Nesburn, and S. L. Wechsler. Virus-induced neuronal apoptosis blocked by the herpes simplex virus latency-associated transcript. *Science*, 287(5457):1500–1503, Feb 2000.

[132] C. Pohl, J. Shishkova, and S. Schneider-Schaulies. Viruses and dendritic cells: enemy mine. *Cell Microbiol*, 9(2):279–289, Feb 2007. doi: 10.1111/j.1462-5822.2006.00863.x. URL `http://dx.doi.org/10.1111/j.1462-5822.2006.00863.x`.

[133] G. Pollara, K. Speidel, L. Samady, M. Rajpopat, Y. McGrath, J. Ledermann, R. S. Coffin, D. R. Katz, and B. Chain. Herpes simplex virus infection of dendritic cells: balance among activation, inhibition, and immunity. *J Infect Dis*, 187(2):165–78, Jan 2003.

[134] G. Pollara, M. Jones, M. E. Handley, M. Rajpopat, A. Kwan, R. S. Coffin, G. Foster, B. Chain, and D. R. Katz. Herpes simplex virus type-1-induced activation of myeloid dendritic cells: the roles of virus cell interaction and paracrine type I IFN secretion. *J Immunol*, 173(6):4108–19, Sep 2004.

[135] M. Poukkula, A. Kaunisto, V. Hietakangas, K. Denessiouk, T. Katajamäki, M. S. Johnson, L. Sistonen, and J. E. Eriksson. Rapid turnover of c-flipshort is determined by its unique c-terminal tail. *J Biol Chem*, 280(29):27345–27355, Jul 2005. doi: 10.1074/jbc.M504019200. URL `http://dx.doi.org/10.1074/jbc.M504019200`.

[136] H. C. Probst, K. McCoy, T. Okazaki, T. Honjo, and M. van den Broek. Resting dendritic cells induce peripheral cd8+ t cell tolerance through pd-1 and ctla-4. *Nat Immunol*, 6(3):280–286, Mar 2005. doi: 10.1038/ni1165. URL `http://dx.doi.org/10.1038/ni1165`.

[137] M. Raftery, C. Behrens, A. Müller, P. Krammer, H. Walczak, and G. Schönrich. Herpes simplex virus type 1 infection of activated cytotoxic T cells: Induction of fratricide as a mechanism of viral immune evasion. *J Exp Med*, 190(8):1103–14, Oct 1999.

[138] M. J. Raftery, A. A. Kraus, R. Ulrich, D. H. Krüger, and G. Schönrich. Hantavirus infection of dendritic cells. *J Virol*, 76(21):10724–10733, Nov 2002.

[139] J. Rajcáni, V. Andrea, and R. Ingeborg. Peculiarities of herpes simplex virus (hsv) transcription: an overview. *Virus Genes*, 28(3):293–310, Apr 2004.

[140] M. Rescigno, M. Martino, C. Sutherland, M. Gold, and P. Ricciardi-Castagnoli. Dendritic cell survival and maturation are regulated by different signaling pathways. *J Exp Med*, 188(11):2175–80, Dec 1998.

[141] M. Rescigno, V. Piguet, B. Valzasina, S. Lens, R. Zubler, L. French, V. Kindler, J. Tschopp, and P. Ricciardi-Castagnoli. Fas engagement induces the maturation of dendritic cells (DCs), the release of interleukin (IL)-1beta, and the production of interferon gamma in the absence of IL-12 during DC-T cell cognate interaction: a new role for Fas ligand in inflammatory responses. *J Exp Med*, 192(11):1661–8, Dec 2000.

[142] B. Roizman, D. M. Knipe, and R. J. Whitley. *Fields virology 5th ed.*, volume II, chapter Herpes simplex viruses, pages 2501–2602. Lippincott, Williams & Wilkins, Philadelphia, PA, 5th edition, 2007.

[143] M. Salio, M. Cella, M. Suter, and A. Lanzavecchia. Inhibition of dendritic cell maturation by herpes simplex virus. *Eur J Immunol*, 29(10):3245–53, Oct 1999.

[144] F. Sallusto and A. Lanzavecchia. Efficient presentation of soluble antigen by cultured human dendritic cells is maintained by granulocyte/macrophage colony-stimulating factor plus interleukin 4 and downregulated by tumor necrosis factor alpha. *J Exp Med*, 179(4):1109–1118, Apr 1994.

[145] L. A. Samaniego, L. Neiderhiser, and N. A. DeLuca. Persistence and expression of the herpes simplex virus genome in the absence of immediate-early proteins. *J Virol*, 72(4):3307–3320, Apr 1998.

[146] R. M. Sandri-Goldin. The many roles of the regulatory protein icp27 during herpes simplex virus infection. *Front Biosci*, 13:5241–5256, 2008.

[147] C. M. Sanfilippo and J. A. Blaho. Icp0 gene expression is a herpes simplex virus type 1 apoptotic trigger. *J Virol*, 80(14):6810–6821, Jul 2006. doi: 10.1128/JVI.00334-06. URL `http://dx.doi.org/10.1128/JVI.00334-06`.

[148] C. Scaffidi, I. Schmitz, P. Krammer, and M. Peter. The role of c-FLIP in modulation of CD95-induced apoptosis. *J Biol Chem*, 274(3):1541–8, Jan 1999.

[149] T. Schacker, J. Zeh, H. L. Hu, E. Hill, and L. Corey. Frequency of symptomatic and asymptomatic herpes simplex virus type 2 reactivations among human immunodeficiency virus-infected men. *J Infect Dis*, 178(6):1616–1622, Dec 1998.

[150] K. E. SCHNEWEIS. [serological studies on the type differentiation of herpesvirus hominis.]. *Z Immun exp ther*, 124:24–48, Sep 1962.

[151] D. R. Schultz and W. J. Harrington. Apoptosis: programmed cell death at a molecular level. *Semin Arthritis Rheum*, 32(6):345–369, Jun 2003. doi: 10.1053/sarh.2003.50005. URL `http://dx.doi.org/10.1053/sarh.2003.50005`.

[152] W. Shen, M. S. e Silva, T. Jaber, O. Vitvitskaia, S. Li, G. Henderson, and C. Jones. Two small rnas encoded within the first 1.5 kilobases of the herpes simplex virus type 1 latency-associated transcript can inhibit productive infection and cooperate to inhibit apoptosis. *J Virol*, 83(18):9131–9139, Sep 2009. doi: 10.1128/JVI.00871-09. URL http://dx.doi.org/10.1128/JVI.00871-09.

[153] D. Siegmund, P. Hadwiger, K. Pfizenmaier, H.-P. Vornlocher, and H. Wajant. Selective inhibition of FLICE-like inhibitory protein expression with small interfering RNA oligonucleotides is sufficient to sensitize tumor cells for TRAIL-induced apoptosis. *Mol Med*, 8(11):725–32, Nov 2002.

[154] I. L. Smith, M. A. Hardwicke, and R. M. Sandri-Goldin. Evidence that the herpes simplex virus immediate early protein icp27 acts post-transcriptionally during infection to regulate gene expression. *Virology*, 186(1):74–86, Jan 1992.

[155] L. F. R. Span, A. H. M. Pennings, G. Vierwinden, J. B. M. Boezeman, R. A. P. Raymakers, and T. de Witte. The dynamic process of apoptosis analyzed by flow cytometry using annexin-v/propidium iodide and a modified in situ end labeling technique. *Cytometry*, 47(1):24–31, Jan 2002.

[156] R. M. Steinman and J. Banchereau. Taking dendritic cells into medicine. *Nature*, 449(7161):419–426, Sep 2007. doi: 10.1038/nature06175. URL http://dx.doi.org/10.1038/nature06175.

[157] R. M. Steinman and Z. A. Cohn. Identification of a novel cell type in peripheral lymphoid organs of mice. i. morphology, quantitation, tissue distribution. *J Exp Med*, 137(5):1142–1162, May 1973.

[158] S. W. Stingley, J. J. Ramirez, S. A. Aguilar, K. Simmen, R. M. Sandri-Goldin, P. Ghazal, and E. K. Wagner. Global analysis of herpes simplex virus type 1 transcription using an oligonucleotide-based dna microarray. *J Virol*, 74(21):9916–9927, Nov 2000.

[159] D. Su, Z. Su, J. Wang, S. Yang, and J. Ma. Ucf-101, a novel omi/htra2 inhibitor, protects against cerebral ischemia/reperfusion injury in rats. *Anat Rec (Hoboken)*, 292(6):854–861, Jun 2009. doi: 10.1002/ar.20910. URL http://dx.doi.org/10.1002/ar.20910.

[160] A. Sun, G. V. Devi-Rao, M. K. Rice, L. W. Gary, D. C. Bloom, R. M. Sandri-Goldin, P. Ghazal, and E. K. Wagner. Immediate-early expression of the herpes simplex virus type 1 icp27 transcript is not critical for efficient replication in vitro or in vivo. *J Virol*, 78(19):10470–10478, Oct 2004. doi: 10.1128/JVI.78.19.10470-10478.2004. URL http://dx.doi.org/10.1128/JVI.78.19.10470-10478.2004.

[161] A. Sun, G. V. Devi-Rao, M. K. Rice, L. W. Gary, D. C. Bloom, R. M. Sandri-Goldin, P. Wagner, and E. K. Wager. The tatgarat box of the hsv-1 icp27 gene is essential

for immediate early expression but not critical for efficient replication in vitro or in vivo. *Virus Genes*, 29(3):335–343, Dec 2004. doi: 10.1007/s11262-004-7437-9. URL http://dx.doi.org/10.1007/s11262-004-7437-9.

[162] Y. Suzuki, Y. Imai, H. Nakayama, K. Takahashi, K. Takio, and R. Takahashi. A serine protease, htra2, is released from the mitochondria and interacts with xiap, inducing cell death. *Mol Cell*, 8(3):613–621, Sep 2001.

[163] B. Taddeo, W. Zhang, F. Lakeman, and B. Roizman. Cells lacking NF-kappaB or in which NF-kappaB is not activated vary with respect to ability to sustain herpes simplex virus 1 replication and are not susceptible to apoptosis induced by a replication-incompetent mutant virus. *J Virol*, 78(21):11615–21, Nov 2004. doi: 10.1128/JVI.78.21.11615-11621.2004. URL http://dx.doi.org/10.1128/JVI.78.21.11615-11621.2004.

[164] W. A. Tatarowicz, C. E. Martin, A. S. Pekosz, S. L. Madden, F. J. Rauscher, S. Y. Chiang, T. A. Beerman, and N. W. Fraser. Repression of the hsv-1 latency-associated transcript (lat) promoter by the early growth response (egr) proteins: involvement of a binding site immediately downstream of the tata box. *J Neurovirol*, 3(3):212–224, Jun 1997.

[165] M. Thome, P. Schneider, K. Hofmann, H. Fickenscher, E. Meinl, F. Neipel, C. Mattmann, K. Burns, J. Bodmer, M. Schröter, C. Scaffidi, P. Krammer, M. Peter, and J. Tschopp. Viral FLICE-inhibitory proteins (FLIPs) prevent apoptosis induced by death receptors. *Nature*, 386(6624):517–21, Apr 1997.

[166] S. C. Thornton, S. N. Mueller, and E. M. Levine. Human endothelial cells: use of heparin in cloning and long-term serial cultivation. *Science*, 222(4624):623–625, Nov 1983.

[167] D. Toullec, P. Pianetti, H. Coste, P. Bellevergue, T. Grand-Perret, M. Ajakane, V. Baudet, P. Boissin, E. Boursier, and F. Loriolle. The bisindolylmaleimide gf 109203x is a potent and selective inhibitor of protein kinase c. *J Biol Chem*, 266(24):15771–15781, Aug 1991.

[168] L. Tourian, H. Zhao, and C. B. Srikant. p38alpha, but not p38beta, inhibits the phosphorylation and presence of c-flips in disc to potentiate fas-mediated caspase-8 activation and type i apoptotic signaling. *J Cell Sci*, 117(Pt 26):6459–6471, Dec 2004. doi: 10.1242/jcs.01573. URL http://dx.doi.org/10.1242/jcs.01573.

[169] J. Tschopp, M. Irmler, and M. Thome. Inhibition of fas death signals by FLIPs. *Curr Opin Immunol*, 10(5):552–8, Oct 1998.

[170] J. L. Umbach, M. F. Kramer, I. Jurak, H. W. Karnowski, D. M. Coen, and B. R. Cullen. Microrna s expressed by herpes simplex virus 1 during latent infection regulate viral mrnas. *Nature*, 454(7205):780–783, Aug 2008. doi: 10.1038/nature07103. URL http://dx.doi.org/10.1038/nature07103.

[171] A. van Lint, M. Ayers, A. G. Brooks, R. M. Coles, W. R. Heath, and F. R. Carbone. Herpes simplex virus-specific cd8+ t cells can clear established lytic infections from skin and nerves and can partially limit the early spread of virus after cutaneous inoculation. *J Immunol*, 172(1):392–397, Jan 2004.

[172] S. Varghese and S. D. Rabkin. Oncolytic herpes simplex virus vectors for cancer virotherapy. *Cancer Gene Ther*, 9(12):967–78, Dec 2002. doi: 10.1038/sj.cgt.7700537. URL `http://dx.doi.org/10.1038/sj.cgt.7700537`.

[173] C. Varol, L. Landsman, D. K. Fogg, L. Greenshtein, B. Gildor, R. Margalit, V. Kalchenko, F. Geissmann, and S. Jung. Monocytes give rise to mucosal, but not splenic, conventional dendritic cells. *J Exp Med*, 204(1):171–180, Jan 2007. doi: 10.1084/jem.20061011. URL `http://dx.doi.org/10.1084/jem.20061011`.

[174] A. M. Verhagen, J. Silke, P. G. Ekert, M. Pakusch, H. Kaufmann, L. M. Connolly, C. L. Day, A. Tikoo, R. Burke, C. Wrobel, R. L. Moritz, R. J. Simpson, and D. L. Vaux. Htra2 promotes cell death through its serine protease activity and its ability to antagonize inhibitor of apoptosis proteins. *J Biol Chem*, 277(1):445–454, Jan 2002. doi: 10.1074/jbc.M109891200. URL `http://dx.doi.org/10.1074/jbc.M109891200`.

[175] A. Verschoor, M. A. Brockman, M. Gadjeva, D. M. Knipe, and M. C. Carroll. Myeloid c3 determines induction of humoral responses to peripheral herpes simplex virus infection. *J Immunol*, 171(10):5363–5371, Nov 2003.

[176] E. K. Wagner and D. C. Bloom. Experimental investigation of herpes simplex virus latency. *Clin Microbiol Rev*, 10(3):419–443, Jul 1997.

[177] E. K. Wagner, J. J. G. Ramirez, S. W. N. Stingley, S. A. Aguilar, L. Buehler, G. B. Devi-Rao, and P. Ghazal. Practical approaches to long oligonucleotide-based dna microarray: lessons from herpesviruses. *Prog Nucleic Acid Res Mol Biol*, 71:445–491, 2002.

[178] J. Wang, L. Zheng, A. Lobito, F. K. Chan, J. Dale, M. Sneller, X. Yao, J. M. Puck, S. E. Straus, and M. J. Lenardo. Inherited human caspase 10 mutations underlie defective lymphocyte and dendritic cell apoptosis in autoimmune lymphoproliferative syndrome type ii. *Cell*, 98(1):47–58, Jul 1999. doi: 10.1016/S0092-8674(00)80605-4. URL `http://dx.doi.org/10.1016/S0092-8674(00)80605-4`.

[179] F. Willems, Z. Amraoui, N. Vanderheyde, V. Verhasselt, E. Aksoy, C. Scaffidi, M. Peter, P. Krammer, and M. Goldman. Expression of c-FLIP(L) and resistance to CD95-mediated apoptosis of monocyte-derived dendritic cells: inhibition by bisindolylmaleimide. *Blood*, 95(11):3478–82, Jun 2000.

[180] A. M. Woltman, S. W. van der Kooij, P. J. Coffer, R. Offringa, M. R. Daha, and C. van Kooten. Rapamycin specifically interferes with gm-csf signaling in human dendritic cells, leading to apoptosis via increased p27kip1 expression. *Blood*, 101

(4):1439–1445, Feb 2003. doi: 10.1182/blood-2002-06-1688. URL http://dx.doi.org/10.1182/blood-2002-06-1688.

[181] B. R. Wong, R. Josien, S. Y. Lee, B. Sauter, H. L. Li, R. M. Steinman, and Y. Choi. Trance (tumor necrosis factor [tnf]-related activation-induced cytokine), a new tnf family member predominantly expressed in t cells, is a dendritic cell-specific survival factor. *J Exp Med*, 186(12):2075–2080, Dec 1997.

[182] L. Wu and Y.-J. Liu. Development of dendritic-cell lineages. *Immunity*, 26(6):741–750, Jun 2007. doi: 10.1016/j.immuni.2007.06.006. URL http://dx.doi.org/10.1016/j.immuni.2007.06.006.

[183] W. J. Wurzer, O. Planz, C. Ehrhardt, M. Giner, T. Silberzahn, S. Pleschka, and S. Ludwig. Caspase 3 activation is essential for efficient influenza virus propagation. *EMBO J*, 22(11):2717–2728, Jun 2003. doi: 10.1093/emboj/cdg279. URL http://dx.doi.org/10.1093/emboj/cdg279.

[184] B. F. Yang, C. Xiao, W. H. Roa, P. H. Krammer, and C. Hao. Calcium/calmodulin-dependent protein kinase ii regulation of c-flip expression and phosphorylation in modulation of fas-mediated signaling in malignant glioma cells. *J Biol Chem*, 278(9):7043–7050, Feb 2003. doi: 10.1074/jbc.M211278200. URL http://dx.doi.org/10.1074/jbc.M211278200.

[185] I. A. York, C. Roop, D. W. Andrews, S. R. Riddell, F. L. Graham, and D. C. Johnson. A cytosolic herpes simplex virus protein inhibits antigen presentation to cd8+ t lymphocytes. *Cell*, 77(4):525–535, May 1994.

[186] G. Zachos, M. Koffa, C. Preston, J. Clements, and J. Conner. Herpes simplex virus type 1 blocks the apoptotic host cell defense mechanisms that target Bcl-2 and manipulates activation of p38 mitogen-activated protein kinase to improve viral replication. *J Virol*, 75(6):2710–28, Mar 2001. doi: 10.1128/JVI.75.6.2710-2728.2001. URL http://dx.doi.org/10.1128/JVI.75.6.2710-2728.2001.

[187] G. Zhou and B. Roizman. The domains of glycoprotein d required to block apoptosis depend on whether glycoprotein d is present in the virions carrying herpes simplex virus 1 genome lacking the gene encoding the glycoprotein. *J Virol*, 75(13):6166–6172, Jul 2001. doi: 10.1128/JVI.75.13.6166-6172.2001. URL http://dx.doi.org/10.1128/JVI.75.13.6166-6172.2001.

[188] G. Zhou, V. Galvan, G. Campadelli-Fiume, and B. Roizman. Glycoprotein d or j delivered in trans blocks apoptosis in sk-n-sh cells induced by a herpes simplex virus 1 mutant lacking intact genes expressing both glycoproteins. *J Virol*, 74(24):11782–11791, Dec 2000.

[189] G. Zhou, E. Avitabile, G. Campadelli-Fiume, and B. Roizman. The domains of glycoprotein d required to block apoptosis induced by herpes simplex virus 1 are largely distinct from those involved in cell-cell fusion and binding to nectin1. *J Virol*, 77(6):3759–3767, Mar 2003.

[190] Q. Zhou, S. Snipas, K. Orth, M. Muzio, V. M. Dixit, and G. S. Salvesen. Target protease specificity of the viral serpin crma. analysis of five caspases. *J Biol Chem*, 272(12):7797–7800, Mar 1997.

[191] J. C. Zwaagstra, H. Ghiasi, S. M. Slanina, A. B. Nesburn, S. C. Wheatley, K. Lillycrop, J. Wood, D. S. Latchman, K. Patel, and S. L. Wechsler. Activity of herpes simplex virus type 1 latency-associated transcript (lat) promoter in neuron-derived cells: evidence for neuron specificity and for a large lat transcript. *J Virol*, 64(10): 5019–5028, Oct 1990.

List of Figures

List of Tables

Selbständigkeitserklärung

Hiermit erkläre ich, die vorliegende Arbeit selbständig erarbeitet und verfaßt und nur die angegebene Literatur, Hilfen und Hilfsmittel verwendet zu haben.

Berlin, den 01.04.2011 Angela Kather